

Cross-trait prediction accuracy of high-dimensional ridge-type estimators in genome-wide association studies

Bingxin Zhao and Hongtu Zhu

University of North Carolina at Chapel Hill

November 25, 2019

Abstract

Marginal association summary statistics have attracted great attention in statistical genetics, mainly because the primary results of most genome-wide association studies (GWAS) are produced by marginal screening. In this paper, we study the prediction accuracy of marginal estimator in dense (or sparsity free) high-dimensional settings with $(n, p, m) \rightarrow \infty$, $m/n \rightarrow \gamma \in (0, \infty)$, and $p/n \rightarrow \omega \in (0, \infty)$. We consider a general correlation structure among the p features and allow an unknown subset m of them to be signals. As the marginal estimator can be viewed as a ridge estimator with regularization parameter $\lambda \rightarrow \infty$, we further investigate a class of ridge-type estimators in a unifying framework, including the popular best linear unbiased prediction (BLUP) in genetics. We find that the influence of λ on out-of-sample prediction accuracy heavily depends on ω . Though selecting an optimal λ can be important when p and n are comparable, it turns out that the out-of-sample R^2 of ridge-type estimators becomes near-optimal for any $\lambda \in (0, \infty)$ as ω increases. For example, when features are independent, the out-of-sample R^2 is always bounded by $1/\omega$ from above and is largely invariant to λ given large ω (say, $\omega > 5$). We also find that in-sample R^2 has completely different patterns and depends much more on λ than out-of-sample R^2 . In practice, our analysis delivers useful messages for genome-wide polygenic risk prediction and computation-accuracy trade-off in dense high-dimensions. We numerically illustrate our results in simulation studies and a real data example.

Keywords. GWAS; Summary statistics; Marginal screening; Ridge estimator; Best linear unbiased prediction (BLUP); Prediction accuracy; Training error; Relative efficiency.

1 Introduction

Human complex traits often have a polygenic genetic architecture [Boyle et al., 2017, O’Connor et al., 2019, Wray et al., 2018]. That is, a large number of genetic variants have small but nonzero contributions to phenotypic variation [Timpson et al., 2018]. Genome-wide association studies (GWAS) aim to find suspicious genetic risk variants by examining association between complex traits and millions of variants, typically common (minor allele frequency [MAF] ≥ 0.05) single-nucleotide polymorphisms (SNPs) collected across the genome. After a decade of GWAS discovery, more than 100 millions of individuals have been genotyped [Martin et al., 2019] and thousands of unique traits have been studied [Visscher et al., 2017].

In the genetics community, GWAS summary association statistics (e.g., effect size, standard error, p -value) of all SNPs for various traits are shared and assembled into large databases. Summary statistics from more than 4000 GWAS are now publicly available [Watanabe et al., 2019] and the number rises steeply. As individual-level SNP data are massive and are often under strict ethical/regulatory protections, it is an active research area to directly use these GWAS summary statistics for various in-sample and out-of-sample analyses [Pasaniuc and Price, 2017]. For example, GWAS summary statistics are used to prioritize causal variants in fine-mapping analysis [Schaid et al., 2018], to quantify genetic overlaps among different traits [Bulik-Sullivan et al., 2015, Speed and Balding, 2019], to perform causal inference among traits via Mendelian randomization [Zhao et al., 2018], and to carry out integrative association tests with gene expression data [Gamazon et al., 2015, Gusev et al., 2016, Hu et al., 2019]. Owing primarily to the potential to translate GWAS findings to medical advancements, it is of particular interest to predict the personalized genetic risk for new GWAS individuals using results from historical GWAS [Martin et al., 2019, Sugrue and Desikan, 2019, Torkamani et al., 2018]. One of the state-of-art methods for genetic risk prediction of human complex traits is genome-wide polygenic risk score (PRS) [Purcell et al., 2009], which is a weighted sum of millions of SNPs where each SNP is weighted by their estimated effect size from discovery GWAS. As no need to access the personal DNA information of subjects in the training set, PRS is computationally efficient and has widespread applications with more than 3,000 related publications in 2018 [Zhao and Zou, 2019]. Recent efforts have begun to explore the clinical utility of PRS on human diseases, such as heart disease and breast cancer [Khera et al., 2018, Mavaddat et al., 2019].

Though GWAS summary statistics have numerous applications, there is little rigorous theoretical evaluation. Without sufficient understanding of their statistical properties, we risk drawing erroneous decisions on summary statistics database design and construction. Most, if not all, of publicly shared GWAS summary statistics are marginal effects generated from marginal screening. Let \mathbf{y} be an $n \times 1$ vector of continuous trait, a linear polygenic structure between \mathbf{y} and SNP data \mathbf{X} is often assumed in GWAS (e.g., Jiang et al. [2016])

$$\mathbf{y} = \mathbf{X}\boldsymbol{\beta} + \boldsymbol{\epsilon} = \sum_{i=1}^p \mathbf{x}_i \beta_i + \boldsymbol{\epsilon} = \sum_{i=1}^m \mathbf{x}_i \beta_i + \boldsymbol{\epsilon},$$

where $\mathbf{X} = (\mathbf{x}_1, \dots, \mathbf{x}_m, \mathbf{x}_{m+1}, \dots, \mathbf{x}_p)$ is an $n \times p$ SNP data matrix with population-level correlation Σ among the p features, $\boldsymbol{\beta} = (\beta_1, \dots, \beta_m, \beta_{m+1}, \dots, \beta_p)^T$ is a $p \times 1$ vector of genetic effects such that $(\beta_1, \dots, \beta_m)^T$ are m unknown nonzero parameters, and $(\beta_{m+1}, \dots, \beta_p)^T$ are zeros, and the $n \times 1$ vector $\boldsymbol{\epsilon}$ represents independent non-genetic random errors. The single SNP analysis in GWAS is given by

$$\mathbf{y} = \mathbf{1}_n \mu_i + \mathbf{x}_i \beta_i + \boldsymbol{\epsilon}_i^* \quad (1)$$

for $i = 1, \dots, p$, which is a marginal screening approach similar to sure independence screening [Fan and Lv, 2008]. Let $\hat{\boldsymbol{\beta}}_S = (\hat{\beta}_{1S}, \dots, \hat{\beta}_{pS})^T$ be the marginal screening ordinary least squares (OLS) estimator of model (1), the marginal estimators are given by

$$\hat{\beta}_{iS} = (\mathbf{x}_i^T \mathbf{x}_i)^{-1} \mathbf{x}_i^T \mathbf{y}, \quad i = 1, \dots, p,$$

and thus $\hat{\boldsymbol{\beta}}_S = \{\text{Diag}(\mathbf{X}^T \mathbf{X})\}^{-1} \mathbf{X}^T \mathbf{y}$ is the form of nearly all shared GWAS summary statistics for continuous traits, where $\text{Diag}(\mathbf{A})$ is the diagonal of matrix \mathbf{A} .

For human complex traits, the number of causal SNPs m is trait-specific and population-specific, and it can be comparable with n , but is not necessarily p . An overwhelming number of empirical evidence supports the polygenicity and pleiotropy of complex traits (e.g., Martin et al. [2018], Sullivan and Geschwind [2019], Watanabe et al. [2019]), which can be potentially explained by biological complexity and negative selection [O'Connor et al., 2019]. Statistically, we may have a dense (sparsity free) signal model, while not every feature has a nonzero effect on the outcome. This is different from the standard settings in sparse regression (e.g., Fan and Lv [2008], Feng and Zhang [2017], Guo et al. [2019], Zhao and Yu [2006]), which often has sparsity restriction on m .

Motivated by GWAS applications, the goal of this paper is to evaluate the out-of-sample and in-sample behaviors of high-dimensional marginal estimator $\hat{\boldsymbol{\beta}}_S$ in sparsity free settings. As marginal estimator can be viewed as a ridge-type estimator with regularization parameter increases to infinity [Fan and Lv, 2008], we investigate several popular ridge-type estimators in an unifying framework and allow the regularization parameter goes to zero or infinity. We first introduce the whole class of ridge-type estimators studied in this paper.

1.1 The class of ridge-type estimators

In this section, we summarize the estimators investigated in our analysis and highlight their natural connections.

1.1.1 Ridge, marginal, and ridge-less

For simplicity, suppose \mathbf{X} have been column-standardized to have mean zero and variance one, then the marginal estimator can be asymptotically given by

$$\hat{\boldsymbol{\beta}}_S = \{\text{Diag}(\mathbf{X}^T \mathbf{X})\}^{-1} \mathbf{X}^T \mathbf{y} = \{\text{Diag}(\hat{\Sigma}_X)\}^{-1} \cdot n^{-1} \mathbf{X}^T \mathbf{y} = n^{-1} \mathbf{X}^T \mathbf{y}, \quad (2)$$

where $\widehat{\Sigma}_X = n^{-1}X^T X$ is the sample covariance matrix. The ridge-regularized estimator [Hoerl and Kennard, 1970, Tikhonov, 1963] with regularization parameter λ is

$$\widehat{\beta}_R(\lambda) = (X^T X + \lambda n I_p)^{-1} X^T y = (\widehat{\Sigma}_X + \lambda I_p)^{-1} \widehat{\beta}_S, \quad \lambda \in (0, \infty). \quad (3)$$

Here $\widehat{\Sigma}_X + \lambda I_p$ is a linear combination of $\widehat{\Sigma}_X$ and diagonal matrix λI_p , and is called linear shrinkage estimator of Σ [Ledoit and Wolf, 2004]. In equation (3), $\widehat{\beta}_R(\lambda)$ can be viewed as the marginal estimator $\widehat{\beta}_S$ after “accounting for Σ ” through this linear shrinkage estimator. When λ is large enough such that λI_p can dominate $\widehat{\Sigma}_X$, $\widehat{\Sigma}_X + \lambda I_p$ becomes asymptotically a diagonal matrix. Thus, let $\widehat{\beta}_R(\infty) = \lim_{\lambda \rightarrow \infty} \widehat{\beta}_R(\lambda)$, as $\lambda \rightarrow \infty$, we can have

$$\widehat{\beta}_R(\infty) \propto \widehat{\beta}_S.$$

On the other hand, as $\lambda \rightarrow 0^+$ (from the right), we have the ridge-less least squares estimator [Hastie et al., 2019]

$$\widehat{\beta}_R(0^+) = \lim_{\lambda \rightarrow 0^+} \widehat{\beta}_R(\lambda) = (X^T X)^+ X^T y = \widehat{\Sigma}_X^+ \widehat{\beta}_S,$$

where A^+ is the Moore-Penrose pseudoinverse of matrix A . When $n > p$ and suppose X has full column rank, $\widehat{\beta}_R(0^+)$ reduces to the classic OLS estimator $\widehat{\beta}_O$ given by

$$\widehat{\beta}_O = \widehat{\beta}_R(0) = (X^T X)^{-1} X^T y = \widehat{\Sigma}_X^{-1} \widehat{\beta}_S.$$

1.1.2 BLUP and BLUP-less

In addition, ridge estimators have natural connection with the following best linear unbiased prediction (BLUP)

$$\widehat{\beta}_B(\tau) = X^T (X X^T + \tau p I_n)^{-1} y, \quad \tau \in (0, \infty).$$

BLUP is originally from linear mixed effects model (LMM) [Henderson, 1950, 1975] and has been widely applied in genetics to tackle dense genetic effects (e.g., Yang et al. [2010]). Similar to $\widehat{\beta}_R(0^+)$, we can define the BLUP-less estimator $\widehat{\beta}_B(0^+)$ by letting $\tau \rightarrow 0$

$$\widehat{\beta}_B(0^+) = \lim_{\tau \rightarrow 0^+} \widehat{\beta}_B(\tau) = X^T (X X^T)^+ y.$$

When $n < p$ and suppose X has full row rank, $X^T (X X^T)^+$ reduces to $X^T (X X^T)^{-1}$, which has been used for variable selection [Wang and Leng, 2016] and also has many applications in genetics, such as OmicKriging [Wheeler et al., 2014]. It can be shown that [Wang and Leng, 2016]

$$X^T (X X^T + \tau p I_n)^{-1} y = (X^T X + \tau p I_p)^{-1} X^T y.$$

It follows that $\widehat{\beta}_B(\tau) = \widehat{\beta}_R(\tau\omega)$ and there is one-to-one correspondence between ridge estimator and BLUP.

Similar to $\widehat{\beta}_S$, all of the ridge-type *conditional* estimators $\widehat{\beta}_R(\lambda)$, $\widehat{\beta}_B(\tau)$, $\widehat{\beta}_R(0^+)$, $\widehat{\beta}_B(0^+)$,

and $\hat{\beta}_O$ can be shared as GWAS summary-level data for following-up in-sample and out-of-sample applications. However, their computational complexity can be totally different in large training dataset with both n and $p \rightarrow \infty$. Particularly, marginal estimator $\hat{\beta}_S$ is usually much less computationally expensive than conditional estimators. Thus, understanding their connections and differences are important to determine the “best” GWAS summary-level data to share while considering the computation-accuracy trade-off. In the rest of this paper, we analyze and compare these estimators in an unifying framework. We name them the class of ridge-type estimators.

1.2 Overview of main results

Below we briefly summarize some phenomena we observed for high-dimensional dense signal prediction and then provide some practical guidelines on GWAS applications.

- (Cross-validation free) The optimal regularizer λ^* (or τ^*) for out-of-sample R^2 is independent of Σ and is solely determined by ω and the global signal strength h^2 (i.e., the genetic heritability). Given consistent estimator of h^2 [Jiang et al., 2016, Ma and Dicker, 2019], optimal ridge-type estimator can be obtained without the need for cross-validation in ridge estimator or BLUP.
- (Sparsity free) Given ω and h^2 , out-of-sample R^2 depends on the eigenvalue distribution of Σ , but is independent of the unknown m . For example, Σ affects the prediction accuracy of marginal estimator $\hat{\beta}_S$ through the first three moments of its eigenvalue distribution. Thus, the prediction accuracy of feature datasets can be assessed and compared by their eigenvalue distributions, without the knowledge of the sparsity of signals.
- (Is it important to select optimal λ ?) The sensitivity of out-of-sample R^2 to λ highly depends on ω . λ plays an important role when n and p are similar (for example, $\omega \approx 1$), in which $\hat{\beta}_R(\lambda)$ with small λ may be over-fitted and have very poor out-of-sample performance. Particularly, the out-of-sample R^2 of $\hat{\beta}_R(0^+)$ can equal to zero while its in-sample R^2 can be one regardless of h^2 . In addition, model under-fitting with large λ can be substantially suboptimal. However, as ω increases, $\hat{\beta}_R(\lambda)$ becomes near-optimal for any $\lambda \in (0, \infty)$. Therefore, selecting optimal λ for out-of-sample prediction becomes less essential as feature dimensionality increases. Instead, computational efficiency might be more important and thus marginal estimator becomes more favorable.
- (Goodness-of-fit) Compared to out-of-sample R^2 , in-sample R^2 is much more sensitive to λ . For example, the in-sample R^2 of $\hat{\beta}_R(\lambda)$ with small λ is usually larger than h^2 and can easily become one when $\omega > 1$ regardless of h^2 . On the other hand, the in-sample R^2 of $\hat{\beta}_S \propto \hat{\beta}_R(\infty)$ may be lower than h^2 and can only equal to one as $\omega \rightarrow \infty$. Thus, $\hat{\beta}_R(\lambda)$ with different λ may differ a lot for their in-sample goodness-of-fit, though their out-of-sample R^2 can be very similar.
- (Meta-analysis/Distributed computation) Different from ridge-type conditional estimators [Dobriban and Sheng, 2019], marginal estimator $\hat{\beta}_S$ can have zero predic-

tion accuracy loss in distributed computation given optimal weights. This mainly because $\hat{\beta}_S$ has no need of calculating the inverse of sample covariance matrix.

Now we deliver some useful messages for GWAS applications.

- (Diverse populations) We provide analytic results on how the prediction accuracy of GWAS summary statistics is related to the linkage disequilibrium (LD) structure Σ_G of the SNP data. For example, we show that the out-of-sample R^2 of $\hat{\beta}_S$ is determined by the first three moments of eigenvalues of Σ_G . More generally the out-of-sample R^2 of $\hat{\beta}_R(\lambda^*)$ is related to the Stieltjes transform. The LD structure is known to be consistent within each population, but substantially different among different populations. Following our results, we can calculate and compare the population-specific prediction accuracy using some simple functions of eigenvalue distribution.
- (Marginal summary statistics) Since ω remains large in most of current GWAS, we provide statistical guarantees that marginal estimator is computation-accuracy efficient in the sense that it can have near-optimal out-of-sample R^2 and is much faster than ridge-type conditional estimators. Moreover, the zero efficiency loss of $\hat{\beta}_S$ in meta-analysis is desirable for summary-level data sharing and assembling.
- (Comparable n and p) However, one should be aware that as n and p become more comparable, or even $n > p$, $\hat{\beta}_R(\lambda^*)$ (or $\hat{\beta}_B(\tau^*)$) may have substantially better performance than $\hat{\beta}_S$. As GWAS sample size increases dramatically in recent few years, efficient estimation of $\hat{\beta}_R(\lambda^*)$ (or $\hat{\beta}_B(\tau^*)$) can become more important for out-of-sample prediction in the near future. When $n < p$, one good alternative of marginal estimator is the optimal BLUP estimator $\hat{\beta}_B(\tau^*)$ from LMM; and when $n > p$, the optimal ridge estimator $\hat{\beta}_R(\lambda^*)$ is a good choice. Again, τ^* and λ^* have one-to-one correspondence and can both be directly estimated from the data without the need for cross-validation.

1.3 Related work and novelty

The present work is related to literature on the studies of high-dimensional linear model without sparsity assumption, most of which are on the asymptotic behavior of high-dimensional ridge estimator, including Dicker [2013, 2016], Dobriban and Wager [2018], El Karoui [2013, 2018], Hastie et al. [2019], Hsu et al. [2011] and Pluta et al. [2017]. For example, Dicker [2013, 2016] studies dense signal ridge problems with Gaussian assumption of data and allows general correlation structure Σ among predictors. Dobriban and Wager [2018] study ridge estimator without Gaussian assumption and recently extend their results to distributed computing problem [Dobriban and Sheng, 2019]. El Karoui [2013, 2018] studies ridge estimator in robust regression. Motivated by interpolation in machine learning, Hastie et al. [2019] analyze the ridge-less estimator by taking a limit on regularization parameter λ . In addition, our results for $\omega \in (0, 1)$ are related to studies of OLS estimator in moderate-dimensions [Guo and Cheng, 2018, Yang and Cheng, 2018].

Our analysis is also related to previous studies on high-dimensional LMM [Dicker and Erdogdu, 2017, Jiang et al., 2016, Ma and Dicker, 2019, Steinsaltz et al., 2018], in

which the authors mainly focus on the in-sample inference of LMM model parameters (such as h^2) and do not pay attention to BLUP and out-of-sample predictions. On the other hand, BLUP has been a popular method in genetics and agriculture for a long time [Robinson, 1991]. Thus, there are studies of BLUP in genetics community, sometimes named genomic BLUP (gBLUP), such as de los Campos et al. [2013], Daetwyler et al. [2010], Goddard [2009], Speed and Balding [2014], and some Bayesian or ridge alternatives, such as Zhou et al. [2013] and Li et al. [2014].

This study is motivated by the increasing applications of high-dimensional GWAS marginal estimator, especially in out-of-sample polygenic risk prediction. A few studies (such as Chatterjee et al. [2013], Daetwyler et al. [2008], Dudbridge [2013], and Zhao and Zou [2019]) have explored the prediction accuracy of GWAS summary statistics in the special case $\Sigma = I_p$. To the best of our knowledge, there is no study on the behavior of marginal estimator in dense high-dimensional settings with general Σ . In the present work, we build our analysis on random matrix theory (RMT) and allow an arbitrary correlation structure Σ among SNPs. Moreover, we link marginal estimator to ridge estimator and BLUP, and study them in an unifying framework. Driven by real data applications, we also generalize our results to cover cross-trait prediction and meta-analysis.

Different from most of previous studies on ridge-type estimators, we focus on R^2 instead of mean squared prediction error (MSE). R^2 is between zero and one and can be viewed as a normalized version of MSE. Different from MSE, R^2 is invariant to linear transformations of predictors, such as scaling and adding constants. This enables us to quantify and compare the performance of different estimators in a unified manner. More importantly, using R^2 allows us to generalize our analysis to study cross-trait prediction where the traits in training and testing data can be different. From a practical perspective, R^2 and pseudo R^2 are standard measures used in GWAS (and many other areas) to evaluate the out-of-sample prediction performance and in-sample goodness-of-fit. As shown in later sections, R^2 can yield very intuitive asymptotic results when comparing these estimators.

1.4 Outline and notation

This paper proceeds as follows. In Section 2, we introduce the detailed model setups and assumptions for cross-trait prediction. In Section 3, we provide the results for marginal estimator. Section 4 investigates the whole class of ridge-type estimators. Section 5 performs simulation studies and real data analysis to numerically verify our asymptotic results in finite samples. We discuss a few future topics in Section 6. Most of the special case results, MSE analysis, and technical lemmas and details are provided in supplementary file.

We make use of the following notations frequently. $\text{tr}(A)$ is the trace of matrix A , $\text{Diag}(A)$ is the diagonal of matrix A , A^{-} is the inverse of matrix A , A^T is the transpose of matrix A , and A^+ is the Moore-Penrose pseudoinverse of matrix A . \rightarrow denotes the convergence of a series of real numbers, \rightarrow_p represents the in probability convergence of a series of random variables, and $\rightarrow_{a.s.}$ is the almost surely convergence of a series of random variables. $\lambda_i(A)$ is the i th eigenvalue of matrix A , $I(\cdot)$ is the indicator function,

and $\|\mathbf{x}\|^2 = \mathbf{x}^T \mathbf{x} = \sum_{i=1}^p x_i^2$ is the squared l_2 norm of $p \times 1$ vector \mathbf{x} , and $\|\mathbf{x}\|_{\Sigma}^2 = \mathbf{x}^T \Sigma \mathbf{x}$ is the norm induced by Σ . In addition, $o(1)$ and $O(1)$ define the small o and big O , $o_p(1)$ and $O_p(1)$ define the small o and big O in probability, and c, C are some generic constant numbers.

2 Modeling framework

In this section, we introduce the modeling framework, including the genetic architecture, assumptions on SNP data and genetic effects.

2.1 Cross-trait prediction

Consider two independent GWAS that are conducted for two traits with the same p SNPs (features):

- (a). Training GWAS: (\mathbf{X}, \mathbf{y}) , with $\mathbf{X} = [\mathbf{X}_{(1)}, \mathbf{X}_{(2)}] \in \mathbb{R}^{n \times p}$, $\mathbf{X}_{(1)} \in \mathbb{R}^{n \times m_\beta}$, and $\mathbf{y} \in \mathbb{R}^{n \times 1}$.
- (b). Testing GWAS: $(\mathbf{Z}, \mathbf{y}_z)$, with $\mathbf{Z} = [\mathbf{Z}_{(1)}, \mathbf{Z}_{(2)}] \in \mathbb{R}^{n_z \times p}$, $\mathbf{Z}_{(1)} \in \mathbb{R}^{n_z \times m_\eta}$, and $\mathbf{y}_z \in \mathbb{R}^{n_z \times 1}$.

Here \mathbf{y} and \mathbf{y}_z are two continuous phenotypes measured in two independent groups of individuals with sample sizes n and n_z , respectively. The $\mathbf{X}_{(1)}$ is an $n \times m_\beta$ matrix of the SNP data with nonzero effects, and $\mathbf{X}_{(2)}$ is an $n \times (p - m_\beta)$ matrix of the null SNPs, resulting in an $n \times p$ matrix of all SNPs, donated by $\mathbf{X} = [\mathbf{X}_{(1)}, \mathbf{X}_{(2)}] = (\mathbf{x}_1, \dots, \mathbf{x}_{m_\beta}, \mathbf{x}_{m_\beta+1}, \dots, \mathbf{x}_p)$, where \mathbf{x}_i is an $n \times 1$ vector of the SNP i , $i = 1, \dots, p$. Similarly, $\mathbf{Z}_{(1)}$ denotes the causal SNPs of \mathbf{y}_z and $\mathbf{Z}_{(2)}$ donate the null SNPs. We allow \mathbf{y} and \mathbf{y}_z to be two different traits. That is, we consider a general cross-trait prediction problem, such as predicting cognitive ability by educational attainment [Lee et al., 2018] or neuroimaging traits [Zhao et al., 2019], and treat same-trait prediction as a special case. Thus, m_β and m_η can be different numbers and $\mathbf{X}_{(1)}$ and $\mathbf{Z}_{(1)}$ correspond to two different sets of causal SNPs in general. The linear polygenic models assume

$$\mathbf{y} = \mathbf{X}_{(1)} \boldsymbol{\beta}_{(1)} + \boldsymbol{\epsilon} \quad \text{and} \quad \mathbf{y}_z = \mathbf{Z}_{(1)} \boldsymbol{\eta}_{(1)} + \boldsymbol{\epsilon}_z, \quad (4)$$

where $\boldsymbol{\beta}_{(1)}^T = (\beta_1, \dots, \beta_{m_\beta})^T$ and $\boldsymbol{\eta}_{(1)}^T = (\eta_1, \dots, \eta_{m_\eta})^T$ are vectors of nonzero causal SNP effects, and $\boldsymbol{\epsilon}$ and $\boldsymbol{\epsilon}_z$ represent independent random error vectors. We let $\boldsymbol{\beta}^T = (\boldsymbol{\beta}_{(1)}^T, \boldsymbol{\beta}_{(2)}^T)$ and $\boldsymbol{\eta}^T = (\boldsymbol{\eta}_{(1)}^T, \boldsymbol{\eta}_{(2)}^T)$, in which elements in $\boldsymbol{\beta}_{(2)}^T = (\beta_{m_\beta+1}, \dots, \beta_p)^T$ and $\boldsymbol{\eta}_{(2)}^T = (\eta_{m_\eta+1}, \dots, \eta_p)^T$ are all zeros. We model $\boldsymbol{\beta}_{(1)}$ and $\boldsymbol{\eta}_{(1)}$ as random variables [Dobriban and Wager, 2018] and will introduce the detailed distribution assumptions in the following section. The overall genetic heritability of \mathbf{y} and \mathbf{y}_z are given by

$$h_\beta^2 = \frac{\text{Var}(\mathbf{X}\boldsymbol{\beta})}{\text{Var}(\mathbf{y})} = \frac{\boldsymbol{\beta}^T \mathbf{X}^T \mathbf{X} \boldsymbol{\beta}}{\boldsymbol{\beta}^T \mathbf{X}^T \mathbf{X} \boldsymbol{\beta} + \boldsymbol{\epsilon}^T \boldsymbol{\epsilon}} \quad \text{and} \quad h_\eta^2 = \frac{\text{Var}(\mathbf{Z}\boldsymbol{\eta})}{\text{Var}(\mathbf{y}_z)} = \frac{\boldsymbol{\eta}^T \mathbf{Z}^T \mathbf{Z} \boldsymbol{\eta}}{\boldsymbol{\eta}^T \mathbf{Z}^T \mathbf{Z} \boldsymbol{\eta} + \boldsymbol{\epsilon}_z^T \boldsymbol{\epsilon}_z}, \quad (5)$$

which measure the proportion of variation in phenotype that can be explained by additive genetic factors. We assume h_β^2 and $h_\eta^2 \in (0, 1]$.

2.2 Model assumptions and definitions

Since m_β and m_η can be different and the causal SNPs of different traits may partially overlap, we let $m_{\beta\eta} \leq \min(m_\beta, m_\eta)$ be the number of overlapping causal SNPs of \mathbf{y} and \mathbf{y}_z .

SNP data The assumptions on SNP data \mathbf{X} and \mathbf{Z} are summarized in Condition 1.

Condition 1. (a). SNP data satisfy $\mathbf{X} = \mathbf{X}_0 \boldsymbol{\Sigma}^{1/2}$, $\mathbf{Z} = \mathbf{Z}_0 \boldsymbol{\Sigma}^{1/2}$, and entries of \mathbf{X}_0 and \mathbf{Z}_0 are real-value i.i.d. random variables with mean zero, variance one and a finite 12th order moment. $\boldsymbol{\Sigma}$ is a $p \times p$ population level deterministic positive definite matrix with $0 < c \leq \lambda_{\min}(\boldsymbol{\Sigma}) \leq \lambda_{\max}(\boldsymbol{\Sigma}) \leq C$ for all n, p and some constants c, C , where $\lambda_{\min}(\boldsymbol{\Sigma})$ and $\lambda_{\max}(\boldsymbol{\Sigma})$ are the smallest and largest eigenvalues of $\boldsymbol{\Sigma}$, respectively. $\boldsymbol{\Sigma}^{1/2}$ is any nonnegative square root of $\boldsymbol{\Sigma}$. For simplicity, we assume $\Sigma_{ii} = 1$, $i = 1, \dots, p$, or equivalently, \mathbf{X} and \mathbf{Z} have been column-standardized. In summary, $\boldsymbol{\Sigma}$ is assumed to be a correlation matrix with uniformly bounded eigenvalues.

(b). As $\min(n, n_z, m_{\beta\eta}) \rightarrow \infty$, we assume

$$\begin{aligned} m_\beta/n &\rightarrow \gamma, \quad m_\eta/n_z \rightarrow \gamma_z, \quad \text{for } \gamma, \gamma_z \in (0, \infty); \\ p/n &\rightarrow \omega, \quad p/n_z \rightarrow \omega_z, \quad \text{for } \omega, \omega_z \in (0, \infty); \quad \text{and} \\ m_{\beta\eta}/\sqrt{m_\beta m_\eta} &\rightarrow \kappa_{\beta\eta}, \quad \text{for } \kappa_{\beta\eta} \in (0, 1]. \end{aligned}$$

(c). For the $p \times p$ population level correlation matrix $\boldsymbol{\Sigma}$, we define its empirical spectral distribution (ESD) as $F_p^\Sigma(x) = p^{-1} \cdot \sum_{i=1}^p \mathbf{I}(\lambda_i(\boldsymbol{\Sigma}) \leq x)$, $x \in \mathbb{R}$. As $p \rightarrow \infty$, let $\{\boldsymbol{\Sigma}_p\}_{p>1}$ be a sequence of matrices, we assume the sequence of corresponding ESDs $\{F_p^\Sigma(x)\}_{p>1}$ converges weakly to a limit probability distribution $H(x)$, $x \in \mathbb{R}$, named the limiting spectral distribution (LSD) of $\boldsymbol{\Sigma}$.

Conditions 1 (a). and 1 (c). are frequently used in high-dimensional data analysis [Dobriban and Wager, 2018, Hastie et al., 2019, Ledoit and P  ch  , 2011]. In modern GWAS, the number of the SNPs p in Condition 1 (b). is usually in millions [Tam et al., 2019], and the current training GWAS sample size n is often smaller or substantially smaller than p [Watanabe et al., 2019]. The genetics community has striven to increase the GWAS sample size in recent years, and for a few traits the sample size has been larger than one million (e.g., Lee et al. [2018]). With these great efforts, the ω is decreasing from a large number towards one for many traits.

Genetic effects and random errors Let $F(0, V)$ represent a generic distribution with mean zero, (co)variance V , and finite fourth order moments. We introduce the following condition on genetic effects $\boldsymbol{\beta}_{(1)}$ and $\boldsymbol{\eta}_{(1)}$ and random error vectors $\boldsymbol{\epsilon}$ and $\boldsymbol{\epsilon}_z$.

Condition 2. We assume the distributions of $\boldsymbol{\beta}$ and $\boldsymbol{\eta}$ are independent of $\boldsymbol{\Sigma}$. Moreover, nonzero elements β_i and η_j are independent random variables satisfying

$$\beta_i \sim F(0, \sigma_\beta^2/p), \quad i = 1, \dots, m_\beta; \quad \eta_j \sim F(0, \sigma_\eta^2/p), \quad j = 1, \dots, m_\eta.$$

The $m_{\beta\eta}$ overlapping nonzero effects (β_k, η_k) s of $(\mathbf{y}, \mathbf{y}_z)$ satisfy

$$\begin{pmatrix} \beta_k \\ \eta_k \end{pmatrix} \sim F \left[\begin{pmatrix} 0 \\ 0 \end{pmatrix}, p^{-1} \cdot \begin{pmatrix} \sigma_\beta^2 & \sigma_{\beta\eta} \\ \sigma_{\beta\eta} & \sigma_\eta^2 \end{pmatrix} \right],$$

where $\sigma_{\beta\eta} = \rho_{\beta\eta} \cdot \sigma_{\beta} \sigma_{\eta}$. And ϵ_i and ϵ_{z_j} are independent random variables satisfying

$$\epsilon_i \sim F(0, \sigma_\epsilon^2), \quad i = 1, \dots, n; \quad \epsilon_{z_j} \sim F(0, \sigma_{\epsilon_z}^2), \quad j = 1, \dots, n_z.$$

Genetic correlation and heritability Given the above assumptions, we define the genetic correlation between y and y_z as

$$\varphi_{\beta\eta} = \frac{\beta^T \Sigma \eta}{\|\beta\|_{\Sigma} \cdot \|\eta\|_{\Sigma}} \cdot \mathbf{I}(\|\beta\|_{\Sigma} \cdot \|\eta\|_{\Sigma} > 0),$$

and we assume $\varphi_{\beta\eta} \in [-1, 1]$. Following Conditions 1 and 2, as $\min(n, n_z, m_{\beta\eta}) \rightarrow \infty$, the genetic correlation between \mathbf{y} and \mathbf{y}_z is asymptotically given by

$$\varphi_{\beta\eta} = \frac{m_{\beta\eta}\sigma_{\beta\eta}\text{tr}(\Sigma)/p^2}{\{m_{\beta}\sigma_{\beta}^2\text{tr}(\Sigma)/p^2\}^{1/2}\{m_{\eta}\sigma_{\eta}^2\text{tr}(\Sigma)/p^2\}^{1/2}} = \kappa_{\beta\eta} \cdot \rho_{\beta\eta} + o_p(1).$$

Similarly, the heritability h_{β}^2 and h_{η}^2 defined in equation (5) can be asymptotically represented as

$$h_\beta^2 = \frac{\|\beta\|_\Sigma}{\|\beta\|_\Sigma + \sigma_\epsilon^2} = \frac{m_\beta \sigma_\beta^2 \text{tr}(\Sigma) / p^2}{m_\beta \sigma_\beta^2 \text{tr}(\Sigma) / p^2 + \sigma_\epsilon^2} \quad \text{and} \quad h_\eta^2 = \frac{\|\eta\|_\Sigma}{\|\eta\|_\Sigma + \sigma_{\epsilon_z}^2} = \frac{m_\eta \sigma_\eta^2 \text{tr}(\Sigma) / p^2}{m_\eta \sigma_\eta^2 \text{tr}(\Sigma) / p^2 + \sigma_{\epsilon_z}^2}.$$

With $\Sigma_{ii} = 1, i = 1, \dots, p$, we have $\text{tr}(\Sigma)/p = 1$, and thus we have the same definitions of h_{β}^2 and h_{η}^2 as those in Jiang et al. [2016] and Guo et al. [2019] for the special case $\Sigma = \mathbf{I}_p$.

Our theoretical analysis of large-scale GWAS below is based on classic random matrix theory (e.g., Bai and Silverstein [2010], Paul and Aue [2014], Yao et al. [2015]), and some recent advances of trace functionals (e.g., Dobriban and Wager [2018], Hastie et al. [2019], Ledoit and P  ch   [2011], Wang et al. [2015]). We introduce some useful RMT results and our lemmas in Section 7.1 of supplementary file.

3 Marginal estimator

Let $\hat{\beta}$ be a generic $p \times 1$ estimator of β , the out-of-sample predictor and in-sample estimation are given by $\hat{S}_Z = Z\hat{\beta}$ and $\hat{S}_X = X\hat{\beta}$, respectively. The out-of-sample and in-sample R^2 are respectively defined as A^2 and E^2 , where

$$A = \frac{\mathbf{y}_z^T \hat{\mathbf{S}}_Z}{\|\mathbf{y}_z\| \cdot \|\hat{\mathbf{S}}_Z\|} \quad \text{and} \quad E = \frac{\mathbf{y}^T \hat{\mathbf{S}}_X}{\|\mathbf{y}\| \cdot \|\hat{\mathbf{S}}_X\|}. \quad (6)$$

In this section, we present the results of A^2 and E^2 for marginal estimator $\hat{\beta}_S$, donated as A_S^2 and E_S^2 , respectively.

3.1 Asymptotic limits

The asymptotic limits of A_S^2 and E_S^2 are given in the following theorem.

Theorem 1. Under polygenic model (4) and Conditions 1 and 2, as $\min(n, n_z, m_{\beta\eta}, p) \rightarrow \infty$, for any $\omega \in (0, \infty)$, $h_\beta^2, h_\eta^2 \in (0, 1]$, $\varphi_{\beta\eta} \in [-1, 1]$, and Σ , we have

$$\begin{aligned} A_S^2 &= h_\eta^2 \varphi_{\beta\eta}^2 \cdot \frac{n \{ \text{tr}(\hat{\Sigma}_X \hat{\Sigma}_Z) \}^2 \cdot h_\beta^2}{n \text{tr}(\hat{\Sigma}_Z) \text{tr}(\hat{\Sigma}_X \hat{\Sigma}_Z \hat{\Sigma}_X) \cdot h_\beta^2 + \text{tr}(\hat{\Sigma}_Z) \text{tr}(\hat{\Sigma}_X) \text{tr}(\hat{\Sigma}_Z \hat{\Sigma}_X) \cdot (1 - h_\beta^2)} + o_p(1) \\ &= h_\eta^2 \varphi_{\beta\eta}^2 \cdot \left\{ \frac{b_3(\Sigma)}{b_2(\Sigma)^2} + \frac{\omega}{b_2(\Sigma)} \cdot \frac{1}{h_\beta^2} \right\}^{-1} + o_p(1), \end{aligned}$$

and

$$\begin{aligned} E_S^2 &= \frac{\{ n \text{tr}(\hat{\Sigma}_X^2) \cdot h_\beta^2 + \text{tr}(\hat{\Sigma}_X)^2 \cdot (1 - h_\beta^2) \}^2}{n^2 \text{tr}(\hat{\Sigma}_X) \text{tr}(\hat{\Sigma}_X^3) \cdot h_\beta^2 + n \text{tr}(\hat{\Sigma}_X)^2 \text{tr}(\hat{\Sigma}_X^2) \cdot (1 - h_\beta^2)} + o_p(1) \\ &= \frac{\{ b_2(\Sigma) \cdot h_\beta^2 + \omega \}^2}{\{ b_2(\Sigma) \cdot h_\beta^2 + \omega \}^2 + b_2(\Sigma) \omega + \{ b_3(\Sigma) - b_2(\Sigma)^2 \cdot h_\beta^2 \} \cdot h_\beta^2} + o_p(1). \end{aligned}$$

For $\Sigma = I_p$, we have $b_k(\Sigma) = 1$ for any positive integral k , it follows that

$$A_S^2 = h_\eta^2 \varphi_{\beta\eta}^2 \cdot \frac{h_\beta^2}{h_\beta^2 + \omega} + o_p(1) \quad \text{and} \quad E_S^2 = \frac{(h_\beta^2 + \omega)^2}{(h_\beta^2 + \omega)^2 + \omega + h_\beta^2(1 - h_\beta^2)} + o_p(1). \quad (7)$$

Here $h_\eta^2 \varphi_{\beta\eta}^2$ represents the signal strength, which is the ultimate upper bound for out-of-sample prediction. Equation (7) indicates that A_S^2 is linearly decayed by the nonzero ω when $\Sigma = I_p$. It is also easy to see that A_S^2 and E_S^2 are the same if $\omega = 0$ and $\varphi_{\beta\eta} = 1$, but are quite different given nonzero ω . This represents the difference between low and high-dimensions. Next remark further illustrates that Σ has bidirectional effects on A_S^2 when $\omega > 0$.

Remark 1. (Bidirectional influences of feature-wise correlation) For general correlation $\Sigma \neq I_p$, A_S^2 depends on the first three moments of the LSD $H(t)$ of Σ through the two terms $b_2(\Sigma)^2/b_3(\Sigma)$ and $\omega/b_2(\Sigma)$. Note that for general $\Sigma \neq I_p$, $b_3(\Sigma) > b_2(\Sigma)^2$ and $b_2(\Sigma) > 1$ by Cauchy-Schwarz inequality. In classic linear model theory where p is fixed, or $\omega = 0$, we have $A_S^2 = h_\eta^2 \varphi_{\beta\eta}^2 \cdot b_2(\Sigma)^2/b_3(\Sigma)$. Thus, A_S^2 is reduced by a factor $b_2(\Sigma)^2/b_3(\Sigma)$ due to the unadjusted feature-wise correlation. On the other hand, when $\omega > 0$, further decay of A_S^2 is introduced by the nonzero term $\omega/b_2(\Sigma)$. Thanks to the fact that $b_2(\Sigma) > 1$, correlation among features can delay such decay. This makes sense, because correlation among p features can be viewed as a reduction of signal dispersion in high-dimensions. Together, there is a transition point for whether or not feature-wise correlation can help achieve higher prediction accuracy in high-dimensions. Formally,

we can define the *prediction relative efficiency* (PRE) for $\Sigma \neq I_p$ to quantify the bidirectional effects of Σ on A_S^2 and identify the transition point. Let $\delta_S(\Sigma) = A_S^2(\Sigma) / A_S^2(I_p)$, we have

$$\delta_S(\Sigma) = \frac{h_\beta^2 + \omega}{h_\beta^2 \cdot \frac{b_3(\Sigma)}{b_2(\Sigma)^2} + \omega \cdot \frac{1}{b_2(\Sigma)}} + o_p(1),$$

and it follows that

$$\delta_S(\Sigma) \begin{matrix} > \\ < \end{matrix} 1 + o_p(1) \quad \text{if} \quad \omega \begin{matrix} > \\ < \end{matrix} h_\beta^2 \cdot \frac{b_3(\Sigma) - b_2(\Sigma)^2}{b_2(\Sigma)^2 - b_2(\Sigma)}.$$

Remark 2. (In-sample v.s. out-of-sample) For the optimal case where $h_\beta^2 = h_\eta^2 = \varphi_{\beta\eta}^2 = 1$, i.e., predicting fully heritable traits with absolute genetic correlation one, we have

$$A_S^2 = \frac{\{\text{tr}(\hat{\Sigma}_X \hat{\Sigma}_Z)\}^2}{\text{tr}(\hat{\Sigma}_Z) \text{tr}(\hat{\Sigma}_X \hat{\Sigma}_X^2)} + o_p(1) \quad \text{and} \quad E_S^2 = \frac{\{\text{tr}(\hat{\Sigma}_X^2)\}^2}{\text{tr}(\hat{\Sigma}_X) \text{tr}(\hat{\Sigma}_X^3)} + o_p(1).$$

This optimal case reveals more insights into the difference between in-sample and out-of-sample R^2 , and the difference between low- and high-dimensions. We note that $\text{tr}(\hat{\Sigma}_X) = \text{tr}(\hat{\Sigma}_Z) = \text{tr}(\Sigma)$, and $\text{tr}(\hat{\Sigma}_X \hat{\Sigma}_Z) = \text{tr}(\Sigma^2)$. That is, trace of sample covariance is always the same as the trace of population covariance, and similar result holds for the product of two independent sample covariances. However, by Lemma 3 in Section 7.1 of supplementary file, such concordance no longer holds for the trace of higher order products in high-dimensions with nonzero ω . Specifically, we have $\text{tr}(\hat{\Sigma}_X^2) = \text{tr}(\Sigma^2) + \omega \text{tr}(\Sigma)^2$, $\text{tr}(\hat{\Sigma}_X^3) = \text{tr}(\Sigma^3) + 3\omega \text{tr}(\Sigma) \text{tr}(\Sigma^2) + \omega^2 \text{tr}(\Sigma)^3$, and $\text{tr}(\hat{\Sigma}_Z \hat{\Sigma}_X^2) = \text{tr}(\Sigma \hat{\Sigma}_X^2) = \text{tr}(\Sigma^3) + n^{-1} \text{tr}(\Sigma) \text{tr}(\Sigma^2)$. Therefore, we have

$$A_S^2 = \frac{\{\text{tr}(\Sigma^2)\}^2}{\text{tr}(\Sigma) \cdot \{\text{tr}(\Sigma^3) + n^{-1} \text{tr}(\Sigma) \text{tr}(\Sigma^2) + o_p(1)\}} + o_p(1)$$

and

$$E_S^2 = \frac{\{\text{tr}(\Sigma^2) + \omega \text{tr}(\Sigma)^2\}^2}{\text{tr}(\Sigma) \cdot \{\text{tr}(\Sigma^3) + 3\omega \text{tr}(\Sigma) \text{tr}(\Sigma^2) + \omega^2 \text{tr}(\Sigma)^3\}} + o_p(1).$$

It is clear that in-sample and out-of-sample R^2 are completely different and both can be much less than one given nonzero ω .

In summary, the asymptotic performance of marginal estimator is solely determined by heritability, genetic correlation, ω , and the first three moments of $H(t)$. These parameters are independent from the unknown number m . Such properties enable us to easily evaluate the prediction accuracy of given SNP dataset. In addition, the PRE measures the influence of Σ on A_S^2 , which can also be used to compare the prediction accuracy among different structures of feature-wise correlation. In next section, we illustrate how to apply the Theorem 1 to estimate A_S^2 in GWAS applications.

3.2 Prediction accuracy estimation and comparison

In GWAS, different global populations (e.g., African, Latino, East Asian) have different SNP correlation structure Σ , and Σ is known to be largely consistent within each population [Gurdasani et al., 2019]. Thus, given the same ω and $h_\eta^2, h_\beta^2, \varphi_{\beta\eta}^2$, the prediction accuracy of GWAS data varies across different populations. To evaluate and compare the prediction accuracy of GWAS data in diverse populations, we need to study the LSD $H(x)$ of Σ . Here we discuss two approaches to evaluate the prediction accuracy A_S^2 for each global population.

Asymptotic estimator (External reference panel) The asymptotic estimator is based on the asymptotic limits. It is clear that we only need to estimate the first three moments $b_1(\Sigma)$, $b_2(\Sigma)$, $b_3(\Sigma)$ of $H(t)$, which have known relationships with $b_1(\hat{\Sigma})$, $b_2(\hat{\Sigma})$, $b_3(\hat{\Sigma})$ according to Lemma 3. Therefore, we can estimate $b_k(\hat{\Sigma})$ from SNP data then obtain $b_k(\Sigma)$, for $k = 1, 2, 3$. In practice, this can be done using external data in publicly available LD reference panels [Tam et al., 2019], such as the 1000 Genomes Project [1000-Genomes-Project-Consortium., 2015]. Let the reference data be $W \in R^{n_w \times p}$, and let $\hat{\Sigma}_W = n_w^{-1} W^T W$, then $b_k(\hat{\Sigma}_W) = p^{-1} \text{tr}(\hat{\Sigma}_W^k) = p^{-1} \sum_{i=1}^p \lambda_i(\hat{\Sigma}_W)^k$, $k = 1, 2, 3$. Thus, all we need are the eigenvalues of $\hat{\Sigma}_W$, $\lambda_i(\hat{\Sigma}_W)$, $i = 1, \dots, p$. When $n_w < p$, we may instead focus on the $n \times n$ companion matrix $\hat{\Phi}_W = n_w^{-1} W W^T$ to obtain these moments.

Empirical estimator (Individual-level data) When SNP data X and Z are available, one can also directly estimate the prediction accuracy by evaluating the four traces $\text{tr}(\hat{\Sigma}_X)$, $\text{tr}(\hat{\Sigma}_Z)$, $\text{tr}(\hat{\Sigma}_X \hat{\Sigma}_Z)$, and $\text{tr}(\hat{\Sigma}_X^2 \hat{\Sigma}_Z)$. Since $\text{tr}(\hat{\Sigma}_X) = \text{tr}(\hat{\Sigma}_Z) = p$, we only need to estimate $\text{tr}(\hat{\Sigma}_X \hat{\Sigma}_Z)$ and $\text{tr}(\hat{\Sigma}_X^2 \hat{\Sigma}_Z)$. Estimating $\hat{\Sigma}_X$ and $\hat{\Sigma}_Z$ can be computationally expensive when both n and p are large. However, some tools have been developed to tackle this challenge [Das et al., 2016, Quick et al., 2018]. Moreover, we may need to additionally account for the population stratification when population substructures exist [Sun and Lin, 2017]. One common solution is to remove the top few “outlier” eigenvalues, which often represent population substructures if any, since the population substructures are usually much stronger than the local SNP correlations.

To estimate the prediction accuracy for a specific pair of traits y and y_z , we also need to estimate h_β^2 , h_η^2 and $\varphi_{\beta\eta}$. Various estimators of these parameters have been proposed in GWAS context, we provide a brief review and discussion of these estimators in Section 7.2 of supplementary file. Next, we discuss two more potential usages of the prediction accuracy results.

Diverse populations Based on these estimators, one can compare the prediction accuracy among diverse populations using their PREs. For example, suppose population 1 has Σ_1 and population 2 has Σ_2 , then their relative prediction accuracy can be written by the ratio of their PREs

$$\frac{\delta_S(\Sigma_1)}{\delta_S(\Sigma_2)} = \frac{h_\beta^2 \cdot \frac{b_3(\Sigma_2)}{b_2(\Sigma_2)^2} + \omega \cdot \frac{1}{b_2(\Sigma_2)}}{h_\beta^2 \cdot \frac{b_3(\Sigma_1)}{b_2(\Sigma_1)^2} + \omega \cdot \frac{1}{b_2(\Sigma_1)}} + o_p(1).$$

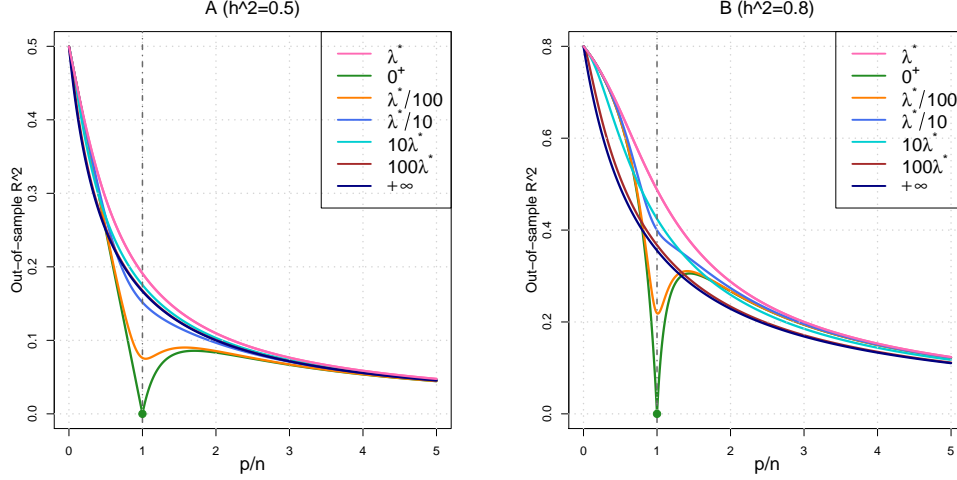


Fig. 1: Out-of-sample R -squared $A_R^2(\lambda)$ of ridge-type estimators given different λ and heritability when $\Sigma = \mathbf{I}_p$. λ^* is the optimal λ value, 0^+ corresponds to the case $\lambda \rightarrow 0^+$, and $+\infty$ represents $\lambda \rightarrow +\infty$. We set $\varphi_{\beta\eta} = 1$, $h_\beta^2 = h_\eta^2 = (0.5, 0.8)$ in A and B, respectively.

It is clear that when ω is much larger than h_β^2 and $b_3(\Sigma)$ is comparable to $b_2(\Sigma)^2$, $b_2(\Sigma)$ plays an important role in the relative prediction accuracy.

LD-based pruning In practice, it is quite common to first perform LD-based pruning with predefined threshold to remove highly related SNPs (e.g., remove one of a pair of SNPs that have correlation larger than the threshold) before out-of-sample prediction. The choice of the predefined threshold is often arbitrary. Using Theorem 1, it is possible to input a series of thresholds, estimate the corresponding prediction accuracies, and then make a decision about the “optimal” threshold for SNP pruning.

3.3 Meta-analysis of marginal estimator

Suppose there are k independent GWAS $(\mathbf{X}_i, \mathbf{y}_i)$, $i = 1, \dots, k$, on the same trait with genetic effects β , we have the following results when aggregating the summary statistics $\hat{\beta}_1, \dots, \hat{\beta}_k$ from the k studies.

Theorem 2. Under polygenic model (4) and Conditions 1 and 2, suppose we have independent GWAS $(\mathbf{X}_i, \mathbf{y}_i)$, with sample sizes (n_1, \dots, n_k) and p SNPs, $i = 1, \dots, k$, $k \in (0, \infty)$, let $\hat{\mathbf{B}} = (\hat{\beta}_1^T, \dots, \hat{\beta}_k^T)$ be the $p \times k$ matrix of marginal estimators from the k GWAS. Let $\mathbf{d} = (d_1, \dots, d_k)^T$ be an $k \times 1$ vector of weights, and let $\hat{\mathbf{B}}(\mathbf{d}) = \hat{\mathbf{B}}\mathbf{d}$ be the aggregated summary statistics. As $\min(n_1, \dots, n_k, n_z, m_{\beta\eta}, p) \rightarrow \infty$, for any $\omega \in (0, \infty)$, $h_\beta^2, h_\eta^2 \in (0, 1]$, $\varphi_{\beta\eta} \in [-1, 1]$, \mathbf{d} , and Σ , we have

$$A_S^2(\mathbf{d}) = h_\eta^2 \varphi_{\beta\eta}^2 \cdot \left\{ \frac{b_3(\Sigma)}{b_2(\Sigma)^2} + \frac{\sum_{i=1}^k d_i^2 / n_i}{(\sum_{i=1}^k d_i)^2} \cdot \frac{p}{b_2(\Sigma) h_\beta^2} \right\}^{-1} + o_p(1).$$

For $\mathbf{d} \equiv \mathbf{d}^* = (n_i, \dots, n_k)^T$, we have

$$A_S^2(\mathbf{d}^*) = h_\eta^2 \varphi_{\beta\eta}^2 \cdot \left\{ \frac{b_3(\boldsymbol{\Sigma})}{b_2(\boldsymbol{\Sigma})^2} + \frac{\tilde{\omega}_k}{h_\beta^2} \cdot \frac{1}{b_2(\boldsymbol{\Sigma})} \right\}^{-1} + o_p(1),$$

where $\tilde{\omega}_k = p / \sum_{i=1}^k n_i$. $A_S^2(\mathbf{d}^*)$ is the same as the out-of-sample R^2 for one single GWAS with sample size $\sum_{i=1}^k n_i$. Particularly, when $\boldsymbol{\Sigma} = \mathbf{I}_p$, we have

$$A_S^2(\mathbf{d}^*) = h_\eta^2 \varphi_{\beta\eta}^2 \cdot \frac{h_\beta^2}{h_\beta^2 + \tilde{\omega}_k} + o_p(1).$$

Theorem 2 shows that marginal screening has no prediction accuracy loss in distributed computation followed by meta-analysis with weights \mathbf{d}^* . Thus, aggregating summary statistics from independent training GWAS has the same asymptotic prediction accuracy as one big GWAS that trains all the individual-level data together. This is a favorable property of high-dimensional marginal estimator. It is known that both OLS [Dobriban and Sheng, 2018] and ridge [Dobriban and Sheng, 2019] estimators may have prediction accuracy loss in high-dimensional distributed computation. Similar results also hold for in-sample R^2 . For example, when $\mathbf{d} = \mathbf{d}^*$, we have

$$E_S^2(\mathbf{d}^*) = \frac{\{b_2(\boldsymbol{\Sigma}) \cdot h_\beta^2 + \tilde{\omega}_k\}^2}{\{b_2(\boldsymbol{\Sigma}) \cdot h_\beta^2 + \tilde{\omega}_k\}^2 + b_2(\boldsymbol{\Sigma})\tilde{\omega}_k + \{b_3(\boldsymbol{\Sigma}) - b_2(\boldsymbol{\Sigma})^2 \cdot h_\beta^2\} \cdot h_\beta^2} + o_p(1).$$

And for $\boldsymbol{\Sigma} = \mathbf{I}_p$, we further have

$$E_S^2(\mathbf{d}^*) = \frac{(h_\beta^2 + \tilde{\omega}_k)^2}{(h_\beta^2 + \tilde{\omega}_k)^2 + \tilde{\omega}_k + h_\beta^2(1 - h_\beta^2)} \cdot \{1 + o_p(1)\}.$$

4 The class of ridge-type estimators

In this section, we present the results for the following ridge-type conditional estimators: $\{\hat{\beta}_R(\lambda), \hat{\beta}_B(\tau), \hat{\beta}_R(0^+), \hat{\beta}_B(0^+), \hat{\beta}_O\}$. We define their out-of-sample R^2 as $\{A_R^2(\lambda), A_B^2(\tau), A_R^2(0^+), A_B^2(0^+), A_O^2\}$, and in-sample R^2 as $\{E_R^2(\lambda), E_B^2(\tau), E_R^2(0^+), E_B^2(0^+), E_O^2\}$.

4.1 Out-of-sample R -squared

We have the following results on $\{A_R^2(\lambda), A_B^2(\tau), A_R^2(0^+), A_B^2(0^+), A_O^2\}$.

Theorem 3. Under polygenic model (4) and Conditions 1 and 2, as $\min(n, n_z, m_{\beta\eta}, p) \rightarrow \infty$, for any $\omega \in (0, \infty)$, $h_\beta^2, h_\eta^2 \in (0, 1]$, $\varphi_{\beta\eta} \in [-1, 1]$, and $\boldsymbol{\Sigma}$, we have

$$\begin{aligned} A_R^2(\lambda) &= A_B^2(\lambda/\omega) \\ &= h_\eta^2 \varphi_{\beta\eta}^2 \cdot \frac{\left[1 + \frac{\lambda}{\omega} \left\{1 - \frac{1}{\lambda v(-\lambda)}\right\}\right]^2 \cdot h_\beta^2}{\left[1 + \frac{\lambda}{\omega} \left\{2 - \frac{1}{\lambda v(-\lambda)} - \frac{v'(-\lambda)}{v(-\lambda)^2}\right\}\right] \cdot h_\beta^2 + \left\{\frac{v'(-\lambda)}{v(-\lambda)^2} - 1\right\} \cdot (1 - h_\beta^2)} + o_p(1), \end{aligned}$$

and

$$A_R^2(0^+) = A_B^2(0^+) = h_\eta^2 \varphi_{\beta\eta}^2 \cdot \frac{\left\{1 - \frac{1}{v(0^+)\omega}\right\}^2 \cdot h_\beta^2}{\left\{1 - \frac{1}{v(0^+)\omega}\right\} \cdot h_\beta^2 + \left\{\frac{v'(0^+)}{v(0^+)^2} - 1\right\} \cdot (1 - h_\beta^2)} + o_p(1),$$

where $v(0^+) = \lim_{\lambda \rightarrow 0^+} v(-\lambda)$ and $v'(0^+) = \lim_{\lambda \rightarrow 0^+} v'(-\lambda)$. $A_R^2(0^+)$ reduces to A_O^2 if $\omega < 1$, which is given by

$$A_O^2 = h_\eta^2 \varphi_{\beta\eta}^2 \cdot \left\{1 + \frac{1 - h_\beta^2}{h_\beta^2} \cdot \frac{\omega}{1 - \omega}\right\}^{-1} + o_p(1).$$

If $h_\beta^2 \in (0, 1)$, $A_R^2(\lambda)$ is maximized at $\lambda = \lambda^* \equiv \omega \cdot (1 - h_\beta^2)/h_\beta^2$, and the optimal out-of-sample R^2 is given by

$$A_R^2(\lambda^*) = A_B^2(\lambda^*/\omega) = h_\eta^2 \varphi_{\beta\eta}^2 \cdot \left\{\frac{1}{h_\beta^2} - \frac{1}{v(-\lambda^*)\omega}\right\} + o_p(1).$$

If $h_\beta^2 = 1$, i.e., \mathbf{y} is a fully heritable trait, the optimal out-of-sample R^2 is obtained as $\lambda \rightarrow 0^+$, and we have

$$A_R^2(0^+) = A_B^2(0^+) = \begin{cases} h_\eta^2 \varphi_{\beta\eta}^2 + o_p(1), & \text{if } \omega < 1; \\ h_\eta^2 \varphi_{\beta\eta}^2 \cdot \left\{1 - \frac{1}{v(0^+)\omega}\right\} + o_p(1), & \text{if } \omega > 1. \end{cases}$$

Theorem 3 shows that A_O^2 is invariant to Σ and always has closed-form expression. For other estimators, due to the linear shrinkage induced by nonzero λ , Σ still has influence on A^2 through the limits of Stieltjes transform $v(-\lambda)$ and its first order derivative $v'(-\lambda)$. When $\lambda = \lambda^*$, $v'(-\lambda)$ cancels out and thus the optimal out-of-sample R^2 depends on Σ only through $v(-\lambda)$. Let $\text{STN}(h_\beta^2) = h_\beta^2/(1 - h_\beta^2)$ be the signal to noise ratio, λ^* can be rewritten as

$$\lambda^* = \omega / \text{STN}(h_\beta^2).$$

Thus, in linear shrinkage estimator $\hat{\Sigma}_X + \lambda \mathbf{I}_p$, the optimal weight for \mathbf{I}_p is proportional to ω and inversely proportional to the signal to noise ratio, matching previous results on MSE [Dobriban and Wager, 2018].

When $\Sigma = \mathbf{I}_p$, the closed-form expressions for $v(-\lambda)$ and $v'(-\lambda)$ are available, and thus we have closed-form expressions for $\{A_R^2(\lambda), A_B^2(\tau), A_R^2(0^+), A_B^2(0^+), A_O^2\}$, which are given in the following corollary.

Corollary 1. Under the same conditions as in Theorem 3, when $\Sigma = \mathbf{I}_p$, we have

$$A_R^2(\lambda) = A_B^2(\lambda/\omega) = h_\eta^2 \varphi_{\beta\eta}^2 \cdot \frac{\left\{1 - \lambda g(-\lambda)\right\}^2 \cdot h_\beta^2}{\left\{1 - 2\lambda g(-\lambda) + \lambda^2 g'(-\lambda)\right\} \cdot h_\beta^2 + \left\{\omega g(-\lambda) - \omega \lambda g'(-\lambda)\right\} \cdot (1 - h_\beta^2)} + o_p(1),$$

where closed-form expressions of $g(\cdot)$ and $g'(\cdot)$ can be found in equations (8) and (9). In

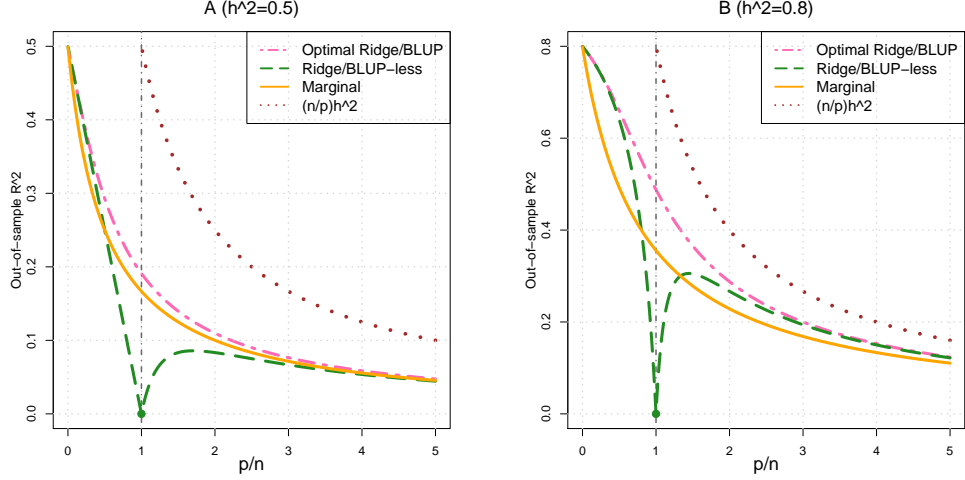


Fig. 2: Out-of-sample R -squared of optimal ridge/BLUP estimators ($A_R^2(\lambda^*) = A_B^2(\lambda^*/\omega)$), ridge/BLUP-less estimators ($A_R^2(0^+) = A_B^2(0^+)$), and marginal estimator (A_S^2) when $\Sigma = I_p$. We set $\varphi_{\beta\eta} = 1$, $h_\beta^2 = h_\eta^2 = (0.5, 0.8)$ in A and B, respectively. The dash line represents the upper limit $(n/p) \cdot h_\beta^2$.

addition,

$$\begin{aligned}
 A_R^2(0^+) &= A_B^2(0^+) = h_\eta^2 \varphi_{\beta\eta}^2 \cdot \frac{\left\{ \frac{1+\omega-|\omega-1|}{2\omega} \right\}^2 \cdot h_\beta^2}{\frac{1+\omega-|\omega-1|}{2\omega} \cdot h_\beta^2 + \frac{\omega+1-|\omega-1|}{2|\omega-1|} \cdot (1-h_\beta^2)} + o_p(1) \\
 &= \begin{cases} h_\eta^2 \varphi_{\beta\eta}^2 \cdot \frac{h_\beta^2}{h_\beta^2 + \frac{\omega}{1-\omega} \cdot (1-h_\beta^2)} + o_p(1), & \text{if } \omega < 1; \\ h_\eta^2 \varphi_{\beta\eta}^2 \cdot \frac{h_\beta^2}{h_\beta^2 \cdot \omega + \frac{\omega^2}{\omega-1} \cdot (1-h_\beta^2)} + o_p(1), & \text{if } \omega > 1. \end{cases}
 \end{aligned}$$

If $h_\beta^2 \in (0, 1)$, $A_R^2(\lambda)$ is maximized at λ^* , and the optimal out-of-sample R^2 is given by

$$\begin{aligned}
 A_R^2(\lambda^*) &= A_B^2(\lambda^*/\omega) = h_\eta^2 \varphi_{\beta\eta}^2 \cdot \{1 - \lambda^* g(-\lambda^*)\} + o_p(1) \\
 &= h_\eta^2 \varphi_{\beta\eta}^2 \cdot \frac{\omega + h_\beta^2 - \sqrt{(\omega - h_\beta^2)^2 + 4\omega h_\beta^2(1 - h_\beta^2)}}{2\omega h_\beta^2} + o_p(1).
 \end{aligned}$$

If $h_\beta^2 = 1$, the optimal $A_R^2(\lambda)$ is obtained as $\lambda \rightarrow 0^+$, and we have

$$A_R^2(0^+) = A_B^2(0^+) = h_\eta^2 \varphi_{\beta\eta}^2 \cdot \frac{\omega + 1 - |\omega - 1|}{2\omega} + o_p(1) = \begin{cases} h_\eta^2 \varphi_{\beta\eta}^2 + o_p(1), & \text{if } \omega < 1; \\ h_\eta^2 \varphi_{\beta\eta}^2 \cdot \frac{1}{\omega} + o_p(1), & \text{if } \omega > 1. \end{cases}$$

In Corollaries S1 and S2 of supplementary file, we quantify the relative prediction accuracy between marginal estimator and the optimal ridge estimator in closed-form expressions for the special case $\Sigma = I_p$. The following remarks provide more insights into high-dimensional dense signal prediction.

Remark 3. (Optimal regularizer and prediction accuracy) The optimal values λ^* and τ^* for out-of-sample R^2 (when $h_\beta^2 \in (0, 1)$) are functions of h_β^2 and ω , and are independent of all other parameters including Σ . Since ω is known and consistent estimator of h_β^2 is available, in practice cross-validation techniques are not required to obtain optimal regularizers for ridge estimator or BLUP. Moreover, $A_R^2(\lambda^*)$ can be estimated by additionally calculating $s_{F_n}(\lambda^*)$, which is a consistent estimator of $v(-\lambda^*, \Sigma)$. To quantify the influence of Σ on $A_R^2(\lambda^*)$, we can define the PRE for $\Sigma \neq I_p$ as $\delta_R(\lambda^*, \Sigma) = A_R^2(\lambda^*, \Sigma) / A_R^2(\lambda^*, I_p)$, and then

$$\delta_R(\lambda^*, \Sigma) = \frac{\omega + h_\beta^2 - \sqrt{(\omega - h_\beta^2)^2 + 4\omega h_\beta^2(1 - h_\beta^2)}}{2\omega - 2h_\beta^2/v(-\lambda^*, \Sigma)} + o_p(1).$$

Remark 4. (Over-and-under fitting) Figure 1 and Supplementary Figure 1 display $A_R^2(\lambda)$ across different λ , ω , and h^2 . It is clear that $A_R^2(\lambda)$ is near-optimal for any λ when ω is big (e.g., $\omega > 5$), especially when h^2 is not high. In contrast, when $\omega \approx 1$, model over-fitting with small λ should be avoided and model under-fitting with large λ can be substantially suboptimal. Notably, $A_R^2(0^+)$ can become surprisingly small. For $\omega > 1$, $A_R^2(0^+)$ is not a monotone function of ω , and the optimal value is achieved at $\omega = 1 + \sqrt{1 - h_\beta^2}$. When ω decreases from $1 + \sqrt{1 - h_\beta^2}$ towards 1, $A_R^2(0^+)$ reduces dramatically.

Remark 5. (Blessing of dimensionality) When ω is large, $A_R^2(\lambda)$ has almost identical performance for all λ . Particularly, the out-of-sample R^2 of $\hat{\beta}_S$ is similar to that of $\hat{\beta}_R(\lambda^*)$, then $\hat{\beta}_S$ can be a good choice for out-of-sample applications because it is much more computationally efficient than $\hat{\beta}_R(\lambda^*)$. High dimensionality indeed reduces the required computational burden to obtain good prediction performance, which is quite counterintuitive.

Remark 6. (Curse of dimensionality) On the other hand, the upper limit of the prediction accuracy of all ridge-type estimators might be not satisfactory when ω is large. For example, when $\Sigma = I_p$, consider the optimal case where $h_\eta^2 = h_\beta^2 = \varphi_{\beta\eta}^2 = 1$, the asymptotic optimal out-of-sample R^2 of ridge-type estimators is one for $n > p$. However, when $n < p$, the out-of-sample R^2 has an upper bound of $n/p = 1/\omega$, which can be viewed as the ratio of sample size and model complexity. These results reveal the fundamental challenge in high-dimensional dense signal prediction. In addition, $1/\omega$ can hardly be achieved in practical situations if any. To see this, consider $h_\eta^2 = h_\beta^2 \in (0, 1)$ and $\varphi_{\beta\eta}^2 = 1$, we can rewrite the optimal out-of-sample R^2 as

$$A_R^2(\lambda^*) = A_B^2(\lambda^*/\omega) = \frac{p + nh_\beta^2 - |p - nh_\beta^2| \cdot \sqrt{1 + \Delta}}{2p} + o_p(1),$$

where $\Delta = 4h_\beta^2(1 - h_\beta^2)/(\omega^{1/2} - \omega^{-1/2}h_\beta^2)^2 > 0$. Note that $\Delta \approx 0$ only for large ω and $h_\beta^2 \approx 1$. Then $A_R^2(\lambda^*)$ is close to the upper bound $n/p \cdot h_\beta^2$ only when ω is large for highly heritable traits prediction (Figure 2 and Supplementary Figure 2). For general Σ , similar to the case of marginal estimator, feature-wise correlation can delay the negative influences of growing dimensionality, but the general pattern remains the same.

Remark 7. [Unboundedness of $\text{tr}\{(\mathbf{X}^T \mathbf{X})^{-1}\}$] $\hat{\beta}_R(\lambda^*)$ has better out-of-sample R^2 than $\hat{\beta}_O$ for $\omega \in (0, 1)$. As shown in Figure 2, when ω is close to zero, $\hat{\beta}_R(\lambda^*)$ and $\hat{\beta}_O$ are close to each other, which matches the classic results in linear models. However, as ω moves towards one, the performance of $\hat{\beta}_O$ is much worse than $\hat{\beta}_R(\lambda^*)$. One way to explain this surprising behavior of $\hat{\beta}_O$ is that $\text{tr}\{(\mathbf{X}^T \mathbf{X})^{-1}\}$ can become very large when $\omega \rightarrow 1^-$. To see this, when $\omega < 1$, note that

$$A_O^2 = A_R^2(0) = h_\eta^2 \varphi_{\beta\eta}^2 \cdot \frac{h_\beta^2}{h_\beta^2 + \text{tr}\{(\mathbf{X}^T \mathbf{X})^{-1}\} \cdot (1 - h_\beta^2)} + o_p(1).$$

In Gaussian case, $(\mathbf{X}^T \mathbf{X})^{-1}$ follows the inverse Wishart distribution and the mean of $\text{tr}\{(\mathbf{X}^T \mathbf{X})^{-1}\}$ is $\omega/(1 - \omega - 1/n)$, which can be large as $\omega \rightarrow 1^-$ [Guo and Cheng, 2018]. Without the need for Gaussianity, Hastie et al. [2019] show that $\text{tr}\{(\mathbf{X}^T \mathbf{X})^{-1}\} = \lim_{\lambda \rightarrow 0^+} \omega g(-\lambda) = \omega/(1 - \omega)$. Then, a tiny small nonzero error term $1 - h_\beta^2$ can ruin the out-of-sample performance of OLS estimator (and also ridge-less/BLUP-less estimators) when ω is close to one. Ridge estimator $\hat{\beta}_R(\lambda)$ avoids the unboundedness of $\text{tr}\{(\mathbf{X}^T \mathbf{X})^{-1}\}$ by introducing a nonzero shrinkage term λ . In marginal estimator $\hat{\beta}_S$, the estimator of $(\mathbf{X}^T \mathbf{X})^{-1}$ is simply $\{\text{Diag}(\mathbf{X}^T \mathbf{X})\}^{-1}$, which can be viewed as an extreme case of banded covariance estimator [Bickel and Levina, 2008] with zero bandwidth. Thus, $\hat{\beta}_S$ can avoid the issue of $\text{tr}\{(\mathbf{X}^T \mathbf{X})^{-1}\}$. However, the price is that $\hat{\beta}_S$ may have larger squared bias. See Section 7.4 of supplementary file for more details, in which we illustrate the bias-variance decomposition using mean squared prediction errors of these estimators.

4.2 In-sample R -squared

In this section, we present the results for in-sample R^2 , which measures the goodness-of-fit and is related to the performance of many in-sample applications of GWAS summary statistics (e.g., Barbeira et al. [2018]). In-sample R^2 has completely different pattern compared to out-of-sample R^2 . The asymptotic results are summarized in the following theorem.

Theorem 4. Under polygenic model (4) and Conditions 1 and 2, as $\min(n, m_\beta, p) \rightarrow \infty$, for any $\omega \in (0, \infty)$, $h_\beta^2 \in (0, 1]$ and Σ , we have

$$\begin{aligned} E_R^2(\lambda) &= E_B^2(\lambda/\omega) \\ &= \frac{\left[h_\beta^2 \cdot \{1 - \lambda + \lambda^2 g(-\lambda)\} + (1 - h_\beta^2) \cdot \omega \{1 - \lambda g(-\lambda)\} \right]^2}{h_\beta^2 \cdot \{1 - 2\lambda + 3\lambda^2 g(-\lambda) - \lambda^3 g'(-\lambda)\} + (1 - h_\beta^2) \cdot \omega \{1 - 2\lambda + \lambda^2 g'(-\lambda)\}} + o_p(1). \end{aligned}$$

$E_R^2(\lambda)$ is maximized as $\lambda \rightarrow 0^+$, and we have

$$E_R^2(0^+) = E_B^2(0^+) = \left\{ h_\beta^2 + (1 - h_\beta^2) \cdot \frac{\omega + 1 - |\omega - 1|}{2} \right\} + o_p(1) = \begin{cases} E_O^2, & \text{if } \omega < 1; \\ 1 + o_p(1), & \text{if } \omega > 1, \end{cases}$$

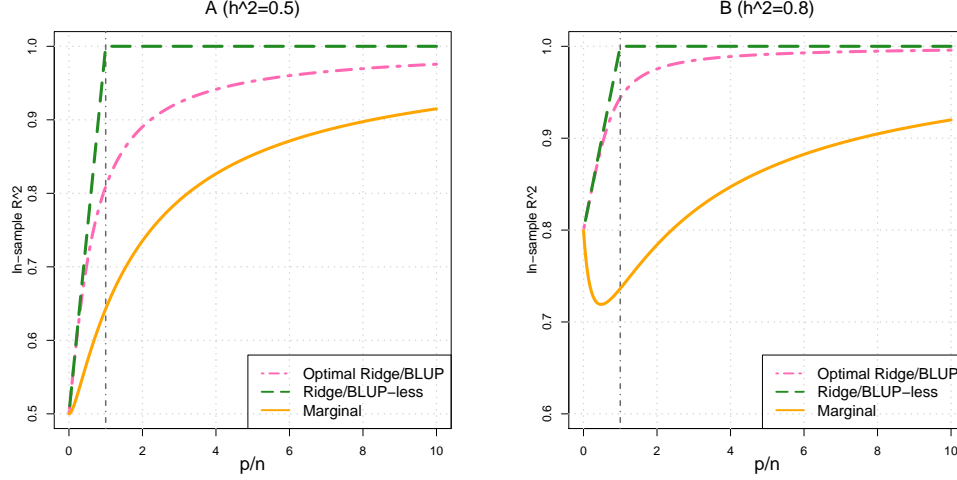


Fig. 3: In-sample R -squared of ridge/BLUP-less estimators ($E_R^2(0^+) = E_B^2(0^+)$), optimal (out-of-sample) ridge/BLUP estimators ($E_R^2(\lambda^*) = E_B^2(\lambda^*/\omega)$), and marginal estimator (E_S^2) when $\Sigma = \mathbf{I}_p$. We set $h_\beta^2 = (0.5, 0.8)$ in A and B, respectively.

where $E_O^2 = \{h_\beta^2 + (1 - h_\beta^2) \cdot \omega\} + o_p(1)$. In addition, we have

$$E_R^2(\lambda^*) = \frac{h_\beta^2}{1 - \lambda^* + \lambda^{*2}g(-\lambda^*)} + o_p(1).$$

When $\Sigma = \mathbf{I}_p$, the closed-form expression of $E_R^2(\lambda^*)$ is given by

$$E_R^2(\lambda^*) = \frac{2h_\beta^6}{(1 - h_\beta^2) \cdot \{\sqrt{(\omega - h_\beta^2)^2 + 4\omega h_\beta^2(1 - h_\beta^2)} - \omega\} + h_\beta^2 \cdot (3h_\beta^2 - 1)} + o_p(1).$$

The optimal in-sample R -squared $E_R^2(0^+) \geq h_\beta^2$ for any $h_\beta^2 \in (0, 1]$ and is a linear function of $\omega \in (0, 1)$ (Figure 3 and Supplementary Figure 3). The term $(1 - h_\beta^2) \cdot \omega$ in E_O^2 represents the degree of model over-fitting due to spurious correlations [Fan et al., 2012, 2018]. For $\omega > 1$, the limit of $E_R^2(0^+)$ is one, which indicates that the ridge-less estimator can have zero training error for \mathbf{y} given any $h_\beta^2 \in (0, 1]$. On the other hand, E_S^2 may not be a monotone function of ω . When $h_\beta^2 \in (0, 0.5]$, E_S^2 increases with ω . When $h_\beta^2 \in (0.5, 1]$, interestingly, E_S^2 decreases first as ω increases and can become much smaller than h_β^2 . More results of in-sample R^2 can be found in Corollary S3 of supplementary file.

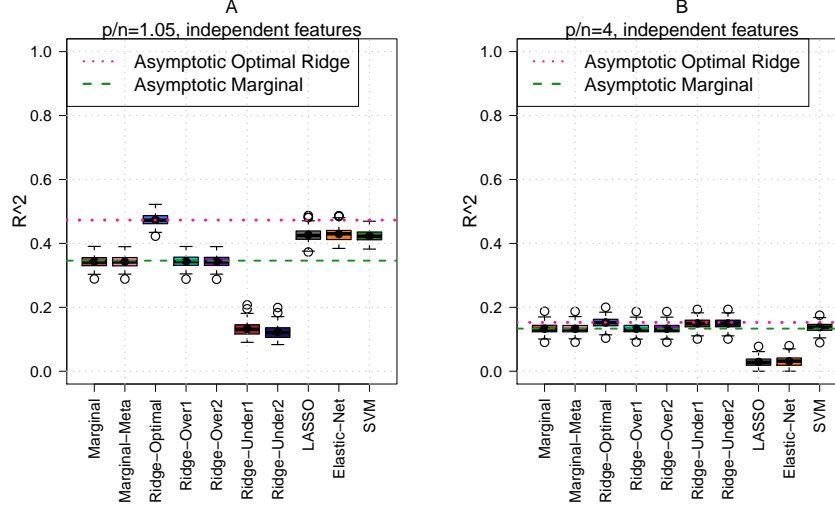


Fig. 4: Out-of-sample R -squared of different estimators for independent features. Marginal: $\hat{\beta}_S$; Marginal-meta: meta-analyzed $\hat{\beta}_S$; Ridge-Optimal: $\hat{\beta}_R(\lambda^*)$; Ridge-Over1: $\hat{\beta}_R(n\lambda^*)$; Ridge-Over2: $\hat{\beta}_R(n^2\lambda^*)$; Ridge-Under1: $\hat{\beta}_R(\lambda^*/n)$; Ridge-Under2: $\hat{\beta}_R(\lambda^*/n^2)$; We set $n = 2000$, and $\omega = 1.05$ and 4 in A and B, respectively. The dash lines represent the asymptotic limits of ridge (red) and marginal (green) estimators.

5 Numerical results

5.1 Simulation

We first numerically evaluate our theoretical results with $n = 2000$, and $\omega = 1.05, 2, 4$ and 8 . Each entry of X and Z is independently generated from $N(0, 1/p)$, and the ratio m/p is set to be 0.8 . We simulate a trait with heritability 0.8 from model (4), and predict the same trait in the testing data (i.e., $h_\beta^2 = h_\eta^2 = 0.8$, $\varphi_{\beta\eta} = 1$, $\beta_{(1)} = \eta_{(1)}$). The nonzero genetic effects $\beta_{(1)}$ and entries of ϵ and ϵ_z are generated from Normal distribution according to Condition 2. We evaluate the following estimators: 1) marginal estimator defined in model (2) (Marginal); 2) a meta-analyzed version of marginal estimator with weights equal to sample sizes (400 and 1600, respectively; Marginal-meta); 3) ridge estimator defined in model (3) with optimal regularizer λ^* (Ridge-Optimal); 3) ridge estimator with $n\lambda^*$ (Ridge-Over1); 4) ridge estimator with $n^2\lambda^*$ (Ridge-Over2); 5) ridge estimator with λ^*/n (Ridge-Under1); and 6) ridge estimator with λ^*/n^2 (Ridge-Under2). In addition, we examine three other methods in our settings, including Lasso [Tibshirani, 1996], Elastic-Net [Zou and Hastie, 2005], and support vector machines (SVM) [Cortes and Vapnik, 1995]. A total of 100 replicates is conducted, and we calculate the in-sample and out-of-sample R -squared (A^2 and E^2) defined in equation (6). The results are summarized in Figure 4 and Supplementary Figures 5 - 6. As expected, the finite sample performance of marginal and ridge estimators supports our asymptotic results. For example, when $\omega = 1.05$, the optimal ridge estimator clearly outperforms marginal estimator, and marginal estimator has similar R^2 to ridge estimator with large λ (Figure 4). Ridge

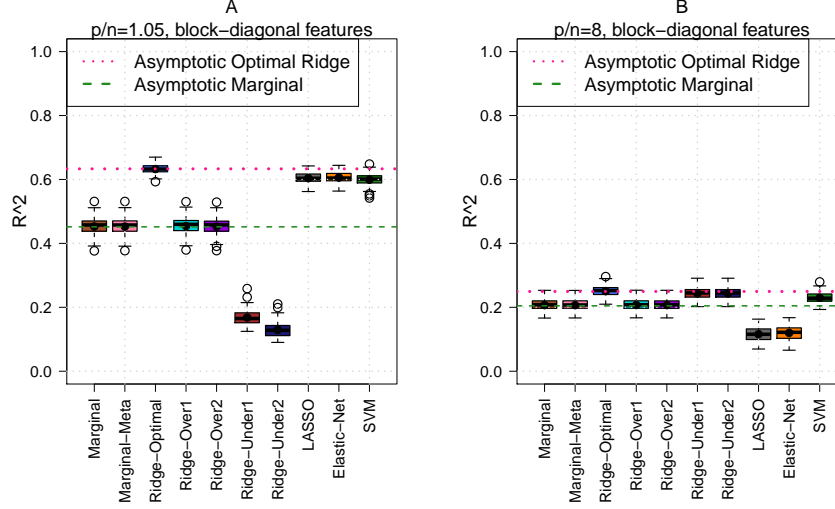


Fig. 5: Out-of-sample R -squared of different methods for features with block-diagonal correlation structure. See Figure 4 for figure notations. We set $n = 2000$, and $\omega = 1.05$ and 8 in A and B, respectively. The dash lines represent the asymptotic limits of ridge (red) and marginal (green) estimators.

estimator with small λ performs poorly for $\omega = 1.05$. However, when ω becomes 4 , marginal estimator and all ridge estimators have similar R^2 . In addition, meta-analyzed marginal estimator shows no decay of prediction accuracy. Lasso and Elastic-Net have poor performances for both A^2 and E^2 as ω becomes large, and SVM shows similar pattern to ridge estimators (Supplementary Figures 5- 6). We also observe that the in-sample R^2 has smaller variance compared to out-of-sample R^2 .

To mimic the LD structure of SNP data, we also construct Σ with a block-diagonal structure (block size = 20). Features within the block have pair-wise correlation $\rho_b = 0.8$, and features belong to different blocks are independent. Other settings are exactly the same as in $\Sigma = I_p$. The results are shown in Figure 5 and Supplementary Figures 7 - 8. Again, the performance of marginal and ridge estimators matches our theoretical limits, and the general pattern remains the same as in $\Sigma = I_p$. In addition, the prediction accuracy is improved due to the feature-wise correlation, verifying that the decay of prediction accuracy due to dimensionality can be delayed by correlation among features. In this situation, it is easier for the optimal ridge estimator to outperform marginal estimator.

5.2 UKB data simulation

Next, we perform simulation based on real GWAS data from the UK Biobank (UKB) resources [Sudlow et al., 2015]. There are $461,488$ common genotyped genetic variants (most of which are unimputed SNPs) after standard quality control (QC) procedures detailed in the supplementary file. We randomly select $10,000$ individuals of British ancestry as training samples, and test the prediction accuracy of these genetic variants on

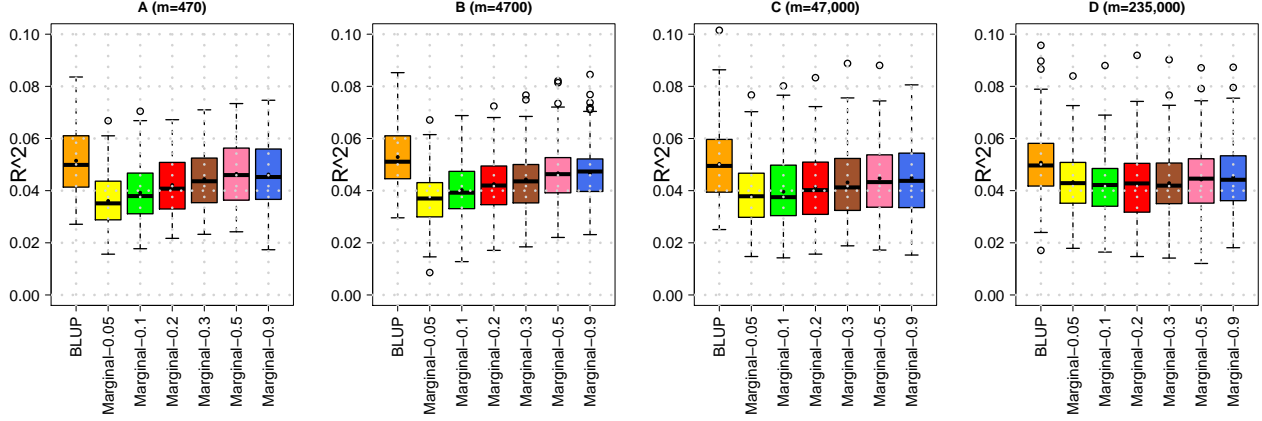


Fig. 6: Out-of-sample R -squared A^2 of different BLUP and marginal estimator across different sparsity m/p .

another 1,000 randomly selected individuals. Causal variants are randomly selected, and the number m is set to 470, 4700, 47,000, and 235,000, respectively. The nonzero genetic effects are independently generated from $N(0, 1/p)$, and the heritability h^2 is set to 80%. Marginal estimator is generated using PLINK [Purcell et al., 2007]. Following practical guidelines [Choi et al., 2018], we perform LD-based clumping for the marginal estimator via PLINK to obtain a list of relatively independent genetic variants for prediction. With the default window size (250 kb), we vary the clumping parameter C_r^2 and set it to 0.05, 0.1, 0.2, 0.3, 0.5, and 0.9. Smaller C_r^2 results in more stringent selection and more filtered variants by clumping. When $C_r^2 = 0.9$, most of the variants remain. The BLUP is obtained from GCTA [Yang et al., 2011] using all genetic variants.

The results are displayed in Figure 6, which shows that BLUP has slightly better prediction accuracy than marginal estimator across signal sparsity m and clumping parameter C_r^2 . The slightly higher prediction accuracy matches our theoretical results. We also find that strict clumping with small C_r^2 may reduce the prediction accuracy when genetic signals are sparse. As m/p increases, marginal estimator has more consistent performance across clumping parameters.

5.3 Real data analysis

In this real data example, we aim to use the GWAS results of neuroimaging traits to predict cognitive test scores. We focus on 14 volumetric traits of seven left/right pairs of brain regions of interest (refer to as ROI volumes), including left/right thalamus proper, left/right caudate, left/right putamen, left/right pallidum, left/right hippocampus, left/right amygdala, and left/right accumbens area. These subcortical ROI volumes are quantified by magnetic resonance imaging (MRI) and are known to be associated with cognitive functions [Miller et al., 2016]. We use the UKB samples ($n = 19,629$, $p = 8,944,375$) as training data for these 14 ROI volumes, and using the UKB results to predict two cognitive test scores (IBAM and list sort total scores) on subjects in the Pediatric Imaging, Neurocognition, and Genetics (PING, $n = 905$) study [Jernigan et al., 2016]. More

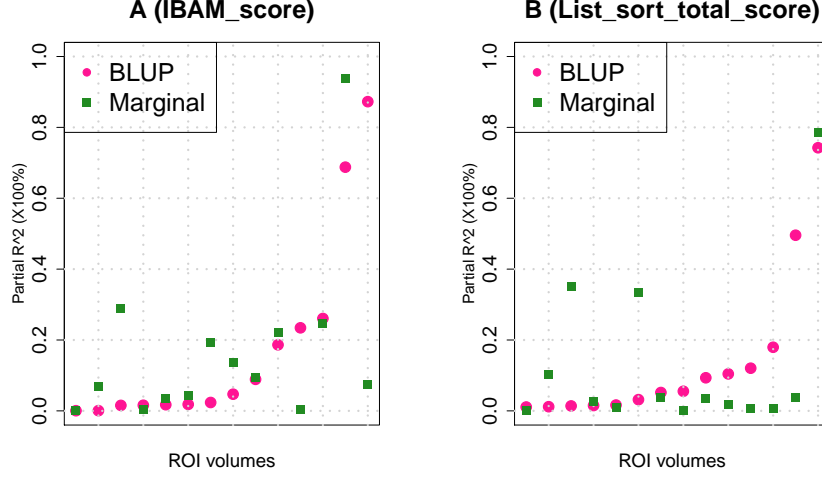


Fig. 7: Partial R -squared ($\times 100\%$) of 14 subcortical ROI volumes to predict IBAM and LST cognitive test scores in the PING cohort. Each point represents one ROI volume phenotype. The partial R -squared is estimated from linear regression while adjusting for the effects of age and gender. BLUP: best linear unbiased prediction; Marginal: marginal estimator. IBAM: IBAM score; LST: list sort total score.

details about data processing, quality control procedures, and cohort information can be found in supplementary file. We perform prediction using both marginal estimator (with $C_r^2 = 0.2$) and BLUP with all overlapping genetic variants between training and testing data. The UKB marginal estimators are from <https://github.com/BIG-S2/GWAS/>, and the BLUP is generated from the GCTA tool. The association between the predicted and observed phenotype is estimated and tested in linear regression, adjusting for the effects of age and sex. The associated partial R^2 is used to measure the prediction accuracy. The partial R^2 of BLUP and marginal estimator on the two cognitive tests are displayed in Supplementary Table 1. We find that BLUP has slightly higher prediction accuracy than marginal estimator, but their partial R^2 are within similar range (Supplementary Figure 10). For example, the mean partial R^2 of IBAM score are 0.176% and 0.168% for BLUP and marginal estimator, respectively. Such small partial R^2 are widely reported in GWAS prediction of cognitive and mental health traits [Bogdan et al., 2018], which may due to the small genetic effects and the extremely polygenic architecture of brain-related complex traits [O'Connor et al., 2019].

6 Discussion

In this paper, we study out-of-sample predictions on large-scale GWAS data with general Σ using random matrix theory. We investigate the prediction accuracy of marginal estimator with R^2 and generalize the results to consider cross-trait prediction and meta-analysis. We also examine and compare the class of ridge-type estimators, and highlight the different or even reverse behaviors of in-sample and out-of-sample R^2 . Our theo-

retical results can be useful to evaluate the prediction accuracy in GWAS, and may also guide more future works in dense high-dimensional prediction.

A few interesting future problems can be studied in high-dimensional dense signal settings. First, ridge-type estimators represent linear shrinkage estimation on Σ and its inverse Σ^{-1} . It might be interesting to explore whether we can improve the prediction accuracy with nonlinear shrinkage estimators, such as Ledoit and Wolf [2018]. Second, if prior knowledge is known on the structure of Σ , it is also possible to perform structured covariance estimation on Σ , see Cai et al. [2016] for a review of this area. For example, since the Σ of SNP data is known to have a block-diagonal structure, it can be modeled as a bandable covariance matrix [Bickel and Levina, 2008] with fast decay of feature correlation as their physical distance increases. Indeed, as mentioned before, marginal estimator can be viewed as a special banded covariance estimator of Σ with zero bandwidth, which may represent an extreme estimator that over-bands Σ . Finally, other extensions such as binary outcomes, time-to-event data, and SNP annotations and selections are also of great interest following the presented framework.

Acknowledgement

We are grateful to Fei Zou for many helpful conversations, which motivate us to work on this problem in the first place. We would also like to thank Ziliang Zhu for helpful discussion on random matrix theory. This research was partially supported by U.S. NIH grants MH086633 and MH116527, and a grant from the Cancer Prevention Research Institute of Texas. This research has been conducted using the UK Biobank resource (application number 22783), subject to a data transfer agreement. We thank Tengfei Li and other members of the UNC BIG-S2 lab for processing the raw brain imaging data. We thank the individuals represented in the UK Biobank and PING studies for their participation and the research teams for their work in collecting, processing and disseminating these datasets for analysis. More information of PING study can be found in supplementary file.

References

- 1000-Genomes-Project-Consortium. (2015) A global reference for human genetic variation. *Nature*, **526**, 68–74.
- Avants, B. B., Tustison, N. J., Song, G., Cook, P. A., Klein, A. and Gee, J. C. (2011) A reproducible evaluation of ants similarity metric performance in brain image registration. *Neuroimage*, **54**, 2033–2044.
- Bai, Z. and Silverstein, J. W. (2010) *Spectral analysis of large dimensional random matrices*, vol. 20. Springer.
- Barbeira, A. N., Dickinson, S. P., Bonazzola, R., Zheng, J., Wheeler, H. E., Torres, J. M., Torstenson, E. S., Shah, K. P., Garcia, T., Edwards, T. L. et al. (2018) Exploring the

- phenotypic consequences of tissue specific gene expression variation inferred from gwas summary statistics. *Nature Communications*, **9**, 1825.
- Bickel, P. J. and Levina, E. (2008) Regularized estimation of large covariance matrices. *The Annals of Statistics*, **36**, 199–227.
- Bogdan, R., Baranger, D. A. and Agrawal, A. (2018) Polygenic risk scores in clinical psychology: bridging genomic risk to individual differences. *Annual Review of Clinical Psychology*, **14**, 119–157.
- Boyle, E. A., Li, Y. I. and Pritchard, J. K. (2017) An expanded view of complex traits: from polygenic to omnigenic. *Cell*, **169**, 1177–1186.
- Bulik-Sullivan, B., Finucane, H. K., Anttila, V., Gusev, A., Day, F. R., Loh, P.-R., Duncan, L., Perry, J. R., Patterson, N., Robinson, E. B. et al. (2015) An atlas of genetic correlations across human diseases and traits. *Nature Genetics*, **47**, 1236–1241.
- Cai, T. T., Ren, Z. and Zhou, H. H. (2016) Estimating structured high-dimensional covariance and precision matrices: Optimal rates and adaptive estimation. *Electronic Journal of Statistics*, **10**, 1–59.
- de los Campos, G., Vazquez, A. I., Fernando, R., Klimentidis, Y. C. and Sorensen, D. (2013) Prediction of complex human traits using the genomic best linear unbiased predictor. *PLoS Genetics*, **9**, e1003608.
- Chatterjee, N., Wheeler, B., Sampson, J., Hartge, P., Chanock, S. J. and Park, J.-H. (2013) Projecting the performance of risk prediction based on polygenic analyses of genome-wide association studies. *Nature Genetics*, **45**, 400–405.
- Choi, S. W., Heng Mak, T. S. and O'Reilly, P. F. (2018) A guide to performing polygenic risk score analyses. *bioRxiv*. URL: <https://www.biorxiv.org/content/early/2018/09/14/416545>.
- Cortes, C. and Vapnik, V. (1995) Support-vector networks. *Machine Learning*, **20**, 273–297.
- Daetwyler, H. D., Pong-Wong, R., Villanueva, B. and Woolliams, J. A. (2010) The impact of genetic architecture on genome-wide evaluation methods. *Genetics*, **185**, 1021–1031.
- Daetwyler, H. D., Villanueva, B. and Woolliams, J. A. (2008) Accuracy of predicting the genetic risk of disease using a genome-wide approach. *PLoS One*, **3**, e3395.
- Das, S., Forer, L., Schönherr, S., Sidore, C., Locke, A. E., Kwong, A., Vrieze, S. I., Chew, E. Y., Levy, S., McGue, M. et al. (2016) Next-generation genotype imputation service and methods. *Nature Genetics*, **48**, 1284–1287.
- Dicker, L. H. (2013) Optimal equivariant prediction for high-dimensional linear models with arbitrary predictor covariance. *Electronic Journal of Statistics*, **7**, 1806–1834.
- (2016) Ridge regression and asymptotic minimax estimation over spheres of growing dimension. *Bernoulli*, **22**, 1–37.

- Dicker, L. H. and Erdogdu, M. A. (2017) Flexible results for quadratic forms with applications to variance components estimation. *The Annals of Statistics*, **45**, 386–414.
- Dobriban, E. and Sheng, Y. (2018) Distributed linear regression by averaging. *arXiv preprint arXiv:1810.00412*.
- (2019) One-shot distributed ridge regression in high dimensions. *arXiv preprint arXiv:1903.09321*.
- Dobriban, E. and Wager, S. (2018) High-dimensional asymptotics of prediction: Ridge regression and classification. *The Annals of Statistics*, **46**, 247–279.
- Dudbridge, F. (2013) Power and predictive accuracy of polygenic risk scores. *PLoS Genetics*, **9**, e1003348.
- El Karoui, N. (2013) Asymptotic behavior of unregularized and ridge-regularized high-dimensional robust regression estimators: rigorous results. *arXiv preprint arXiv:1311.2445*.
- (2018) On the impact of predictor geometry on the performance on high-dimensional ridge-regularized generalized robust regression estimators. *Probability Theory and Related Fields*, **170**, 95–175.
- Evans, L., Tahmasbi, R., Vrieze, S., Abecasis, G., Das, S., Gazal, S., Bjelland, D., Goddard, M., Neale, B., Yang, J. et al. (2018) Comparison of methods that use whole genome data to estimate the heritability and genetic architecture of complex traits. *Nature Genetics*, **50**, 737–745.
- Fan, J., Guo, S. and Hao, N. (2012) Variance estimation using refitted cross-validation in ultrahigh dimensional regression. *Journal of the Royal Statistical Society: Series B (Statistical Methodology)*, **74**, 37–65.
- Fan, J. and Lv, J. (2008) Sure independence screening for ultrahigh dimensional feature space. *Journal of the Royal Statistical Society: Series B (Statistical Methodology)*, **70**, 849–911.
- Fan, J., Shao, Q.-M. and Zhou, W.-X. (2018) Are discoveries spurious? distributions of maximum spurious correlations and their applications. *The Annals of Statistics*, **46**, 989–1017.
- Feng, L. and Zhang, C.-H. (2017) Sorted concave penalized regression. *arXiv preprint arXiv:1712.09941*.
- Gamazon, E. R., Wheeler, H. E., Shah, K. P., Mozaffari, S. V., Aquino-Michaels, K., Carroll, R. J., Eyler, A. E., Denny, J. C., Nicolae, D. L., Cox, N. J. et al. (2015) A gene-based association method for mapping traits using reference transcriptome data. *Nature Genetics*, **47**, 1091–1098.

- Goddard, M. (2009) Genomic selection: prediction of accuracy and maximisation of long term response. *Genetica*, **136**, 245–257.
- Guo, X. and Cheng, G. (2018) Moderate-dimensional inferences on quadratic functionals in ordinary least squares. *arXiv preprint arXiv:1810.01323*.
- Guo, Z., Wang, W., Cai, T. T. and Li, H. (2019) Optimal estimation of genetic relatedness in high-dimensional linear models. *Journal of the American Statistical Association*, **114**, 358–369.
- Gurdasani, D., Barroso, I., Zeggini, E. and Sandhu, M. S. (2019) Genomics of disease risk in globally diverse populations. *Nature Reviews Genetics*, in press.
- Gusev, A., Ko, A., Shi, H., Bhatia, G., Chung, W., Penninx, B. W., Jansen, R., De Geus, E. J., Boomsma, D. I., Wright, F. A. et al. (2016) Integrative approaches for large-scale transcriptome-wide association studies. *Nature Genetics*, **48**, 245–252.
- Hastie, T., Montanari, A., Rosset, S. and Tibshirani, R. J. (2019) Surprises in high-dimensional ridgeless least squares interpolation. *arXiv preprint arXiv:1903.08560*.
- Henderson, C. R. (1950) Estimation of genetic parameters (abstract). *Annals of Mathematical Statistics*, **21**, 309–310.
- (1975) Best linear unbiased estimation and prediction under a selection model. *Biometrics*, **31**, 423–447.
- Hoerl, A. E. and Kennard, R. W. (1970) Ridge regression: Biased estimation for nonorthogonal problems. *Technometrics*, **12**, 55–67.
- Holmes, J. B., Speed, D. and Balding, D. J. (2019) Summary statistic analyses can mistake confounding bias for heritability. *bioRxiv*. URL: <https://www.biorxiv.org/content/early/2019/06/04/532069>.
- Hsu, D., Kakade, S. M. and Zhang, T. (2011) Random design analysis of ridge regression. *arXiv preprint arXiv:1106.2363*.
- Hu, Y., Li, M., Lu, Q., Weng, H., Wang, J., Zekavat, S., Yu, Z., Li, B., Gu, J., Muchnik, S. et al. (2019) A statistical framework for cross-tissue transcriptome-wide association analysis. *Nature Genetics*, **51**, 568–576.
- Jernigan, T. L., Brown, T. T., Hagler Jr, D. J., Akshoomoff, N., Bartsch, H., Newman, E., Thompson, W. K., Bloss, C. S., Murray, S. S., Schork, N. et al. (2016) The pediatric imaging, neurocognition, and genetics (ping) data repository. *Neuroimage*, **124**, 1149–1154.
- Jiang, J., Li, C., Paul, D., Yang, C. and Zhao, H. (2016) On high-dimensional misspecified mixed model analysis in genome-wide association study. *The Annals of Statistics*, **44**, 2127–2160.

- Khera, A. V., Chaffin, M., Aragam, K. G., Haas, M. E., Roselli, C., Choi, S. H., Natarajan, P., Lander, E. S., Lubitz, S. A., Ellinor, P. T. et al. (2018) Genome-wide polygenic scores for common diseases identify individuals with risk equivalent to monogenic mutations. *Nature Genetics*, **50**, 1219–1224.
- Klein, A. and Tourville, J. (2012) 101 labeled brain images and a consistent human cortical labeling protocol. *Frontiers in Neuroscience*, **6**, 171.
- Ledoit, O. and Péché, S. (2011) Eigenvectors of some large sample covariance matrix ensembles. *Probability Theory and Related Fields*, **151**, 233–264.
- Ledoit, O. and Wolf, M. (2004) A well-conditioned estimator for large-dimensional covariance matrices. *Journal of Multivariate Analysis*, **88**, 365–411.
- (2018) Optimal estimation of a large-dimensional covariance matrix under stein’s loss. *Bernoulli*, **24**, 3791–3832.
- Lee, J. J., Wedow, R., Okbay, A., Kong, E., Maghzian, O., Zacher, M., Nguyen-Viet, T. A., Bowers, P., Sidorenko, J., Linnér, R. K. et al. (2018) Gene discovery and polygenic prediction from a genome-wide association study of educational attainment in 1.1 million individuals. *Nature Genetics*, **50**, 1112–1121.
- Li, C., Yang, C., Gelernter, J. and Zhao, H. (2014) Improving genetic risk prediction by leveraging pleiotropy. *Human Genetics*, **5**, 639–650.
- Loh, P.-R., Bhatia, G., Gusev, A., Finucane, H. K., Bulik-Sullivan, B. K., Pollack, S. J., de Candia, T. R., Lee, S. H., Wray, N. R., Kendler, K. S. et al. (2015) Contrasting genetic architectures of schizophrenia and other complex diseases using fast variance-components analysis. *Nature Genetics*, **47**, 1385–1392.
- Ma, R. and Dicker, L. H. (2019) The mahalanobis kernel for heritability estimation in genome-wide association studies: fixed-effects and random-effects methods. *arXiv preprint arXiv:1901.02936*.
- Marchenko, V. A. and Pastur, L. A. (1967) Distribution of eigenvalues for some sets of random matrices. *Matematicheskii Sbornik*, **114**, 507–536.
- Martin, A. R., Daly, M. J., Robinson, E. B., Hyman, S. E. and Neale, B. M. (2018) Predicting polygenic risk of psychiatric disorders. *Biological Psychiatry*, in press.
- Martin, A. R., Kanai, M., Kamatani, Y., Okada, Y., Neale, B. M. and Daly, M. J. (2019) Clinical use of current polygenic risk scores may exacerbate health disparities. *Nature Genetics*, **51**, 584–591.
- Mavaddat, N., Michailidou, K., Dennis, J., Lush, M., Fachal, L., Lee, A., Tyrer, J. P., Chen, T.-H., Wang, Q., Bolla, M. K. et al. (2019) Polygenic risk scores for prediction of breast cancer and breast cancer subtypes. *The American Journal of Human Genetics*, **104**, 21–34.

- Miller, K. L., Alfaro-Almagro, F., Bangerter, N. K., Thomas, D. L., Yacoub, E., Xu, J., Bartsch, A. J., Jbabdi, S., Sotiropoulos, S. N., Andersson, J. L. et al. (2016) Multimodal population brain imaging in the uk biobank prospective epidemiological study. *Nature neuroscience*, **19**, 1523.
- O'Connor, L. J., Schoech, A. P., Hormozdiari, F., Gazal, S., Patterson, N. and Price, A. L. (2019) Extreme polygenicity of complex traits is explained by negative selection. *The American Journal of Human Genetics*, **105**, 456–476.
- Pasaniuc, B. and Price, A. L. (2017) Dissecting the genetics of complex traits using summary association statistics. *Nature Reviews Genetics*, **18**, 117–127.
- Paul, D. and Aue, A. (2014) Random matrix theory in statistics: A review. *Journal of Statistical Planning and Inference*, **150**, 1–29.
- Pluta, D., Ombao, H., Chen, C., Xue, G., Moyzis, R. and Yu, Z. (2017) Adaptive mantel test for association testing in imaging genetics data. *arXiv preprint arXiv:1712.07270*.
- Purcell, S., Neale, B., Todd-Brown, K., Thomas, L., Ferreira, M. A., Bender, D., Maller, J., Sklar, P., De Bakker, P. I., Daly, M. J. et al. (2007) Plink: a tool set for whole-genome association and population-based linkage analyses. *The American Journal of Human Genetics*, **81**, 559–575.
- Purcell, S. M., Wray, R., Stone, L., Visscher, M., O'Donovan, C., Sullivan, F., Sklar, P., Ruderfer, M., McQuillin, A., Morris, W. et al. (2009) Common polygenic variation contributes to risk of schizophrenia and bipolar disorder. *Nature*, **460**, 748–752.
- Quick, C., Fuchsberger, C., Taliun, D., Abecasis, G., Boehnke, M. and Kang, H. M. (2018) emerald: rapid linkage disequilibrium estimation with massive datasets. *Bioinformatics*, **35**, 164–166.
- van Rheenen, W., Peyrot, W. J., Schork, A. J., Lee, S. H. and Wray, N. R. (2019) Genetic correlations of polygenic disease traits: from theory to practice. *Nature Reviews Genetics*, in press.
- Robinson, G. K. (1991) That blup is a good thing: the estimation of random effects. *Statistical Science*, **6**, 15–32.
- Schaid, D., Chen, W. and Larson, N. (2018) From genome-wide associations to candidate causal variants by statistical fine-mapping. *Nature Reviews Genetics*, **19**, 491–504.
- Silverstein, J. W. (1995) Strong convergence of the empirical distribution of eigenvalues of large dimensional random matrices. *Journal of Multivariate Analysis*, **55**, 331–339.
- Speed, D. and Balding, D. (2014) Multiblup: improved snp-based prediction for complex traits. *Genome Research*, **24**, 1550–1557.
- (2019) Sumher better estimates the snp heritability of complex traits from summary statistics. *Nature Genetics*, **51**, 277–284.

- Steinsaltz, D., Dahl, A. and Wachter, K. W. (2018) Statistical properties of simple random-effects models for genetic heritability. *Electronic Journal of Statistics*, **12**, 321–358.
- Sudlow, C., Gallacher, J., Allen, N., Beral, V., Burton, P., Danesh, J., Downey, P., Elliott, P., Green, J., Landray, M. et al. (2015) Uk biobank: an open access resource for identifying the causes of a wide range of complex diseases of middle and old age. *PLoS Medicine*, **12**, e1001779.
- Sugrue, L. P. and Desikan, R. S. (2019) What are polygenic scores and why are they important? *JAMA*, **321**, 1820–1821.
- Sullivan, P. F. and Geschwind, D. H. (2019) Defining the genetic, genomic, cellular, and diagnostic architectures of psychiatric disorders. *Cell*, **177**, 162–183.
- Sun, R. and Lin, X. (2017) Set-based tests for genetic association using the generalized berk-jones statistic. *arXiv preprint arXiv:1710.02469*.
- Tam, V., Patel, N., Turcotte, M., Bossé, Y., Paré, G. and Meyre, D. (2019) Benefits and limitations of genome-wide association studies. *Nature Reviews Genetics*, in press.
- Tibshirani, R. (1996) Regression shrinkage and selection via the lasso. *Journal of the Royal Statistical Society. Series B (Methodological)*, **58**, 267–288.
- Tikhonov, A. N. (1963) On the solution of ill-posed problems and the method of regularization. In *Doklady Akademii Nauk*, vol. 151, 501–504. Russian Academy of Sciences.
- Timpson, N. J., Greenwood, C. M., Soranzo, N., Lawson, D. J. and Richards, J. B. (2018) Genetic architecture: the shape of the genetic contribution to human traits and disease. *Nature Reviews Genetics*, **19**, 110–125.
- Torkamani, A., Wineinger, N. E. and Topol, E. J. (2018) The personal and clinical utility of polygenic risk scores. *Nature Reviews Genetics*, **19**, 581–590.
- Tustison, N. J., Cook, P. A., Klein, A., Song, G., Das, S. R., Duda, J. T., Kandel, B. M., van Strien, N., Stone, J. R., Gee, J. C. et al. (2014) Large-scale evaluation of ants and freesurfer cortical thickness measurements. *Neuroimage*, **99**, 166–179.
- Visscher, P. M., Wray, N. R., Zhang, Q., Sklar, P., McCarthy, M. I., Brown, M. A. and Yang, J. (2017) 10 years of gwas discovery: biology, function, and translation. *The American Journal of Human Genetics*, **101**, 5–22.
- Wang, C., Pan, G., Tong, T. and Zhu, L. (2015) Shrinkage estimation of large dimensional precision matrix using random matrix theory. *Statistica Sinica*, **25**, 993–1008.
- Wang, X. and Leng, C. (2016) High dimensional ordinary least squares projection for screening variables. *Journal of the Royal Statistical Society: Series B (Statistical Methodology)*, **78**, 589–611.

- Watanabe, K., Stringer, S., Frei, O., Mirkov, M. U., de Leeuw, C., Polderman, T. J., van der Sluis, S., Andreassen, O. A., Neale, B. M. and Posthuma, D. (2019) A global overview of pleiotropy and genetic architecture in complex traits. *Nature Genetics*, **51**, 1339–1348.
- Wheeler, H. E., Aquino-Michaels, K., Gamazon, E. R., Trubetskoy, V. V., Dolan, M. E., Huang, R. S., Cox, N. J. and Im, H. K. (2014) Poly-omic prediction of complex traits: Omickriging. *Genetic Epidemiology*, **38**, 402–415.
- Wray, N. R., Wijmenga, C., Sullivan, P. F., Yang, J. and Visscher, P. M. (2018) Common disease is more complex than implied by the core gene omnigenic model. *Cell*, **173**, 1573–1580.
- Yang, J., Benyamin, B., McEvoy, B. P., Gordon, S., Henders, A. K., Nyholt, D. R., Madden, P. A., Heath, A. C., Martin, N. G., Montgomery, G. W. et al. (2010) Common snps explain a large proportion of the heritability for human height. *Nature Genetics*, **42**, 565–569.
- Yang, J., Lee, S. H., Goddard, M. E. and Visscher, P. M. (2011) Gcta: a tool for genome-wide complex trait analysis. *The American Journal of Human Genetics*, **88**, 76–82.
- Yang, J., Zeng, J., Goddard, M. E., Wray, N. R. and Visscher, P. M. (2017) Concepts, estimation and interpretation of snp-based heritability. *Nature Genetics*, **49**, 1304–1310.
- Yang, Q. and Cheng, G. (2018) Quadratic discriminant analysis under moderate dimension. *arXiv preprint arXiv:1808.10065*.
- Yao, J., Zheng, S. and Bai, Z. (2015) *Sample covariance matrices and high-dimensional data analysis*, vol. 2. Cambridge University Press Cambridge.
- Zhao, B., Luo, T., Li, T., Li, Y., Zhang, J., Shan, Y., Wang, X., Yang, L., Zhou, F., Zhu, Z. et al. (2019) Genome-wide association analysis of 19,629 individuals identifies variants influencing regional brain volumes and refines their genetic co-architecture with cognitive and mental health traits. *Nature Genetics*, **51**, 1637–1644.
- Zhao, B. and Zou, F. (2019) On prs for complex polygenic trait prediction. *bioRxiv*. URL: <https://www.biorxiv.org/content/early/2019/06/04/447797>.
- Zhao, P. and Yu, B. (2006) On model selection consistency of lasso. *Journal of Machine Learning Research*, **7**, 2541–2563.
- Zhao, Q., Wang, J., Hemani, G., Bowden, J. and Small, D. S. (2018) Statistical inference in two-sample summary-data mendelian randomization using robust adjusted profile score. *arXiv preprint arXiv:1801.09652*.
- Zhou, X., Carbonetto, P. and Stephens, M. (2013) Polygenic modeling with bayesian sparse linear mixed models. *PLoS Genetics*, **9**, e1003264.
- Zou, H. and Hastie, T. (2005) Regularization and variable selection via the elastic net. *Journal of the Royal Statistical Society: Series B (Statistical Methodology)*, **67**, 301–320.

7 Supplementary material

7.1 RMT lemmas

We introduce some known results from classic random matrix theory (RMT, e.g., Bai and Silverstein [2010], Paul and Aue [2014], Yao et al. [2015]) and some recent advances of trace functionals (e.g., Dobriban and Wager [2018], Hastie et al. [2019], Ledoit and P       [2011], Wang et al. [2015]), which are foundations for our theoretical analysis of the large-scale GWAS data (\mathbf{X}, \mathbf{Z}) . Below we mainly use the training data \mathbf{X} as an example, but all the lemmas are applicable for the testing SNP data \mathbf{Z} as well.

The ESD of $\hat{\Sigma} = n^{-1}\mathbf{X}^T\mathbf{X}$ is given by $F_p^{\hat{\Sigma}}(x) = p^{-1} \sum_{i=1}^p \mathbf{I}\{\lambda_i(\hat{\Sigma}) \leq x\}, x \in \mathbb{R}$. We are interested in the limit behavior of $F_p^{\hat{\Sigma}}(x)$, which has one-to-one correspondence with the limit behavior of its Stieltjes transform. For a general distribution $G(x)$ with support $I \subset \mathbb{R}$, the Stieltjes transform (e.g., page 514 of Bai and Silverstein [2010]) and its first order derivative (evaluated at z) are given by $s_G(z) = \int_{x \in I} (x - z)^{-1} dG(x)$ and $s'_G(z) = \int_{x \in I} (x - z)^{-2} dG(x)$, respectively, for $z \in \mathbb{C} \setminus I$. Therefore, let $I = [0, \infty)$, as $\min(n, p) \rightarrow \infty$, the Stieltjes transform of $F_p^{\hat{\Sigma}}(x)$ and its first order derivative are given by $s_{F_p}(z) = p^{-1} \text{tr}\{(\hat{\Sigma} - zI_p)^{-1}\}$ and $s'_{F_p}(z) = p^{-1} \text{tr}\{(\hat{\Sigma} - zI_p)^{-2}\}$, respectively, for $z \in \mathbb{C} \setminus I$. The asymptotic behavior of $F_p^{\hat{\Sigma}}(x)$ can be characterized in the following lemma [Marchenko and Pastur, 1967, Silverstein, 1995] by its Stieltjes transform. See, for example, Theorem 2.4 of Yao et al. [2015].

Lemma 1. Under Condition 1, as $\min(n, p) \rightarrow \infty$, $F_p^{\hat{\Sigma}}(x)$ converges weakly to a limit probability distribution $M(x)$ with probability one, $x \in \mathbb{R}$. The Stieltjes transform of $M(x)$, donated as $s_M(z)$, is implicitly defined by the Marchenko-Pastur (M-P) equation

$$s_M(z) = \int \frac{1}{t\{1 - \omega - \omega z s_M(z)\} - z} dH(t).$$

In general, $s_M(z)$ has no closed-form expression, but all information about the LSD $M(x)$ is contained in this equation. For the special case $\Sigma = I_p$, we have $s_M(z) = \{1 - \omega - \omega z s_M(z) - z\}^{-1}$, it follows that (e.g., page 52 of Bai and Silverstein [2010])

$$s_M(z) = \frac{\sqrt{(1 - \omega - z)^2 - 4\omega z} - (1 - \omega - z)}{-2\omega z}, \quad \text{and} \quad (8)$$

$$s'_M(z) = \frac{(\omega - 1)\sqrt{(-z - \omega + 1)^2 - 4\omega z} - (\omega + 1)z + (\omega - 1)^2}{2\omega z^2 \sqrt{(-z - \omega + 1)^2 - 4\omega z}}, \quad (9)$$

respectively, for $z \in \mathbb{C} \setminus I$. Moreover, the LDS $M(x)$ in this special case is named the M-P law, and its probability density function is given by

$$p(x)_\omega = \frac{1}{2\pi\omega x} \cdot \sqrt{\{b_+(\omega) - x\}\{x - b_-(\omega)\}},$$

if $x \in [b_-(\omega), b_+(\omega)]$; and $p(x)_\omega = 0$ if $x \notin [b_-(\omega), b_+(\omega)]$; and $p(x)_\omega$ has a point mass $1 - 1/\omega$ at the origin if $\omega > 1$, where $b_\pm(\omega) = (1 \pm \sqrt{\omega})^2$.

Stieltjes transforms can also be used to study the limit of trace functionals of $F_p^{\Sigma}(x)$. Below we denote $g(z) \equiv s_M(z)$ and $g'(z) \equiv s'_M(z)$, respectively. Sometimes, it is more convenient to use the notation defined on the $n \times n$ companion matrix $\hat{\Phi} = n^{-1} \mathbf{X} \mathbf{X}^T$ [Dobriban and Wager, 2018]. Let $F_n^{\hat{\Phi}}(x) = n^{-1} \sum_{i=1}^n \mathbb{I}\{\lambda_i(\hat{\Phi}) \leq x\}$ be the ESD of $\hat{\Phi}$, $x \in \mathbb{R}$, and let $P(x)$ be the limiting distribution of $F_n^{\hat{\Phi}}(x)$. Define the Stieltjes transform of $F_n^{\hat{\Phi}}(x)$ and its first order derivative as $s_{F_n}(z) = n^{-1} \text{tr}\{(\hat{\Phi} - z \mathbf{I}_n)^{-1}\}$ and $s'_{F_n}(z) = n^{-1} \text{tr}\{(\hat{\Phi} - z \mathbf{I}_n)^{-2}\}$, respectively, and define the Stieltjes transform of $P(x)$ and its first order derivative as $v(z) \equiv s_P(z)$, and $v'(z) \equiv s'_P(z)$, respectively. We summarize the connections among $s_{F_p}(z)$, $s'_{F_p}(z)$, $g(z)$, $g'(z)$, $s_{F_n}(z)$, $s'_{F_n}(z)$, $v(z)$ and $v'(z)$ in the following lemma [Dobriban and Wager, 2018, Ledoit and Péché, 2011].

Lemma 2. Under Condition 1, as $\min(n, p) \rightarrow \infty$, for any $z \in \mathbb{C} \setminus I$, we have

$$\begin{aligned} s_{F_p}(z) &= p^{-1} \text{tr}\{(\widehat{\Sigma} - zI_p)^{-1}\} \rightarrow_{a.s.} g(z), & s'_{F_p}(z) &= p^{-1} \text{tr}\{(\widehat{\Sigma} - zI_p)^{-2}\} \rightarrow_{a.s.} g'(z), \\ s_{F_n}(z) &= n^{-1} \text{tr}\{(\widehat{\Phi} - zI_n)^{-1}\} \rightarrow_{a.s.} v(z), & s'_{F_n}(z) &= n^{-1} \text{tr}\{(\widehat{\Phi} - zI_n)^{-2}\} \rightarrow_{a.s.} v'(z), \\ p^{-1} \text{tr}\{\Sigma(\widehat{\Sigma} - zI_p)^{-1}\} &\rightarrow_{a.s.} \frac{1}{\omega} \left\{ \frac{1}{-zv(z)} - 1 \right\}, & p^{-1} \text{tr}\{\Sigma(\widehat{\Sigma} - zI_p)^{-2}\} &\rightarrow_{a.s.} \frac{v(z) + zv'(z)}{\omega \{-zv(z)\}^2}, \\ \omega\{g(z) + z^{-1}\} &= v(z) + z^{-1}, & \text{and} & \quad \omega\{g'(z) - z^{-2}\} = v'(z) - z^{-2}. \end{aligned}$$

In general, little is known about the connection between population LSD $H(t)$ and empirical LDS $M(t)$. However, there is one-to-one correspondence between the moments of $H(t)$ and those of $M(t)$. For any positive integer k , define the k th moment of $H(t)$ as $b_k(\Sigma) = \int_{\mathbb{R}} t^k dH(t) = p^{-1} \text{tr}(\Sigma^k)$, and the k th moment of $M(t)$ as $b_k(\hat{\Sigma}) = \int_{\mathbb{R}} t^k dM(t) = p^{-1} \text{tr}(\hat{\Sigma}^k)$. Then by Lemma 1, we have the following Lemma on the two sets of moments (Lemma 2.16 of Yao et al. [2015]).

Lemma 3. Under Condition 1, as $\min(n, p) \rightarrow \infty$, for any positive integer k , $b_k(\widehat{\Sigma})$ is a function of $b_l(\Sigma)$, for $0 < l \leq k$, and ω . Specifically, the first three moments of $H(t)$ and the first three moments of $M(t)$ are linked as $b_1(\widehat{\Sigma}) = b_1(\Sigma)$, $b_2(\widehat{\Sigma}) = b_2(\Sigma) + \omega b_1(\Sigma)^2$, and $b_3(\widehat{\Sigma}) = b_3(\Sigma) + 3\omega b_1(\Sigma)b_2(\Sigma) + \omega^2 b_1(\Sigma)^3$. Moreover, when $\Sigma = I_p$, we have $b_k(\Sigma) \equiv 1$ and $b_k(\widehat{\Sigma}) = \sum_{r=0}^{k-1} (r+1)^{-1} \binom{k}{r} \binom{k-1}{r-1} \omega^r$.

For any positive integer k , since $\lambda_i(\Sigma)$ is uniformly bounded, $i = 1, \dots, p$, $b_k(\Sigma)$ and $b_k(\hat{\Sigma})$ are also bounded for any $\omega \in (0, \infty)$. Thus, we have the following lemma on the concentration of quadratic forms.

Lemma 4. Under Condition 1, as $\min(n, p) \rightarrow \infty$, for any positive integer k , we have $0 < c \leq b_k(\Sigma) \leq b_k(\hat{\Sigma}) \leq C$. In addition, let $\hat{\Sigma}_X = n^{-1}X^T X$, $\hat{\Sigma}_Z = n_z^{-1}Z^T Z$, $B_{k_1, k_2} = \hat{\Sigma}_X^{k_1} \hat{\Sigma}_Z^{k_2}$, and define $A^0 = I$ for any matrix A . Then for any non-negative integers k_1, k_2 , we have

$$\frac{\text{tr}(\mathbf{B}_{k_1, k_2} \mathbf{B}_{k_1, k_2}^T)}{\{\text{tr}(\mathbf{B}_{k_1, k_2})\}^2} = O\left(\frac{1}{p}\right) = o(1).$$

Moreover, let α be a p -dimensional random vector of i.i.d. elements with mean zero,

variance σ_α^2 , and finite fourth order moment, we have

$$\alpha^T \mathbf{B}_{k_1, k_2} \alpha = \sigma_\alpha^2 \cdot \text{tr}(\mathbf{B}_{k_1, k_2}) \cdot \{1 + o_p(1)\}.$$

The proof of Lemma 4 is based on the Lemma B.26 of Bai and Silverstein [2010] and the Markov's inequality. Lemma 4 shows that the quadratic forms of \mathbf{B}_{k_1, k_2} concentrate around their means. We note that $\omega \in (0, \infty)$ is a key condition. When $\omega = \infty$, the concentration still holds when either k_1 or k_2 is zero, but may not hold when both k_1 and k_2 are nonzero.

7.2 Heritability and genetic correlation

In GWAS, genetics signal strength and their genetics overlaps are often quantified as heritability and genetic correlation, and are standard measures to report. Reliable estimators for h_β^2 , h_η^2 and $\varphi_{\beta\eta}$ are available from various models in genetics, using either individual-level data [Loh et al., 2015, Yang et al., 2011] or summary-level data [Bulik-Sullivan et al., 2015, Speed and Balding, 2019]. Particularly, Jiang et al. [2016] shows that the REML estimator of h^2 is consistent in high-dimensional LMM regardless of m , and this estimator \hat{h}^2 (named GREML) has been implemented in the popular genetic tool GCTA (<http://cnsgenomics.com/software/gcta/#GREML>). The theoretical results on h^2 in Jiang et al. [2016] are built on the special case $\Sigma = \mathbf{I}_p$, and the \hat{h}^2 might be biased given general Σ [Ma and Dicker, 2019] or hidden confounding effects [Holmes et al., 2019], though such bias is often believed to be small and acceptable in practice. See Yang et al. [2017] and van Rheenen et al. [2019] for overviews of these genetic concepts, and a detailed numerical comparison of population methods in Evans et al. [2018].

7.3 Relative prediction accuracy

In this section, we study the relative prediction accuracy of marginal estimator compared to the optimal ridge estimator. We focus on the case $\Sigma = \mathbf{I}_p$, in which we can quantify the efficiency loss in closed-form expressions.

Corollary S1. Let $R_R(h_\beta^2, \omega) = A_R^2(\lambda^*) / A_S^2$. Under polygenic model (4) and Conditions 1 and 2, as $\min(n, n_z, m_{\beta\eta}, p) \rightarrow \infty$, for any $h_\beta^2, h_\eta^2 \in (0, 1]$, $\varphi_{\beta\eta} \in [-1, 1]$, and $\Sigma = \mathbf{I}_p$, we have

$$R_R(h_\beta^2, \omega) = \frac{(\omega + h_\beta^2) \{ (\omega + h^2) - \sqrt{(\omega + h_\beta^2)^2 - 4\omega h_\beta^4} \}}{2h_\beta^4 \omega} + o_p(1) > 1 + o_p(1).$$

Moreover, for any fixed $\omega \in (0, \infty)$, $\frac{dR}{dh_\beta^2} R_B(h_\beta^2, \omega) > 0$ on $h_\beta^2 \in (0, 1)$; and for any given

$h_\beta^2 \in (0, 1]$, we have

$$\frac{dR}{d\omega} R_R(h_\beta^2, \omega) \begin{cases} > 0, & \text{if } 0 < \omega < h_\beta^2; \\ = 0, & \text{if } \omega = h_\beta^2; \\ < 0, & \text{if } \omega > h_\beta^2. \end{cases}$$

Corollary S1 shows that $\hat{\beta}_R(\lambda^*)$ always has better asymptotic out-of-sample R^2 than $\hat{\beta}_S$. $R_R(h_\beta^2, \omega)$ is higher for larger h_β^2 and is not a monotone function of ω . For given h_β^2 , $R_R(h_\beta^2, \omega)$ is maximized at $\omega = h_\beta^2$, with the maximum value

$$R_R^*(h_\beta^2, \omega) = \frac{2 - 2\sqrt{1 - h_\beta^2}}{h_\beta^2} + o_p(1).$$

$R_R^*(h_\beta^2, \omega)$ is an increasing function of h_β^2 on $h_\beta^2 \in (0, 1]$ and the maximum value is 2 at $h_\beta^2 = 1$. That is, for a fully heritable trait and $p = n$ in the training GWAS, we have $R_B(h_\beta^2, \omega) = A_R^2(\lambda^*)/A_S^2 = 2$. This represents the difference between n/p and $n/(n+p)$. As ω becomes large, $R_B(h_\beta^2, \omega)$ decreases, which can be viewed as a blessing of dimensionality due to the fact that the difference between n/p and $n/(n+p)$ decreases. Another interesting question is the relative prediction accuracy between $\hat{\beta}_S$ and $\hat{\beta}_R(0^+)$, which is quantified in the following corollary.

Corollary S2. Let $R_{R^0}(h_\beta^2, \omega) = A_R^2(0^+)/A_S^2$. Under polygenic model (4) and Conditions 1 and 2, as $\min(n, n_z, m_{\beta\eta}, p) \rightarrow \infty$, for any $h_\beta^2, h_\eta^2 \in (0, 1]$, $\varphi_{\beta\eta} \in [-1, 1]$, and $\Sigma = I_p$, we have

$$R_{R^0}(h_\beta^2, \omega) = \begin{cases} \frac{h_\beta^2 + \frac{\omega}{1-\omega} \cdot (1-h_\beta^2)}{h_\beta^2 + \omega} + o_p(1), & \text{if } \omega < 1; \\ \frac{h_\beta^2 \omega + (1-h_\beta^2) \frac{\omega^2}{\omega-1}}{h_\beta^2 + \omega} + o_p(1), & \text{if } \omega > 1. \end{cases}$$

It follows that for $h_\beta^2 \in (0, 1/2]$, we have

$$R_{R^0}(h_\beta^2, \omega) \begin{cases} > 1 + o_p(1), & \text{if } \omega < h_\beta^2; \\ = 1 + o_p(1), & \text{if } \omega = h_\beta^2; \\ < 1 + o_p(1), & \text{if } \omega > h_\beta^2; \end{cases}$$

and for $h_\beta^2 \in (1/2, 1)$, we have

$$R_{R^0}(h_\beta^2, \omega) \begin{cases} > 1 + o_p(1), & \text{if } \omega < h_\beta^2 \text{ or } \omega > h_\beta^2/(2h_\beta^2 - 1); \\ = 1 + o_p(1), & \text{if } \omega = h_\beta^2 \text{ or } \omega = h_\beta^2/(2h_\beta^2 - 1); \\ < 1 + o_p(1), & \text{if } h_\beta^2 < \omega < h_\beta^2/(2h_\beta^2 - 1). \end{cases}$$

And if $h_\beta^2 = 1$, then $R_{R^0}(h_\beta^2, \omega) > 1 + o_p(1)$ for any ω .

As $\hat{\beta}_R(0^+)$ reduces to $\hat{\beta}_O$ when $\omega < 1$, our results indicate that $\hat{\beta}_S$ can have better out-of-sample R^2 than $\hat{\beta}_O$ when $1 > \omega > h_\beta^2$. Thus, $\hat{\beta}_S$ can easily outperform $\hat{\beta}_O$ when

h_β^2 is low. Moreover, if $h_\beta^2 \leq 0.5$, $\hat{\beta}_R(0^+)$ is worse than $\hat{\beta}_S$ for $1 < \omega$. If $h_\beta^2 > 0.5$, however, $\hat{\beta}_R(0^+)$ is better when ω is large.

7.4 Mean squared prediction errors

In this section, we study the MSE of marginal estimator and illustrate the bias-variance trade-off of each estimator. We focus on the same trait prediction case in which $\beta = \eta$. The MSE and bias-variance decomposition (e.g., Hastie et al. [2019]) of a generic $p \times 1$ estimator $\hat{\beta}$ trained on GWAS dataset (X, y) can be defined as

$$\begin{aligned} M^2 &= E\{\|\hat{\beta} - \beta\|_\Sigma^2 | X, y\} = E\{(\hat{\beta} - \beta)^T \Sigma (\hat{\beta} - \beta) | X, y\} \\ &= \{E(\hat{\beta} | X, y) - \beta\}^T \Sigma \{E(\hat{\beta} | X, y) - \beta\} + \text{tr}[\text{Cov}(\hat{\beta} | X, y) \Sigma] \equiv B^2 + V^2, \end{aligned}$$

where B^2 represents the squared bias of $\hat{\beta}$, and V^2 measures the total variance of the $\hat{\beta}$ due to the random error term. We define $M_S^2 = B_S^2 + V_S^2$, $M_R^2(\lambda) = B_R^2(\lambda) + V_R^2(\lambda)$, $M_R^2(0^+) = B_R^2(0^+) + V_R^2(0^+)$, $M_O^2 = B_O^2 + V_O^2$, $M_B^2(\tau) = B_B^2(\tau) + V_B^2(\tau)$, and $M_B^2(0^+) = B_B^2(0^+) + V_B^2(0^+)$, for marginal, ridge, ridge-less, OLS, BLUP and BLUP-less estimators, respectively.

Proposition S1. Under polygenic model (4) and Conditions 1 and 2, as $\min(n, n_z, m_\beta, p) \rightarrow \infty$, for any $h_\beta^2 \in (0, 1]$ and Σ , we have

$$\begin{aligned} M_S^2 &= \left[m\sigma_\beta^2/p \cdot \{\omega b_2(\Sigma) + b_3(\Sigma) - 2b_2(\Sigma) + 1\} + \sigma_\epsilon^2 \cdot \omega b_2(\Sigma) \right] \cdot \{1 + o_p(1)\}, \\ M_R^2(\lambda) &= M_B^2(\lambda/\omega) = \left[m\sigma_\beta^2/p \cdot \frac{v(-\lambda) - \lambda v'(-\lambda)}{v(-\lambda)^2 \omega} + \sigma_\epsilon^2 \cdot \left\{ \frac{v'(-\lambda)}{v(-\lambda)^2} - 1 \right\} \right] \cdot \{1 + o_p(1)\}, \\ M_R^2(0^+) &= M_B^2(0^+) = \left[m\sigma_\beta^2/p \cdot \frac{1}{v(0^+) \omega} + \sigma_\epsilon^2 \cdot \left\{ \frac{v'(0^+)}{v(0^+)^2} - 1 \right\} \right] \cdot \{1 + o_p(1)\}, \quad \text{and} \\ M_O^2 &= \sigma_\epsilon^2 \cdot \frac{\omega}{1 - \omega} \cdot \{1 + o_p(1)\} \quad (\omega < 1). \end{aligned}$$

Moreover, if $h_\beta^2 \in (0, 1)$, $M_R^2(\lambda)$ is minimized at λ^* with the minimize value

$$M_R^2(\lambda^*) = M_B^2(\lambda^*/\omega) = m\sigma_\beta^2/p \cdot \left\{ \frac{1}{v(-\lambda^*) \omega} - \frac{\lambda^*}{\omega} \right\} \cdot \{1 + o_p(1)\}.$$

And if $h_\beta^2 = 1$, $M_R^2(\lambda)$ is minimized as $\lambda \rightarrow 0^+$, and thus the minimize value is $M_R^2(0^+)$.

Supplementary Figure 4 illustrates the different patterns of MSE for optimal ridge, ridge-less/OLS, and marginal estimators when $\Sigma = I_p$. For OLS estimator $\hat{\beta}_O$, we have $B_O^2 = 0$, but $V_O^2 = \sigma_\epsilon^2 \cdot \omega/(1 - \omega)$ can become unbounded as $\omega \rightarrow 1^-$. Similar issue occurs for ridge-less and BLUP-less estimators as $\omega \rightarrow 1^+$. On the other hand, the MSE of marginal estimator $\hat{\beta}_S$ is linear in ω , and thus can be much larger than those of other ridge-type estimators when ω is large. Specifically, V_S^2 is linear in ω and is always smaller than V_O^2 . However, B_S^2 is also linear in ω , and thus the MSE of $\hat{\beta}_S$ linearly grows up with ω . When $\Sigma = I_p$, we have the following closed-form expressions on MSE of ridge-type estimators.

Proposition S2. Under polygenic model (4) and Conditions 1 and 2, as $\min(n, n_z, m_\beta, p) \rightarrow \infty$, when $\Sigma = I_p$, for any $h_\beta^2 \in (0, 1)$, we have

$$M_S^2 = (m\sigma_\beta^2/p \cdot \omega + \sigma_\epsilon^2 \cdot \omega) \cdot \{1 + o_p(1)\},$$

$$M_R^2(\lambda) = M_B^2(\lambda/\omega) = \left[m\sigma_\beta^2/p \cdot \lambda^2 g'(-\lambda) + \sigma_\epsilon^2 \cdot \omega \{g(-\lambda) - \lambda g'(-\lambda)\} \right] \cdot \{1 + o_p(1)\},$$

and

$$M_R^2(0^+) = M_B^2(0^+) = \left[m\sigma_\beta^2/p \cdot \frac{(\omega - 1) + |\omega - 1|}{2\omega} + \sigma_\epsilon^2 \cdot \frac{\omega + 1 - |\omega - 1|}{2|\omega - 1|} \right] \cdot \{1 + o_p(1)\}$$

$$= \begin{cases} M_O^2, & \text{if } \omega < 1; \\ \left\{ m\sigma_\beta^2/p \cdot \frac{\omega - 1}{\omega} + \sigma_\epsilon^2 \cdot \frac{1}{\omega - 1} \right\} \cdot \{1 + o_p(1)\}, & \text{if } \omega > 1. \end{cases}$$

Moreover, for $h_\beta^2 \in (0, 1)$, $M_R^2(\lambda)$ is minimized at λ^* with the minimize value

$$M_R^2(\lambda^*) = M_B^2(\lambda^*/\omega) = m\sigma_\beta^2 \cdot \lambda^* g(-\lambda^*)$$

$$= m\sigma_\beta^2/p \cdot \frac{2\omega h_\beta^2 + \sqrt{(\omega - h_\beta^2)^2 + 4\omega h_\beta^2(1 - h_\beta^2)} - \omega - h_\beta^2}{2\omega h_\beta^2} \cdot \{1 + o_p(1)\}.$$

For $h_\beta^2 = 1$, $M_R^2(\lambda)$ is minimized at $\lambda^* \rightarrow 0^+$, and the minimize value is

$$M_R^2(0^+) = \begin{cases} o_p(1), & \text{if } \omega < 1; \\ m\sigma_\beta^2/p \cdot \frac{\omega - 1}{\omega} \cdot \{1 + o_p(1)\}, & \text{if } \omega > 1. \end{cases}$$

Proposition S3. Under the same conditions as in Proposition S2, we have for any ω

$$\frac{M_S^2}{M_R^2(\lambda^*)} = \frac{1}{(1 - h_\beta^2)g(-\lambda^*)} = \frac{2\omega^2}{\sqrt{(\omega + h_\beta^2)^2 - 4h_\beta^4\omega + h_\beta^2(2\omega - 1)} - \omega} > 1 + o_p(1).$$

Moreover, we have

$$\frac{M_S^2}{M_O^2} = \frac{1 - \omega}{1 - h_\beta^2} \begin{cases} > 1 + o_p(1), & \text{if } 0 < \omega < h_\beta^2; \\ = 1 + o_p(1), & \text{if } \omega = h_\beta^2; \\ < 1 + o_p(1), & \text{if } \omega > h_\beta^2. \end{cases}$$

When $h_\beta^2 = 1$, we have $M_S^2/M_O^2 > 1 + o_p(1)$ and $M_S^2/M_B^2(0^+) = M_S^2/M_R^2(0^+) > 1 + o_p(1)$ for any ω .

7.5 Relative goodness-of-fit

The following corollary provides the comparison between $E_R^2(\lambda^*)$ and E_S^2 , and some interesting properties of E_S^2 .

Corollary S3. Let $Q_R(h^2, \omega) = E_R^2(\lambda^*)/E_S^2$. Under polygenic model (4) and Conditions 1

and 2, as $\min(n, n_z, m_\beta, p) \rightarrow \infty$, for any $h_\beta^2 \in (0, 1]$, $\omega \in (0, \infty)$, and $\Sigma = I_p$, we have

$$Q_R(h^2, \omega) > 1 + o_p(1).$$

Moreover, if $h^2 \in (0, 0.5]$, we have

$$\frac{dE}{d\omega} E_S^2(h_\beta^2, \omega) > 1 + o_p(1).$$

which indicates that $E_S^2(h_\beta^2, \omega)$ is a monotone function of ω . If $h_\beta^2 \in (0.5, 1]$, however, we have

$$\frac{dE}{d\omega} E_S^2(h_\beta^2, \omega) \begin{cases} < 0, & \text{if } 0 < \omega < h_\beta^2 \cdot (2h_\beta^2 - 1); \\ = 0, & \text{if } \omega = h_\beta^2 \cdot (2h_\beta^2 - 1); \\ > 0, & \text{if } \omega > h_\beta^2 \cdot (2h_\beta^2 - 1), \end{cases}$$

and $E_S^2(h_\beta^2, \omega) = 4h_\beta^4 / (4h_\beta^4 + 1) + o_p(1)$ at $\omega = h_\beta^2 \cdot (2h_\beta^2 - 1)$.

7.6 Lemmas

7.6.1 Marginal estimator

Proof of Lemma 4 (concentration of quadratic forms)

Let α be a p -dimensional random vector of i.i.d. elements with mean zero and finite fourth order moment, and A be a fixed $p \times p$ matrix. Without loss of generality, we let $E(\alpha_1^2) = 1$. Then, by Lemma B.26 of Bai and Silverstein [2010], for any $q \geq 1$, we have

$$E\left[\{\alpha^T A \alpha - \text{tr}(A)\}^q\right] \leq c_q \cdot \left[E(\alpha_1^4) \text{tr}(A A^T)\right]^{q/2} + E(\alpha_1^{2q}) \text{tr}\{(A A^T)^{q/2}\},$$

where c_q is some constant that only depends on q . Let $q = 2$, it follows that

$$\text{Var}\left\{\frac{\alpha^T A \alpha}{\text{tr}(A)}\right\} = E\left[\left\{\frac{\alpha^T A \alpha}{\text{tr}(A)} - 1\right\}^2\right] \leq c_q \cdot \left[\frac{E(\alpha_1^4) \text{tr}(A A^T)}{\text{tr}(A)^2} + \frac{E(\alpha_1^4) \text{tr}(A A^T)}{\text{tr}(A)^2}\right].$$

Let $B_{k_1, k_2} = \hat{\Sigma}_X^{k_1} \hat{\Sigma}_Z^{k_2}$, $\hat{\Sigma}_X = n^{-1} X^T X$, and $\hat{\Sigma}_Z = n_z^{-1} Z^T Z$. Then, for bounded ω and any Σ with uniformly bounded eigenvalues, we have

$$\text{tr}(B_{k_1, k_2}) = p \cdot b_1(\hat{\Sigma}_X^{k_1} \hat{\Sigma}_Z^{k_2}) \leq p \cdot b_{k_1 + k_2}(\hat{\Sigma}_X) = O(p).$$

Then, we have

$$\frac{\text{tr}(B_{k_1, k_2} B_{k_1, k_2}^T)}{\{\text{tr}(B_{k_1, k_2})\}^2} = \frac{\text{tr}(B_{2k_1, 2k_2})}{\{\text{tr}(B_{k_1, k_2})\}^2} = O\left(\frac{p}{p^2}\right) = O\left(\frac{1}{p}\right) = o(1).$$

It follows that

$$\text{Var}\left\{\frac{\alpha^T B_{k_1, k_2} \alpha}{\text{tr}(B_{k_1, k_2})}\right\} = E\left[\left\{\frac{\alpha^T B_{k_1, k_2} \alpha}{\sigma_\alpha^2 \text{tr}(B_{k_1, k_2})} - 1\right\}^2\right] = o(1).$$

Thus, by Markov's inequality, we have

$$\alpha^T \mathbf{B}_{k_1, k_2} \alpha = \sigma_\alpha^2 \cdot \text{tr}(\mathbf{B}_{k_1, k_2}) \cdot \{1 + o_p(1)\}.$$

7.6.2 Useful trace results for ridge-type estimators

Here we summarize some results that are used frequently in our analysis of ridge-type estimators, which are based on Lemma 2.

Lemma S1. Under Condition 1 of the main paper, as $\min(n, p) \rightarrow \infty$, for any $\lambda > 0$, we have

$$\begin{aligned} \text{tr}\{\Sigma(\mathbf{X}^T \mathbf{X} + \lambda n \mathbf{I}_p)^{-1}\} &\rightarrow_{a.s.} \frac{1}{\lambda v(-\lambda)} - 1, \quad \text{and} \\ \text{tr}\{\Sigma(\mathbf{X}^T \mathbf{X} + \lambda n \mathbf{I}_p)^{-2}\} &\rightarrow_{a.s.} \frac{1}{n} \cdot \frac{v(-\lambda) - \lambda v'(-\lambda)}{(\lambda v(-\lambda))^2} \end{aligned}$$

When $\Sigma = \mathbf{I}_p$, we have closed-form limits

$$\begin{aligned} \text{tr}\{(\mathbf{X}^T \mathbf{X} + \lambda n \mathbf{I}_p)^{-1}\} &\rightarrow_{a.s.} \omega g(-\lambda) = \frac{\sqrt{(1-\omega+\lambda)^2 + 4\omega\lambda} - (1-\omega+\lambda)}{2\lambda}, \quad \text{and} \\ \text{tr}\{(\mathbf{X}^T \mathbf{X} + \lambda n \mathbf{I}_p)^{-2}\} &\rightarrow_{a.s.} \frac{p}{n^2} \cdot g'(-\lambda) = \frac{p}{n^2} \cdot \frac{(\omega-1) + \frac{(\omega+1)\lambda + (\omega-1)^2}{\sqrt{(1-\omega+\lambda)^2 + 4\omega\lambda}}}{2\omega\lambda^2}. \end{aligned}$$

Moreover, at the optimal $\lambda^* = \omega \cdot (1 - h_\beta^2) / h_\beta^2$, we have

$$\begin{aligned} A_R^2(\lambda^*) &= h_\eta^2 \varphi_{\beta\eta}^2 \cdot \{1 - \lambda^* g(-\lambda^*)\} + o_p(1) \\ &= h_\eta^2 \varphi_{\beta\eta}^2 \cdot \frac{\omega + h_\beta^2 - \sqrt{(h_\beta^2 - 2\omega h_\beta^2 + \omega)^2 + 4\omega^2 h_\beta^2 (1 - h_\beta^2)}}{2\omega h_\beta^2} + o_p(1) \\ &= h_\eta^2 \varphi_{\beta\eta}^2 \cdot \frac{\omega + h_\beta^2 - \sqrt{(\omega + h_\beta^2)^2 - 4\omega h_\beta^4}}{2\omega h_\beta^2} + o_p(1) \\ &= h_\eta^2 \varphi_{\beta\eta}^2 \cdot \frac{\omega + h_\beta^2 - \sqrt{(\omega - h_\beta^2)^2 + 4\omega h_\beta^2 (1 - h_\beta^2)}}{2\omega h_\beta^2} + o_p(1). \end{aligned}$$

Lemma S2. Under Condition 1 of the main paper, when $\Sigma = \mathbf{I}_p$, as $\min(n, p) \rightarrow \infty$, $\lambda \rightarrow 0^+$, we have the following closed-form limits

$$\begin{aligned} g(-\lambda) &\rightarrow_{a.s.} \frac{\frac{1+\omega}{|1-\omega|} - 1}{2\omega}, \quad \lambda g(-\lambda) \rightarrow_{a.s.} \frac{|1-\omega| - (1-\omega)}{2\omega} \\ \lambda g'(-\lambda) &\rightarrow_{a.s.} \frac{2\lambda}{\{(1-\omega+\lambda)^2 + 4\omega\lambda\}^{3/2}} = 0, \quad \text{and} \quad \lambda^2 g'(-\lambda) \rightarrow_{a.s.} \frac{(\omega-1) + |1-\omega|}{2\omega} \end{aligned}$$

The following lemma is used to show the equivalence of prediction accuracy of ridge

estimator and BLUP, which can be easily proved by applying singular value decomposition on \mathbf{X} .

Lemma S3. Under Condition 1 of the main paper, as $\min(n, p) \rightarrow \infty$, for any $\lambda > 0$ and arbitrary Σ , we have

$$\begin{aligned}\text{tr}\{(\mathbf{X}\mathbf{X}^T + \lambda\mathbf{I}_n)^{-1}\mathbf{X}\Sigma\mathbf{X}^T\} &= \text{tr}\{(\mathbf{X}^T\mathbf{X} + \lambda\mathbf{I}_p)^{-1}\mathbf{X}^T\mathbf{X}\Sigma\} \quad \text{and} \\ \text{tr}\{(\mathbf{X}\mathbf{X}^T + \lambda\mathbf{I}_n)^{-2}\mathbf{X}\Sigma\mathbf{X}^T\} &= \text{tr}\{(\mathbf{X}^T\mathbf{X} + \lambda\mathbf{I}_p)^{-2}\mathbf{X}^T\mathbf{X}\Sigma\}.\end{aligned}$$

7.7 Proofs of marginal estimator

Out-of-sample

Proposition S4. Under polygenic model (4) and Conditions 1 and 2, as $\min(n, n_z, m_{\beta\eta}, p) \rightarrow \infty$, for any $\omega \in (0, \infty)$, $h_\beta^2, h_\eta^2 \in (0, 1]$, $\varphi_{\beta\eta} \in [-1, 1]$, and Σ , we have

$$\begin{aligned}\frac{(\mathbf{Z}_{(1)}\boldsymbol{\eta}_{(1)} + \boldsymbol{\epsilon}_z)^T(\mathbf{Z}_{(1)}\boldsymbol{\eta}_{(1)} + \boldsymbol{\epsilon}_z)}{n_z m_\eta \cdot \sigma_\eta^2 / p + n_z \cdot \sigma_{\epsilon_z}^2} &= 1 + o_p(1), \\ \frac{(\mathbf{X}_{(1)}\boldsymbol{\beta}_{(1)} + \boldsymbol{\epsilon})^T \mathbf{X} \mathbf{Z}^T \mathbf{Z} \mathbf{X}^T (\mathbf{X}_{(1)}\boldsymbol{\beta}_{(1)} + \boldsymbol{\epsilon})}{nn_z m_\beta \cdot \{(n+1)b_3(\Sigma) + pb_2(\Sigma)\} \cdot \sigma_\beta^2 / p + nn_z pb_2(\Sigma) \cdot \sigma_\epsilon^2} &= 1 + o_p(1),\end{aligned}$$

and

$$\frac{(\mathbf{Z}_{(1)}\boldsymbol{\eta}_{(1)} + \boldsymbol{\epsilon}_z)^T \mathbf{Z} \mathbf{X}^T (\mathbf{X}_{(1)}\boldsymbol{\beta}_{(1)} + \boldsymbol{\epsilon})}{nn_z m_{\beta\eta} b_2(\Sigma) \cdot \sigma_{\beta\eta} / p} = 1 + o_p(1).$$

By continuous mapping theorem, we have

$$A_S^2 = h_\eta^2 \varphi_{\beta\eta}^2 \cdot \left\{ \frac{b_3(\Sigma)}{b_2(\Sigma)^2} + \frac{\omega}{h_\beta^2} \cdot \frac{1}{b_2(\Sigma)} \right\}^{-1} + o_p(1).$$

Meta-analysis

Under polygenic model (4) and Conditions 1 and 2, suppose we have independent GWAS $(\mathbf{X}_i, \mathbf{y}_i)$, with sample sizes (n_1, \dots, n_k) and p SNPs, $i = 1, \dots, k$, $k \in (0, \infty)$, let $\widehat{\mathbf{B}} = [\widehat{\boldsymbol{\beta}}_1^T, \dots, \widehat{\boldsymbol{\beta}}_k^T]$ be the $p \times k$ matrix of marginal estimators from the k GWAS. Let $\mathbf{d} = (d_1, \dots, d_k)^T$ be an $k \times 1$ vector of weights, and let $\widehat{\mathbf{B}}(\mathbf{d}) = \widehat{\mathbf{B}}\mathbf{d}$ be the aggregated summary statistics. As $\min(n_1, \dots, n_k, n_z, m_{\beta\eta}, p) \rightarrow \infty$, for any $\omega \in (0, \infty)$, $h_\beta^2, h_\eta^2 \in (0, 1]$, $\varphi_{\beta\eta} \in [-1, 1]$, \mathbf{d} , and Σ , we have

$$A_S^2(\mathbf{d}) = \left\{ \frac{(\sum_{i=1}^k d_i \widehat{\boldsymbol{\beta}}_i)^T \mathbf{Z}^T (\mathbf{Z}\boldsymbol{\eta} + \boldsymbol{\epsilon}_z)}{\|\mathbf{Z}\boldsymbol{\eta} + \boldsymbol{\epsilon}_z\| \|\mathbf{Z}\widehat{\mathbf{B}}\mathbf{d}\|} \right\}^2 = h_\eta^2 \varphi_{\beta\eta}^2 \cdot \frac{(\sum_{i=1}^k d_i)^2 \cdot b_2(\Sigma)^2}{(\sum_{i=1}^k d_i \widehat{\boldsymbol{\beta}}_i)^T \mathbf{Z}^T \mathbf{Z} (\sum_{i=1}^k d_i \widehat{\boldsymbol{\beta}}_i)} + o_p(1).$$

Note that for $i \neq j$, $(i, j) \in (1, \dots, k)$, we have

$$(\mathbf{Z}\widehat{\boldsymbol{\beta}}_i)^T (\mathbf{Z}\widehat{\boldsymbol{\beta}}_j) = \frac{1}{n_i n_j} \mathbb{E}(\boldsymbol{\beta}^T \mathbf{X}_i^T \mathbf{X}_i \mathbf{Z}^T \mathbf{Z} \mathbf{X}_j^T \mathbf{X}_j \boldsymbol{\beta}) \cdot \{1 + o_p(1)\} = m_\beta n_z \cdot b_3(\Sigma) \cdot \sigma_\beta^2 / p \cdot \{1 + o_p(1)\}$$

and

$$\begin{aligned} (\mathbf{Z}\hat{\boldsymbol{\beta}}_i)^T (\mathbf{Z}\hat{\boldsymbol{\beta}}_i) &= \frac{1}{n_i^2} \mathbb{E}(\boldsymbol{\beta}^T \mathbf{X}_i^T \mathbf{X}_i \mathbf{Z}^T \mathbf{Z} \mathbf{X}_i^T \mathbf{X}_i \boldsymbol{\beta} + \boldsymbol{\epsilon}_i^T \mathbf{X}_i^T \mathbf{Z}^T \mathbf{Z} \mathbf{X}_i^T \boldsymbol{\epsilon}_i) \cdot \{1 + o_p(1)\} \\ &= m_\beta n_z \cdot \{b_3(\boldsymbol{\Sigma}) + \frac{p}{n_i h_\beta^2} b_2(\boldsymbol{\Sigma})\} \cdot \sigma_\beta^2 / p \cdot \{1 + o_p(1)\}. \end{aligned}$$

It follows that

$$\begin{aligned} A_S^2(\mathbf{d}) &= h_\eta^2 \varphi_{\beta\eta}^2 \cdot \frac{(\sum_{i=1}^k d_i)^2 \cdot b_2(\boldsymbol{\Sigma})^2}{\sum_{i=1}^k d_i^2 \cdot \{b_3(\boldsymbol{\Sigma}) + \frac{p}{n_i h_\beta^2} b_2(\boldsymbol{\Sigma})\} + 2 \sum_{i \neq j}^{(i,j) \in (1, \dots, k)} d_i d_j \cdot b_3(\boldsymbol{\Sigma})} + o_p(1) \\ &= h_\eta^2 \varphi_{\beta\eta}^2 \cdot \frac{(\sum_{i=1}^k d_i)^2 \cdot b_2(\boldsymbol{\Sigma})^2}{(\sum_{i=1}^k d_i)^2 \cdot b_3(\boldsymbol{\Sigma}) + (\sum_{i=1}^k d_i^2 \frac{p}{n_i h_\beta^2}) \cdot b_2(\boldsymbol{\Sigma})} + o_p(1) \\ &= h_\eta^2 \varphi_{\beta\eta}^2 \cdot \left\{ \frac{b_3(\boldsymbol{\Sigma})}{b_2(\boldsymbol{\Sigma})^2} + \frac{\sum_{i=1}^k d_i^2 / n_i}{(\sum_{i=1}^k d_i)^2} \cdot \frac{p}{b_2(\boldsymbol{\Sigma}) h_\beta^2} \right\}^{-1} + o_p(1). \end{aligned}$$

Therefore, when $d_i = n_i$, we have

$$A_S^2(\mathbf{a}^*) = h_\eta^2 \varphi_{\beta\eta}^2 \cdot \left\{ \frac{b_3(\boldsymbol{\Sigma})}{b_2(\boldsymbol{\Sigma})^2} + \frac{p}{\sum_{i=1}^k n_i} \cdot \frac{1}{b_2(\boldsymbol{\Sigma}) h_\beta^2} \right\}^{-1} + o_p(1).$$

In-sample

Proposition S5. Under polygenic model (4) and Conditions 1 and 2, as $\min(n, n_z, m_\beta, p) \rightarrow \infty$, for any $\omega \in (0, \infty)$, $h_\beta^2 \in (0, 1]$, and $\boldsymbol{\Sigma}$, we have

$$\begin{aligned} \frac{(\mathbf{X}_{(1)} \boldsymbol{\beta}_{(1)} + \boldsymbol{\epsilon})^T (\mathbf{X}_{(1)} \boldsymbol{\beta}_{(1)} + \boldsymbol{\epsilon})}{nm_\beta \cdot \sigma_\beta^2 / p + n \cdot \sigma_\epsilon^2} &= 1 + o_p(1), \\ \frac{(\mathbf{X}_{(1)} \boldsymbol{\beta}_{(1)} + \boldsymbol{\epsilon})^T \mathbf{X} \mathbf{X}^T \mathbf{X} \mathbf{X}^T (\mathbf{X}_{(1)} \boldsymbol{\beta}_{(1)} + \boldsymbol{\epsilon})}{n^3 m_\beta \cdot \{b_3(\boldsymbol{\Sigma}) + 3\omega b_2(\boldsymbol{\Sigma}) + \omega^2\} \cdot \sigma_\beta^2 / p + n^2 p \cdot \{b_2(\boldsymbol{\Sigma}) + \omega\} \cdot \sigma_\epsilon^2} &= 1 + o_p(1), \end{aligned}$$

and

$$\frac{(\mathbf{X}_{(1)} \boldsymbol{\beta}_{(1)} + \boldsymbol{\epsilon})^T \mathbf{X} \mathbf{X}^T (\mathbf{X}_{(1)} \boldsymbol{\beta}_{(1)} + \boldsymbol{\epsilon})}{n^2 m_\beta \{b_2(\boldsymbol{\Sigma}) + \omega\} \cdot \sigma_\beta^2 / p + np \cdot \sigma_\epsilon^2} = 1 + o_p(1).$$

By continuous mapping theorem, we have

$$E_S^2 = \frac{\{b_2(\boldsymbol{\Sigma}) h_\beta^2 + \omega\}^2}{\{b_2(\boldsymbol{\Sigma}) h_\beta^2 + \omega\}^2 + b_2(\boldsymbol{\Sigma}) \omega + \{b_3(\boldsymbol{\Sigma}) - b_2(\boldsymbol{\Sigma})^2 h_\beta^2\} h_\beta^2} + o_p(1).$$

For the special case $\boldsymbol{\Sigma} = \mathbf{I}_p$, we have $b_3(\boldsymbol{\Sigma}) = b_2(\boldsymbol{\Sigma}) = b_1(\boldsymbol{\Sigma}) = 1$ in the above propositions.

7.8 Proofs of ridge-type estimators

OLS estimator, out-of-sample

Proposition S6. Under polygenic model (4) and Conditions 1 and 2, as $\min(n, n_z, m_{\beta\eta}, p) \rightarrow \infty$, for any $\omega \in (0, \infty)$, $h_\beta^2, h_\eta^2 \in (0, 1]$, $\varphi_{\beta\eta} \in [-1, 1]$, and Σ , we have

$$\frac{(X_{(1)}\beta_{(1)} + \epsilon)^T X(X^T X)^{-1} Z^T Z(X^T X)^{-1} X^T (X_{(1)}\beta_{(1)} + \epsilon)}{n_z m_\beta \cdot \sigma_\beta^2 / p + n_z \omega / (1 - \omega) \cdot \sigma_\epsilon^2} = 1 + o_p(1),$$

and

$$\frac{(Z_{(1)}\eta_{(1)} + \epsilon_z)^T Z(X^T X)^{-1} X^T (X_{(1)}\beta_{(1)} + \epsilon)}{n_z m_{\beta\eta} \cdot \sigma_{\beta\eta} / p} = 1 + o_p(1).$$

By continuous mapping theorem, we have

$$A_O^2 = h_\eta^2 \varphi_{\beta\eta}^2 \cdot \left\{ 1 + \frac{1 - h_\beta^2}{h_\beta^2} \cdot \frac{\omega}{1 - \omega} \right\}^{-1} + o_p(1). \quad (\omega < 1)$$

OLS estimator, in-sample

Proposition S7. Under polygenic model (4) and Conditions 1 and 2, as $\min(n, n_z, m_\beta, p) \rightarrow \infty$, for any $\omega \in (0, \infty)$, $h_\beta^2 \in (0, 1]$, and Σ , we have

$$\frac{(X_{(1)}\beta_{(1)} + \epsilon)^T X(X^T X)^{-1} X^T X(X^T X)^{-1} X^T (X_{(1)}\beta_{(1)} + \epsilon)}{n m_\beta \cdot \sigma_\beta^2 / p + p \cdot \sigma_\epsilon^2} = 1 + o_p(1),$$

and

$$\frac{(X_{(1)}\beta_{(1)} + \epsilon)^T X(X^T X)^{-1} X^T (X_{(1)}\beta_{(1)} + \epsilon)}{n m_\beta \cdot \sigma_\beta^2 / p + p \cdot \sigma_\epsilon^2} = 1 + o_p(1).$$

By continuous mapping theorem, we have

$$E_O^2 = \{h_\beta^2 + \omega(1 - h_\beta^2)\} \cdot \{1 + o_p(1)\}. \quad (\omega < 1)$$

Ridge estimator, out-of-sample

Proposition S8. Under polygenic model (4) and Conditions 1 and 2, as $\min(n, n_z, m_{\beta\eta}, p) \rightarrow \infty$, for any $\omega \in (0, \infty)$, $h_\beta^2, h_\eta^2 \in (0, 1]$, $\varphi_{\beta\eta} \in [-1, 1]$, and Σ , we have

$$\frac{(X_{(1)}\beta_{(1)} + \epsilon)^T X(X^T X + \lambda n I_p)^{-1} Z^T Z(X^T X + \lambda n I_p)^{-1} X^T (X_{(1)}\beta_{(1)} + \epsilon)}{V_{R1} + V_{R2}} = 1 + o_p(1),$$

where

$$\begin{aligned} V_{R1} &= n_z m_\beta \cdot \left[1 - \frac{2\lambda}{\omega} \text{tr}\{\Sigma(\mathbf{X}^T \mathbf{X} + \lambda n \mathbf{I}_p)^{-1}\} + \frac{\lambda^2 n}{\omega} \cdot \text{tr}\{\Sigma(\mathbf{X}^T \mathbf{X} + \lambda n \mathbf{I}_p)^{-2}\} \right] \cdot \sigma_\beta^2 / p \\ &= n_z m_\beta \cdot \left[1 - \frac{2\lambda}{\omega} \left\{ \frac{1}{\lambda v(-\lambda)} - 1 \right\} + \frac{\lambda^2}{\omega} \cdot \frac{v(-\lambda) - \lambda v'(-\lambda)}{\{\lambda v(-\lambda)\}^2} \right] \cdot \sigma_\beta^2 / p, \end{aligned}$$

and

$$\begin{aligned} V_{R2} &= n_z \cdot \left[\text{tr}\{\Sigma(\mathbf{X}^T \mathbf{X} + \lambda n \mathbf{I}_p)^{-1}\} + \lambda n \cdot \text{tr}\{\Sigma(\mathbf{X}^T \mathbf{X} + \lambda n \mathbf{I}_p)^{-2}\} \right] \cdot \sigma_\epsilon^2 \\ &= n_z \cdot \left[\left\{ \frac{1}{\lambda v(-\lambda)} - 1 \right\} - \lambda \cdot \frac{v(-\lambda) - \lambda v'(-\lambda)}{\{\lambda v(-\lambda)\}^2} \right] \cdot \sigma_\epsilon^2, \end{aligned}$$

In addition, we have

$$\frac{(\mathbf{Z}_{(1)} \boldsymbol{\eta}_{(1)} + \boldsymbol{\epsilon}_z)^T \mathbf{Z} (\mathbf{X}^T \mathbf{X} + \lambda n \mathbf{I}_p)^{-1} \mathbf{X}^T (\mathbf{X}_{(1)} \boldsymbol{\beta}_{(1)} + \boldsymbol{\epsilon})}{C_{R1}} = 1 + o_p(1),$$

where

$$\begin{aligned} C_{R1} &= n_z m_{\beta\eta} \cdot \left[1 - \frac{\lambda}{\omega} \cdot \text{tr}\{\Sigma(\mathbf{X}^T \mathbf{X} + \lambda n \mathbf{I}_p)^{-1}\} \right] \cdot \sigma_{\beta\eta} / p \\ &= n_z m_{\beta\eta} \cdot \left[1 - \frac{\lambda}{\omega} \cdot \left\{ \frac{1}{\lambda v(-\lambda)} - 1 \right\} \right] \cdot \sigma_{\beta\eta} / p. \end{aligned}$$

By continuous mapping theorem, we have

$$A_R^2(\lambda) = h_\eta^2 \varphi_{\beta\eta}^2 \cdot \frac{\left[1 + \frac{\lambda}{\omega} \left\{ 1 - \frac{1}{\lambda v(-\lambda)} \right\} \right]^2 \cdot h_\beta^2}{h_\beta^2 \cdot \left[1 + \frac{\lambda}{\omega} \left\{ 2 - \frac{1}{\lambda v(-\lambda)} - \frac{v'(-\lambda)}{v(-\lambda)^2} \right\} \right] + (1 - h_\beta^2) \cdot \left\{ \frac{v'(-\lambda)}{v(-\lambda)^2} - 1 \right\}} + o_p(1).$$

Similar to Theorem 2.1 of Dobriban and Wager [2018], $A_R^2(\lambda)$ is optimized at $\lambda^* = \omega \cdot (1 - h_\beta^2) / h_\beta^2$, where the second order term $v'(-\lambda)$ disappears. In Theorem 2.1 of Dobriban and Wager [2018], they set $\gamma = p/n$, and the signal to noise ratio to α^2 , thus, their optimal λ is $\lambda^* = \gamma \alpha^{-2}$. The $A_R^2(0^+)$ can be obtained by taking $\lambda \rightarrow 0^+$, with careful exchanging limits as $n, p \rightarrow \infty$ and $\lambda \rightarrow 0^+$, detailed in Theorem 4 of Hastie et al. [2019]. When $\Sigma = \mathbf{I}_p$, using the results in Lemmas S1 and S2, we have closed-form expressions for $A_R^2(\lambda)$, $A_R^2(\lambda^*)$, and $A_R^2(0^+)$.

Ridge estimator, in-sample

Proposition S9. Under polygenic model (4) and Conditions 1 and 2, as $\min(n, n_z, m_\beta, p) \rightarrow \infty$, for any $\omega \in (0, \infty)$, $h_\beta^2 \in (0, 1]$ and Σ , we have

$$\frac{(\mathbf{X}_{(1)} \boldsymbol{\beta}_{(1)} + \boldsymbol{\epsilon})^T \mathbf{X} (\mathbf{X}^T \mathbf{X} + \lambda n \mathbf{I}_p)^{-1} \mathbf{X}^T \mathbf{X} (\mathbf{X}^T \mathbf{X} + \lambda n \mathbf{I}_p)^{-1} \mathbf{X}^T (\mathbf{X}_{(1)} \boldsymbol{\beta}_{(1)} + \boldsymbol{\epsilon})}{V_{R3} + V_{R4}} = 1 + o_p(1),$$

where

$$\begin{aligned} V_{R3} &= nm_\beta \cdot \left[1 - \frac{2\lambda}{p} \cdot \text{tr}\{\mathbf{X}^T \mathbf{X} (\mathbf{X}^T \mathbf{X} + \lambda n \mathbf{I}_p)^{-1}\} + \frac{\lambda^2}{\omega} \cdot \text{tr}\{\mathbf{X}^T \mathbf{X} (\mathbf{X}^T \mathbf{X} + \lambda n \mathbf{I}_p)^{-2}\} \right] \cdot \sigma_\beta^2 / p \\ &= nm_\beta \cdot \{1 - 2\lambda + 3\lambda^2 g(-\lambda) - \lambda^3 g'(-\lambda)\} \cdot \sigma_\beta^2 / p \end{aligned}$$

and

$$\begin{aligned} V_{R4} &= p \cdot \left[1 - \frac{2\lambda}{\omega} \cdot \text{tr}\{(\mathbf{X}^T \mathbf{X} + \lambda n \mathbf{I}_p)^{-1}\} + \frac{\lambda^2 n}{\omega} \cdot \text{tr}\{(\mathbf{X}^T \mathbf{X} + \lambda n \mathbf{I}_p)^{-2}\} \right] \cdot \sigma_\epsilon^2 \\ &= p \cdot \{1 - 2\lambda g(-\lambda) + \lambda^2 g'(-\lambda)\} \cdot \sigma_\epsilon^2. \end{aligned}$$

In addition, we have

$$\frac{(\mathbf{X}_{(1)} \boldsymbol{\beta}_{(1)} + \boldsymbol{\epsilon})^T \mathbf{X} (\mathbf{X}^T \mathbf{X} + \lambda n \mathbf{I}_p)^{-1} \mathbf{X}^T (\mathbf{X}_{(1)} \boldsymbol{\beta}_{(1)} + \boldsymbol{\epsilon})}{C_{R2}} = 1 + o_p(1),$$

where

$$\begin{aligned} C_{R2} &= nm_\beta \cdot \left[1 - \frac{\lambda}{p} \cdot \text{tr}\{\mathbf{X}^T \mathbf{X} (\mathbf{X}^T \mathbf{X} + \lambda n \mathbf{I}_p)^{-1}\} \right] \cdot \sigma_\beta^2 / p + \text{tr}\{\mathbf{X}^T \mathbf{X} (\mathbf{X}^T \mathbf{X} + \lambda n \mathbf{I}_p)^{-1}\} \cdot \sigma_\epsilon^2 \\ &= nm_\beta \cdot \{1 - \lambda + \lambda^2 g(-\lambda)\} \cdot \sigma_\beta^2 / p + p \cdot \{1 - \lambda g(-\lambda)\} \cdot \sigma_\epsilon^2. \end{aligned}$$

By continuous mapping theorem, we have

$$E_R^2(\lambda) = \frac{\left[h_\beta^2 \cdot \{1 - \lambda + \lambda^2 g(-\lambda)\} + (1 - h_\beta^2) \cdot \omega \{1 - \lambda g(-\lambda)\} \right]^2}{h_\beta^2 \cdot \{1 - 2\lambda + 3\lambda^2 g(-\lambda) - \lambda^3 g'(-\lambda)\} + (1 - h_\beta^2) \cdot \omega \{1 - 2\lambda + \lambda^2 g'(-\lambda)\}} + o_p(1).$$

Different from $A_R^2(\lambda)$, $E_R^2(\lambda)$ is minimized as $\lambda \rightarrow 0$, which means the over-fitting of the model in high-dimensions.

7.9 Proofs of MSE

The main work of studying the out-of-sample MSE of ridge and ridge-less estimators has been done in Dobriban and Wager [2018] and Hastie et al. [2019], which use the key results of Ledoit and P  ch   [2011].

Marginal estimator

$$\begin{aligned} B_\Sigma^2 &= \{E(\hat{\boldsymbol{\beta}}_S | \mathbf{X}, \mathbf{y}) - \boldsymbol{\beta}\}^T \boldsymbol{\Sigma} \{E(\hat{\boldsymbol{\beta}}_S | \mathbf{X}, \mathbf{y}) - \boldsymbol{\beta}\} \\ &= (n^{-1} \mathbf{X}^T \mathbf{X} \boldsymbol{\beta} - \boldsymbol{\beta})^T \boldsymbol{\Sigma} (n^{-1} \mathbf{X}^T \mathbf{X} \boldsymbol{\beta} - \boldsymbol{\beta}) \\ &= n^{-2} \boldsymbol{\beta}^T \mathbf{X}^T \mathbf{X} \boldsymbol{\Sigma} \mathbf{X}^T \mathbf{X} \boldsymbol{\beta} + \boldsymbol{\beta}^T \boldsymbol{\Sigma} \boldsymbol{\beta} - 2n^{-1} \boldsymbol{\beta}^T \boldsymbol{\Sigma} \mathbf{X}^T \mathbf{X} \boldsymbol{\beta} \\ &= \left[m_\beta \cdot \{b_3(\boldsymbol{\Sigma}) + \omega b_2(\boldsymbol{\Sigma}) - 2b_2(\boldsymbol{\Sigma}) + 1\} \cdot \sigma_\beta^2 / p \right] \cdot \{1 + o_p(1)\}. \end{aligned}$$

$$\begin{aligned}
V_S^2 &= \text{tr}\{\text{Cov}(\hat{\beta}_S|\mathbf{X}, \mathbf{y})\boldsymbol{\Sigma}\} \\
&= \text{tr}[\{\text{E}(\hat{\beta}_S\hat{\beta}_S^T|\mathbf{X}, \mathbf{y}) - \text{E}(\hat{\beta}_S|\mathbf{X}, \mathbf{y})\text{E}(\hat{\beta}_S|\mathbf{X}, \mathbf{y})^T\}\boldsymbol{\Sigma}] \\
&= \text{tr}\left[\text{E}\{n^{-1}\mathbf{X}^T(\mathbf{X}\boldsymbol{\beta} + \boldsymbol{\epsilon}) \cdot n^{-1}(\mathbf{X}\boldsymbol{\beta} + \boldsymbol{\epsilon})^T\mathbf{X}\} - (n^{-1}\mathbf{X}^T\mathbf{X}\boldsymbol{\beta})(n^{-1}\mathbf{X}^T\mathbf{X}\boldsymbol{\beta})^T\right]\boldsymbol{\Sigma}] \\
&= n^{-2}\text{tr}(\mathbf{X}^T\boldsymbol{\epsilon}\boldsymbol{\epsilon}^T\mathbf{X}\boldsymbol{\Sigma}) \\
&= n^{-2}\text{tr}(\boldsymbol{\epsilon}^T\mathbf{X}\boldsymbol{\Sigma}\mathbf{X}^T\boldsymbol{\epsilon}) \\
&= \{\omega b_2(\boldsymbol{\Sigma}) \cdot \sigma_\epsilon^2\} \cdot \{1 + o_p(1)\}.
\end{aligned}$$

OLS estimator

$$\begin{aligned}
B_O^2 &= \{\text{E}(\hat{\beta}_O|\mathbf{X}, \mathbf{y}) - \boldsymbol{\beta}\}^T \boldsymbol{\Sigma} \{\text{E}(\hat{\beta}_O|\mathbf{X}, \mathbf{y}) - \boldsymbol{\beta}\} \\
&= (\boldsymbol{\beta} - \boldsymbol{\beta})^T \boldsymbol{\Sigma} (\boldsymbol{\beta} - \boldsymbol{\beta}) = 0.
\end{aligned}$$

$$\begin{aligned}
V_O^2 &= \text{tr}\{\text{Cov}(\hat{\beta}_O|\mathbf{X}, \mathbf{y})\boldsymbol{\Sigma}\} \\
&= \text{tr}[\{\text{E}(\hat{\beta}_O\hat{\beta}_O^T|\mathbf{X}, \mathbf{y}) - \text{E}(\hat{\beta}_O|\mathbf{X}, \mathbf{y})\text{E}(\hat{\beta}_O|\mathbf{X}, \mathbf{y})^T\}\boldsymbol{\Sigma}] \\
&= \text{tr}\{(\mathbf{X}^T\mathbf{X})^{-1}\mathbf{X}^T\boldsymbol{\epsilon}\boldsymbol{\epsilon}^T\mathbf{X}(\mathbf{X}^T\mathbf{X})^{-1}\boldsymbol{\Sigma}\} \\
&= \text{tr}\{(\mathbf{X}^T\mathbf{X})^{-1}\boldsymbol{\Sigma}\} \cdot \sigma_\epsilon^2 \\
&= \frac{\omega}{1-\omega} \cdot \sigma_\epsilon^2 \cdot \{1 + o_p(1)\}. \quad (\omega < 1)
\end{aligned}$$

Ridge estimator

$$\begin{aligned}
B_R^2(\lambda) &= [\text{E}\{\hat{\beta}_R(\lambda)|\mathbf{X}, \mathbf{y}\} - \boldsymbol{\beta}]^T \boldsymbol{\Sigma} [\text{E}\{\hat{\beta}_R(\lambda)|\mathbf{X}, \mathbf{y}\} - \boldsymbol{\beta}] \\
&= \{(\mathbf{X}^T\mathbf{X} + \lambda n\mathbf{I}_p)^{-1}\mathbf{X}^T\mathbf{X}\boldsymbol{\beta} - \boldsymbol{\beta}\}^T \boldsymbol{\Sigma} \{(\mathbf{X}^T\mathbf{X} + \lambda n\mathbf{I}_p)^{-1}\mathbf{X}^T\mathbf{X}\boldsymbol{\beta} - \boldsymbol{\beta}\} \\
&= \boldsymbol{\beta}^T \{(\mathbf{X}^T\mathbf{X} + \lambda n\mathbf{I}_p)^{-1}\mathbf{X}^T\mathbf{X} - \mathbf{I}_p\}^T \boldsymbol{\Sigma} \{(\mathbf{X}^T\mathbf{X} + \lambda n\mathbf{I}_p)^{-1}\mathbf{X}^T\mathbf{X} - \mathbf{I}_p\} \boldsymbol{\beta} \\
&= \left[m_\beta \cdot \left\{ 1 + 2\lambda\omega^{-1} - \frac{1}{v(-\lambda)\omega} - \frac{\lambda v'(-\lambda)}{v(-\lambda)^2\omega} \right\} \cdot \sigma_\beta^2/p + m_\beta \cdot \sigma_\beta^2/p \right. \\
&\quad \left. - 2m_\beta \cdot \left\{ 1 - \frac{1}{v(-\lambda)\omega} + \frac{\lambda}{\omega} \right\} \cdot \sigma_\beta^2/p \right] \cdot \{1 + o_p(1)\}. \\
&= m_\beta \cdot \frac{v(-\lambda) - \lambda v'(-\lambda)}{v(-\lambda)^2\omega} \cdot \sigma_\beta^2/p \cdot \{1 + o_p(1)\}.
\end{aligned}$$

$$\begin{aligned}
V_R^2(\lambda) &= \text{tr}[\text{Cov}\{\widehat{\beta}_R(\lambda)|\mathbf{X}, \mathbf{y}\}\boldsymbol{\Sigma}] \\
&= \text{tr}\{(\mathbf{X}^T\mathbf{X} + \lambda n\mathbf{I}_p)^{-1}\mathbf{X}^T\boldsymbol{\epsilon}\boldsymbol{\epsilon}^T\mathbf{X}(\mathbf{X}^T\mathbf{X} + \lambda n\mathbf{I}_p)^{-1}\boldsymbol{\Sigma}\} \\
&= \text{tr}\{(\mathbf{X}^T\mathbf{X} + \lambda n\mathbf{I}_p)^{-1}\mathbf{X}^T\mathbf{X}(\mathbf{X}^T\mathbf{X} + \lambda n\mathbf{I}_p)^{-1}\boldsymbol{\Sigma}\} \cdot \sigma_\epsilon^2 \cdot \{1 + o_p(1)\} \\
&= \left\{ \frac{1}{\lambda v(-\lambda)} - 1 - \frac{v(-\lambda) - \lambda v(-\lambda)'}{\lambda v(-\lambda)^2} \right\} \cdot \sigma_\epsilon^2 \cdot \{1 + o_p(1)\} \\
&= \left\{ \frac{v(-\lambda)'}{v(-\lambda)^2} - 1 \right\} \cdot \sigma_\epsilon^2 \cdot \{1 + o_p(1)\}.
\end{aligned}$$

Again, similar to Theorem 2.1 of Dobriban and Wager [2018] and Theorem 4 of Hastie et al. [2019], $M_R^2(\lambda)$ is optimized at $\lambda^* = \omega \cdot (1 - h_\beta^2)/h_\beta^2$. The $B_R^2(0^+)$ and $V_R^2(0^+)$ can be obtained by taking $\lambda \rightarrow 0^+$. When $\boldsymbol{\Sigma} = \mathbf{I}_p$, using the results in Lemmas S1 and S2, we have closed-form expressions for $M_R^2(\lambda)$, $M_R^2(\lambda^*)$, and $M_R^2(0^+)$.

7.10 Intermediate results

Marginal estimator

Proposition S10. Under polygenic model (4) and Conditions 1 and 2, as $\min(n, n_z, m_{\beta\eta}, p) \rightarrow \infty$, for any $\omega \in (0, \infty)$, $h_\beta^2, h_\eta^2 \in (0, 1]$, $\varphi_{\beta\eta} \in [-1, 1]$, and $\boldsymbol{\Sigma}$, we have

$$\begin{aligned}
&\mathbb{E}\left\{(\mathbf{Z}_{(1)}\boldsymbol{\eta}_{(1)} + \boldsymbol{\epsilon}_z)^T \mathbf{X} \mathbf{X}^T (\mathbf{X}_{(1)}\boldsymbol{\beta}_{(1)} + \boldsymbol{\epsilon})\right\} = nn_z m_{\beta\eta} b_2(\boldsymbol{\Sigma}) \cdot \sigma_{\beta\eta} / p, \\
&\mathbb{E}\left\{(\mathbf{Z}_{(1)}\boldsymbol{\eta}_{(1)} + \boldsymbol{\epsilon}_z)^T (\mathbf{Z}_{(1)}\boldsymbol{\eta}_{(1)} + \boldsymbol{\epsilon}_z)\right\} = n_z m_\eta \cdot \sigma_\eta^2 / p + n_z \cdot \sigma_{\epsilon_z}^2, \\
&\mathbb{E}\left\{(\mathbf{X}_{(1)}\boldsymbol{\beta}_{(1)} + \boldsymbol{\epsilon})^T \mathbf{X} \mathbf{Z} \mathbf{Z}^T \mathbf{X}^T (\mathbf{X}_{(1)}\boldsymbol{\beta}_{(1)} + \boldsymbol{\epsilon})\right\} \\
&= nn_z m_\beta \cdot \{(n+1)b_3(\boldsymbol{\Sigma}) + p b_2(\boldsymbol{\Sigma})\} \cdot \sigma_\beta^2 / p + nn_z p b_2(\boldsymbol{\Sigma}) \cdot \sigma_\epsilon^2,
\end{aligned}$$

$$\begin{aligned}
&\mathbb{E}\left\{(\mathbf{X}_{(1)}\boldsymbol{\beta}_{(1)} + \boldsymbol{\epsilon})^T \mathbf{X} \mathbf{X}^T (\mathbf{X}_{(1)}\boldsymbol{\beta}_{(1)} + \boldsymbol{\epsilon})\right\} = n^2 m_\beta \{b_2(\boldsymbol{\Sigma}) + \omega\} \cdot \sigma_\beta^2 / p + np \cdot \sigma_\epsilon^2, \\
&\mathbb{E}\left\{(\mathbf{X}_{(1)}\boldsymbol{\beta}_{(1)} + \boldsymbol{\epsilon})^T (\mathbf{X}_{(1)}\boldsymbol{\beta}_{(1)} + \boldsymbol{\epsilon})\right\} = nm_\beta \cdot \sigma_\beta^2 / p + n \cdot \sigma_\epsilon^2, \quad \text{and} \\
&\mathbb{E}\left\{(\mathbf{X}_{(1)}\boldsymbol{\beta}_{(1)} + \boldsymbol{\epsilon})^T \mathbf{X} \mathbf{X}^T \mathbf{X} \mathbf{X}^T (\mathbf{X}_{(1)}\boldsymbol{\beta}_{(1)} + \boldsymbol{\epsilon})\right\} \\
&= n^3 m_\beta \cdot \{b_3(\boldsymbol{\Sigma}) + 3\omega b_2(\boldsymbol{\Sigma}) + \omega^2\} \cdot \sigma_\beta^2 / p + n^2 p \cdot \{b_2(\boldsymbol{\Sigma}) + \omega\} \cdot \sigma_\epsilon^2,
\end{aligned}$$

Then Propositions S4 and S5 follow from Lemma 4, the concentration of marginal estimator quadratic forms.

Ridge-type estimators

Proposition S11. Under polygenic model (4) and Conditions 1 and 2, as $\min(n, n_z, m_{\beta\eta}, p) \rightarrow \infty$, for any $\omega \in (0, \infty)$, $h_\beta^2, h_\eta^2 \in (0, 1]$, $\varphi_{\beta\eta} \in [-1, 1]$, and $\boldsymbol{\Sigma}$, we have almost surely

that

$$\begin{aligned}
& \mathbb{E} \left\{ (\mathbf{Z}_{(1)} \boldsymbol{\eta}_{(1)} + \boldsymbol{\epsilon}_z)^T \mathbf{Z} (\mathbf{X}^T \mathbf{X})^{-1} \mathbf{X}^T (\mathbf{X}_{(1)} \boldsymbol{\beta}_{(1)} + \boldsymbol{\epsilon}) \right\} = n_z m_{\beta\eta} \cdot \sigma_{\beta\eta} / p, \\
& \mathbb{E} \left\{ (\mathbf{X}_{(1)} \boldsymbol{\beta}_{(1)} + \boldsymbol{\epsilon})^T \mathbf{X} (\mathbf{X}^T \mathbf{X})^{-1} \mathbf{Z}^T \mathbf{Z} (\mathbf{X}^T \mathbf{X})^{-1} \mathbf{X}^T (\mathbf{X}_{(1)} \boldsymbol{\beta}_{(1)} + \boldsymbol{\epsilon}) \right\} \\
& \quad = n_z m_{\beta} \cdot \sigma_{\beta}^2 / p + n_z \omega / (1 - \omega) \cdot \sigma_{\epsilon}^2, \\
& \mathbb{E} \left\{ (\mathbf{X}_{(1)} \boldsymbol{\beta}_{(1)} + \boldsymbol{\epsilon})^T \mathbf{X} (\mathbf{X}^T \mathbf{X})^{-1} \mathbf{X}^T (\mathbf{X}_{(1)} \boldsymbol{\beta}_{(1)} + \boldsymbol{\epsilon}) \right\} = n m_{\beta} \cdot \sigma_{\beta}^2 / p + p \cdot \sigma_{\epsilon}^2, \\
& \mathbb{E} \left\{ (\mathbf{X}_{(1)} \boldsymbol{\beta}_{(1)} + \boldsymbol{\epsilon})^T \mathbf{X} (\mathbf{X}^T \mathbf{X})^{-1} \mathbf{X}^T \mathbf{X} (\mathbf{X}^T \mathbf{X})^{-1} \mathbf{X}^T (\mathbf{X}_{(1)} \boldsymbol{\beta}_{(1)} + \boldsymbol{\epsilon}) \right\} = n m_{\beta} \cdot \sigma_{\beta}^2 / p + p \cdot \sigma_{\epsilon}^2, \\
& \mathbb{E} \left\{ (\mathbf{Z}_{(1)} \boldsymbol{\eta}_{(1)} + \boldsymbol{\epsilon}_z)^T \mathbf{Z} (\mathbf{X}^T \mathbf{X} + \lambda n \mathbf{I}_p)^{-1} \mathbf{X}^T (\mathbf{X}_{(1)} \boldsymbol{\beta}_{(1)} + \boldsymbol{\epsilon}) \right\} \\
& \quad = n_z m_{\beta\eta} \cdot \left[1 - \frac{\lambda}{\omega} \cdot \left\{ \frac{1}{\lambda v(-\lambda)} - 1 \right\} \right] \cdot \sigma_{\beta\eta} / p, \\
& \mathbb{E} \left\{ (\mathbf{X}_{(1)} \boldsymbol{\beta}_{(1)} + \boldsymbol{\epsilon})^T \mathbf{X} (\mathbf{X}^T \mathbf{X} + \lambda n \mathbf{I}_p)^{-1} \mathbf{Z}^T \mathbf{Z} (\mathbf{X}^T \mathbf{X} + \lambda n \mathbf{I}_p)^{-1} \mathbf{X}^T (\mathbf{X}_{(1)} \boldsymbol{\beta}_{(1)} + \boldsymbol{\epsilon}) \right\} \\
& \quad = n_z m_{\beta} \cdot \left[1 - \frac{2\lambda}{\omega} \left\{ \frac{1}{\lambda v(-\lambda)} - 1 \right\} + \frac{\lambda^2}{\omega} \cdot \frac{v(-\lambda) - \lambda v'(-\lambda)}{\{\lambda v(-\lambda)\}^2} \right] \cdot \sigma_{\beta}^2 / p + \\
& \quad \quad n_z \cdot \left[\left\{ \frac{1}{\lambda v(-\lambda)} - 1 \right\} - \lambda \cdot \frac{v(-\lambda) - \lambda v'(-\lambda)}{\{\lambda v(-\lambda)\}^2} \right] \cdot \sigma_{\epsilon}^2, \\
& \mathbb{E} \left\{ (\mathbf{X}_{(1)} \boldsymbol{\beta}_{(1)} + \boldsymbol{\epsilon})^T \mathbf{X} (\mathbf{X}^T \mathbf{X} + \lambda n \mathbf{I}_p)^{-1} \mathbf{X}^T (\mathbf{X}_{(1)} \boldsymbol{\beta}_{(1)} + \boldsymbol{\epsilon}) \right\} \\
& \quad = n m_{\beta} \cdot \{1 - \lambda + \lambda^2 g(-\lambda)\} \cdot \sigma_{\beta}^2 / p + p \cdot \{1 - \lambda g(-\lambda)\} \cdot \sigma_{\epsilon}^2, \quad \text{and} \\
& \mathbb{E} \left\{ (\mathbf{X}_{(1)} \boldsymbol{\beta}_{(1)} + \boldsymbol{\epsilon})^T \mathbf{X} (\mathbf{X}^T \mathbf{X} + \lambda n \mathbf{I}_p)^{-1} \mathbf{X}^T \mathbf{X} (\mathbf{X}^T \mathbf{X} + \lambda n \mathbf{I}_p)^{-1} \mathbf{X}^T (\mathbf{X}_{(1)} \boldsymbol{\beta}_{(1)} + \boldsymbol{\epsilon}) \right\} \\
& \quad = n m_{\beta} \cdot \{1 - 2\lambda + 3\lambda^2 g(-\lambda) - \lambda^3 g'(-\lambda)\} \cdot \sigma_{\beta}^2 / p + p \cdot \{1 - 2\lambda g(-\lambda) + \lambda^2 g'(-\lambda)\} \cdot \sigma_{\epsilon}^2,
\end{aligned}$$

These results are based on Lemmas S1 and S2. Then Propositions S6 - S9 follow from the concentration of ridge-type quadratic forms.

7.11 Additional technical details for marginal estimator

The following technical details are useful in proving our theoretical results of marginal estimator.

$$\begin{aligned}
& \mathbb{E} \left\{ (\mathbf{Z}_{(1)} \boldsymbol{\eta}_{(1)} + \boldsymbol{\epsilon}_z)^T \mathbf{Z} \mathbf{X}^T (\mathbf{X}_{(1)} \boldsymbol{\beta}_{(1)} + \boldsymbol{\epsilon}) \right\} \\
&= (m_{\beta\eta}/p) n_z n \text{tr}(\widehat{\boldsymbol{\Sigma}}_X \widehat{\boldsymbol{\Sigma}}_Z) \cdot \sigma_{\beta\eta}/p = (m_{\beta\eta}/p) n_z n \text{tr}(\boldsymbol{\Sigma}^2) \cdot \sigma_{\beta\eta}/p = m_{\beta\eta} n_z n b_2(\boldsymbol{\Sigma}) \cdot \sigma_{\beta\eta}/p, \\
& \mathbb{E} \left\{ (\mathbf{Z}_{(1)} \boldsymbol{\eta}_{(1)} + \boldsymbol{\epsilon}_z)^T (\mathbf{Z}_{(1)} \boldsymbol{\eta}_{(1)} + \boldsymbol{\epsilon}_z) \right\} \\
&= (m_\eta/p) n_z \text{tr}(\widehat{\boldsymbol{\Sigma}}_Z) \cdot \sigma_\eta^2/p + n_z \cdot \sigma_{\epsilon_z}^2 = n_z m_\eta \cdot \sigma_\eta^2/p + n_z \cdot \sigma_{\epsilon_z}^2, \\
& \mathbb{E} \left\{ (\mathbf{X}_{(1)} \boldsymbol{\beta}_{(1)} + \boldsymbol{\epsilon})^T \mathbf{X} \mathbf{X}^T \mathbf{Z} \mathbf{X}^T (\mathbf{X}_{(1)} \boldsymbol{\beta}_{(1)} + \boldsymbol{\epsilon}) \right\} \\
&= (m_\beta/p) n^2 n_z \text{tr}(\widehat{\boldsymbol{\Sigma}}_X \widehat{\boldsymbol{\Sigma}}_Z \widehat{\boldsymbol{\Sigma}}_X) \cdot \sigma_\beta^2/p + n n_z \text{tr}(\widehat{\boldsymbol{\Sigma}}_X \widehat{\boldsymbol{\Sigma}}_Z) \cdot \sigma_\epsilon^2 \\
&= (m_\beta/p) n^2 n_z \left\{ \frac{n+1}{n} \text{tr}(\boldsymbol{\Sigma}^3) + \frac{1}{n} \text{tr}(\boldsymbol{\Sigma}) \text{tr}(\boldsymbol{\Sigma}^2) \right\} \cdot \sigma_\beta^2/p + n n_z \text{tr}(\boldsymbol{\Sigma}^2) \cdot \sigma_\epsilon^2 \\
&= n n_z m_\beta \cdot \{(n+1)b_3(\boldsymbol{\Sigma}) + p b_2(\boldsymbol{\Sigma})\} \cdot \sigma_\beta^2/p + n n_z p b_2(\boldsymbol{\Sigma}) \cdot \sigma_\epsilon^2
\end{aligned}$$

$$\begin{aligned}
& \mathbb{E} \left\{ (\mathbf{X}_{(1)} \boldsymbol{\beta}_{(1)} + \boldsymbol{\epsilon})^T \mathbf{X} \mathbf{X}^T (\mathbf{X}_{(1)} \boldsymbol{\beta}_{(1)} + \boldsymbol{\epsilon}) \right\} \\
&= (m_\beta/p) n^2 \text{tr}(\widehat{\boldsymbol{\Sigma}}_X^2) \cdot \sigma_\beta^2/p + n \text{tr}(\widehat{\boldsymbol{\Sigma}}) \cdot \sigma_\epsilon^2 \\
&= (m_\beta/p) n^2 p b_2(\widehat{\boldsymbol{\Sigma}}_X) \cdot \sigma_\beta^2/p + n p b_1(\widehat{\boldsymbol{\Sigma}}) \cdot \sigma_\epsilon^2 \\
&= m_\beta n^2 \{b_2(\boldsymbol{\Sigma}) + \omega\} \cdot \sigma_\beta^2/p + n p \cdot \sigma_\epsilon^2 \\
& \mathbb{E} \left\{ (\mathbf{X}_{(1)} \boldsymbol{\beta}_{(1)} + \boldsymbol{\epsilon})^T (\mathbf{X}_{(1)} \boldsymbol{\beta}_{(1)} + \boldsymbol{\epsilon}) \right\} \\
&= (m_\beta/p) n \text{tr}(\widehat{\boldsymbol{\Sigma}}_X) \cdot \sigma_\beta^2/p + n_z \cdot \sigma_\epsilon^2 = n m_\beta \cdot \sigma_\beta^2/p + n \cdot \sigma_\epsilon^2, \quad \text{and} \\
& \mathbb{E} \left\{ (\mathbf{X}_{(1)} \boldsymbol{\beta}_{(1)} + \boldsymbol{\epsilon})^T \mathbf{X} \mathbf{X}^T \mathbf{X} \mathbf{X}^T (\mathbf{X}_{(1)} \boldsymbol{\beta}_{(1)} + \boldsymbol{\epsilon}) \right\} \\
&= (m_\beta/p) n^3 \text{tr}(\widehat{\boldsymbol{\Sigma}}_X^3) \cdot \sigma_\beta^2/p + n^2 \text{tr}(\widehat{\boldsymbol{\Sigma}}^2) \cdot \sigma_\epsilon^2 \\
&= n^3 m_\beta \cdot \{b_3(\boldsymbol{\Sigma}) + 3\omega b_2(\boldsymbol{\Sigma}) + \omega^2\} \cdot \sigma_\beta^2/p + n^2 p \cdot \{b_2(\boldsymbol{\Sigma}) + \omega\} \cdot \sigma_\epsilon^2.
\end{aligned}$$

7.12 Real data analysis

Data processing

The raw MRI, covariates and genetic data are downloaded from data resources. We process the MRI data locally using consistent procedures via advanced normalization tools (ANTs, [Avants et al., 2011]) to generate ROI volumes for each dataset. Normalization steps using the ANTs software are detailed in Tustison et al. [2014] and Avants et al. [2011]. We use the standard OASIS-30 Atropos template for registration and Mindboggle-101 atlases for labeling. Details of these templates and processing steps can be found in <https://mindboggle.info/data.html>, Klein and Tourville [2012] and Tustison et al. [2014]. For each phenotype and continuous covariate variable, we further remove values greater than five times the median absolute deviation from the median value. We use imputed SNP data in real data analysis. We perform the following genetic variants data quality controls on each dataset: 1) exclude subjects with more than 10% missing genotypes; 2) exclude variants with minor allele frequency less than 0.01; 3) exclude variants

with larger than 10% missing genotyping rate; 4) exclude variants that fail the Hardy-Weinberg test at 1×10^{-7} level; and 5) remove variants with imputation INFO score less than 0.8. All individuals are aged between 3 and 92 years. More cohort information of these studies can be found in Zhao et al. [2019].

Data acknowledgements

Part of the data collection and sharing for this project was funded by the Pediatric Imaging, Neurocognition and Genetics Study (PING) (U.S. National Institutes of Health Grant RC2DA029475). PING is funded by the National Institute on Drug Abuse and the Eunice Kennedy Shriver National Institute of Child Health & Human Development. PING data are disseminated by the PING Coordinating Center at the Center for Human Development, University of California, San Diego.

PING methods

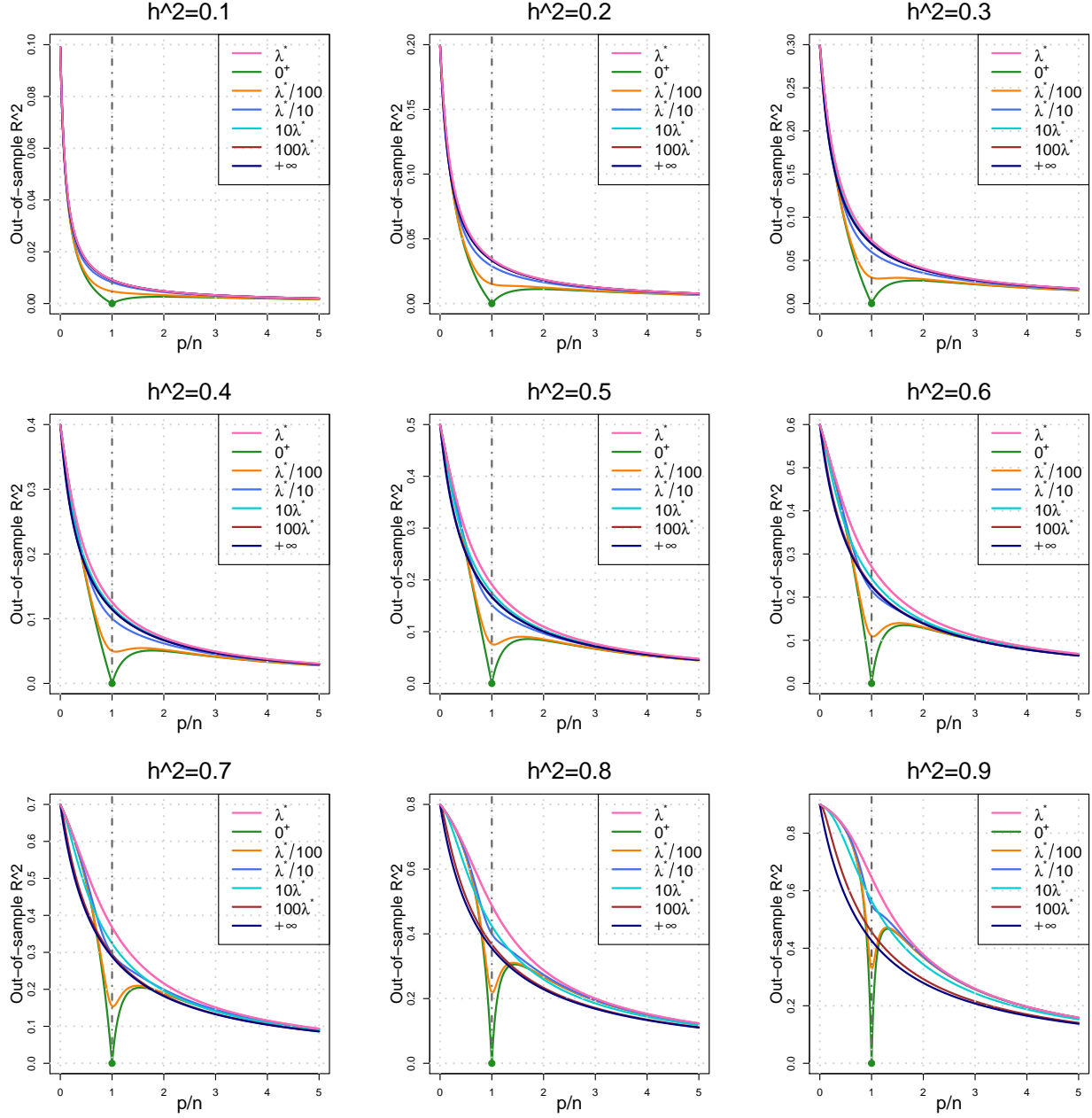
Part of the data used in the preparation of this article were obtained from the Pediatric Imaging, Neurocognition and Genetics (PING) Study database (<http://ping.chd.ucsd.edu/>). PING was launched in 2009 by the National Institute on Drug Abuse (NIDA) and the Eunice Kennedy Shriver National Institute Of Child Health & Human Development (NICHD) as a 2-year project of the American Recovery and Reinvestment Act. The primary goal of PING has been to create a data resource of highly standardized and carefully curated magnetic resonance imaging (MRI) data, comprehensive genotyping data, and developmental and neuropsychological assessments for a large cohort of developing children aged 3 to 20 years. The scientific aim of the project is, by openly sharing these data, to amplify the power and productivity of investigations of healthy and disordered development in children, and to increase understanding of the origins of variation in neurobehavioral phenotypes. For up-to-date information, see <http://ping.chd.ucsd.edu/>.

Pediatric Imaging, Neurocognition and Genetics (PING) authors

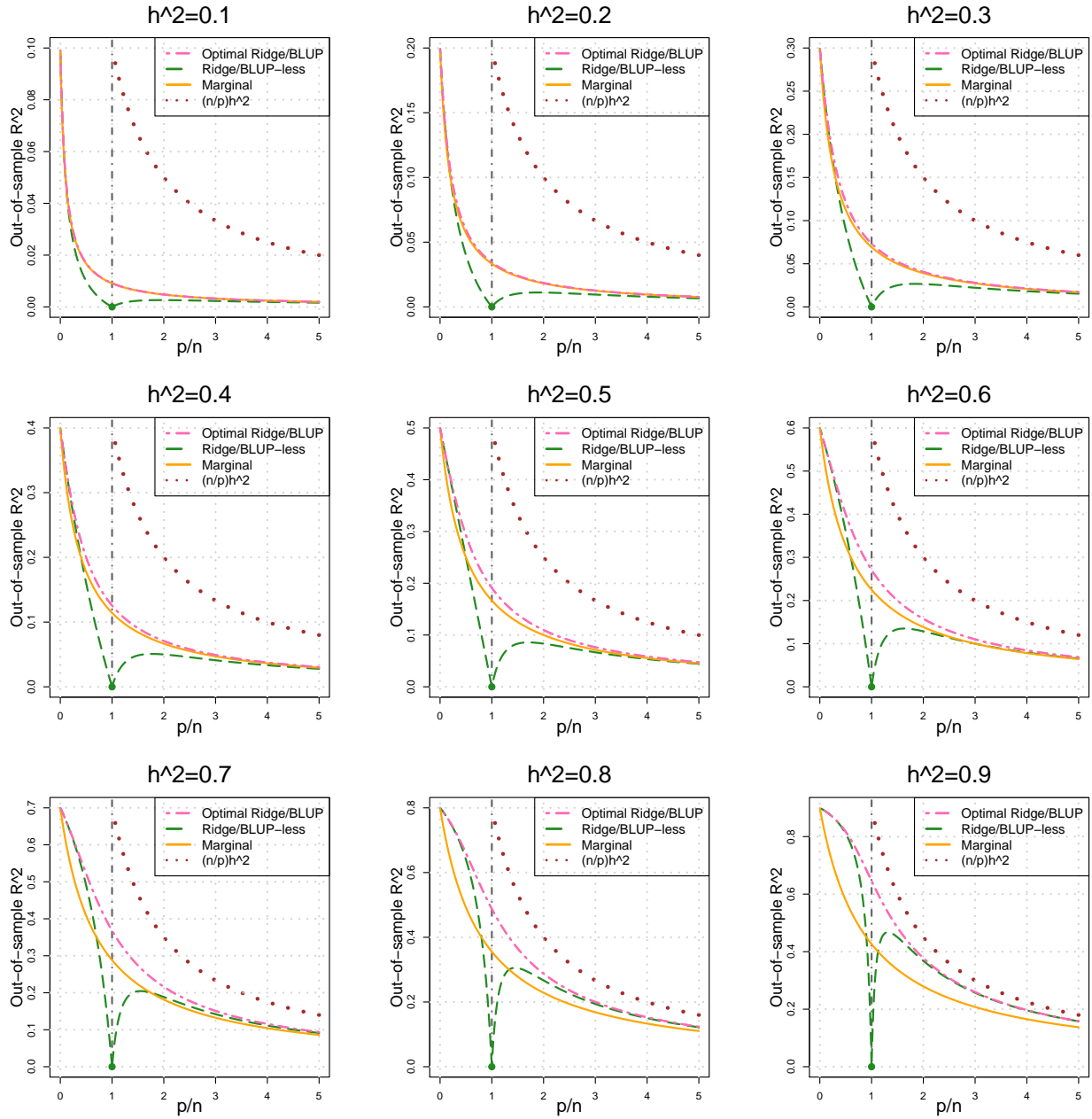
Connor McCabe¹, Linda Chang², Natacha Akshoomoff³, Erik Newman¹, Thomas Ernst², Peter Van Zijl⁴, Joshua Kuperman⁵, Sarah Murray⁶, Cinnamon Bloss⁶, Mark Appelbaum¹, Anthony Gamst¹, Wesley Thompson³, Hauke Bartsch⁵.

¹UC San Diego, La Jolla, CA 92093, USA. ²U Hawaii, Honolulu, HI 96822, USA. ³Department of Psychiatry, University of California, San Diego, La Jolla, California 92093, USA. ⁴Kennedy Krieger Institute, Baltimore, MD 21205, USA. ⁵Multimodal Imaging Laboratory, Department of Radiology, University of California San Diego, La Jolla, California 92037, USA. ⁶Scripps Translational Science Institute, La Jolla, CA 92037, USA.

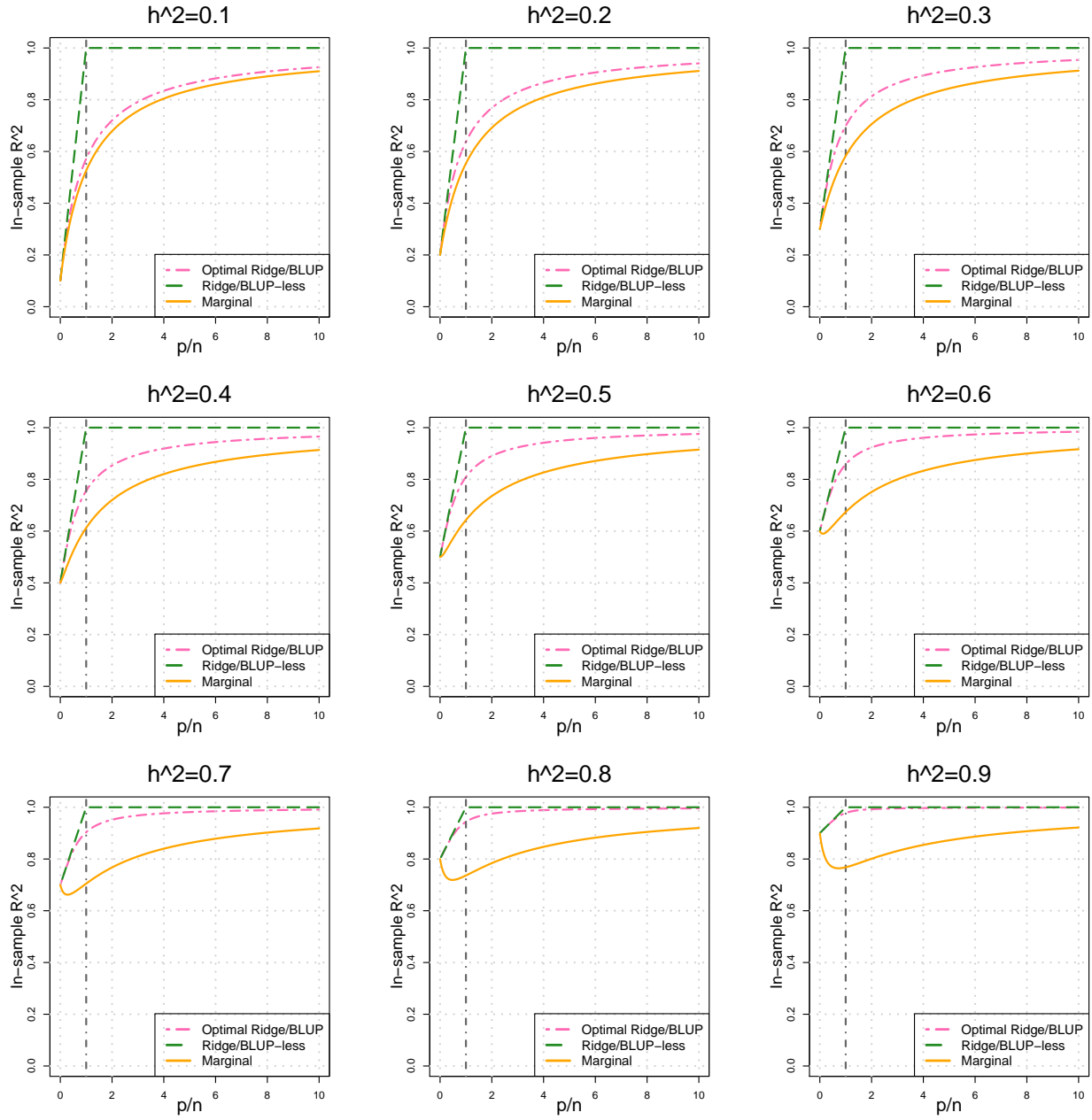
7.13 Supplementary figures



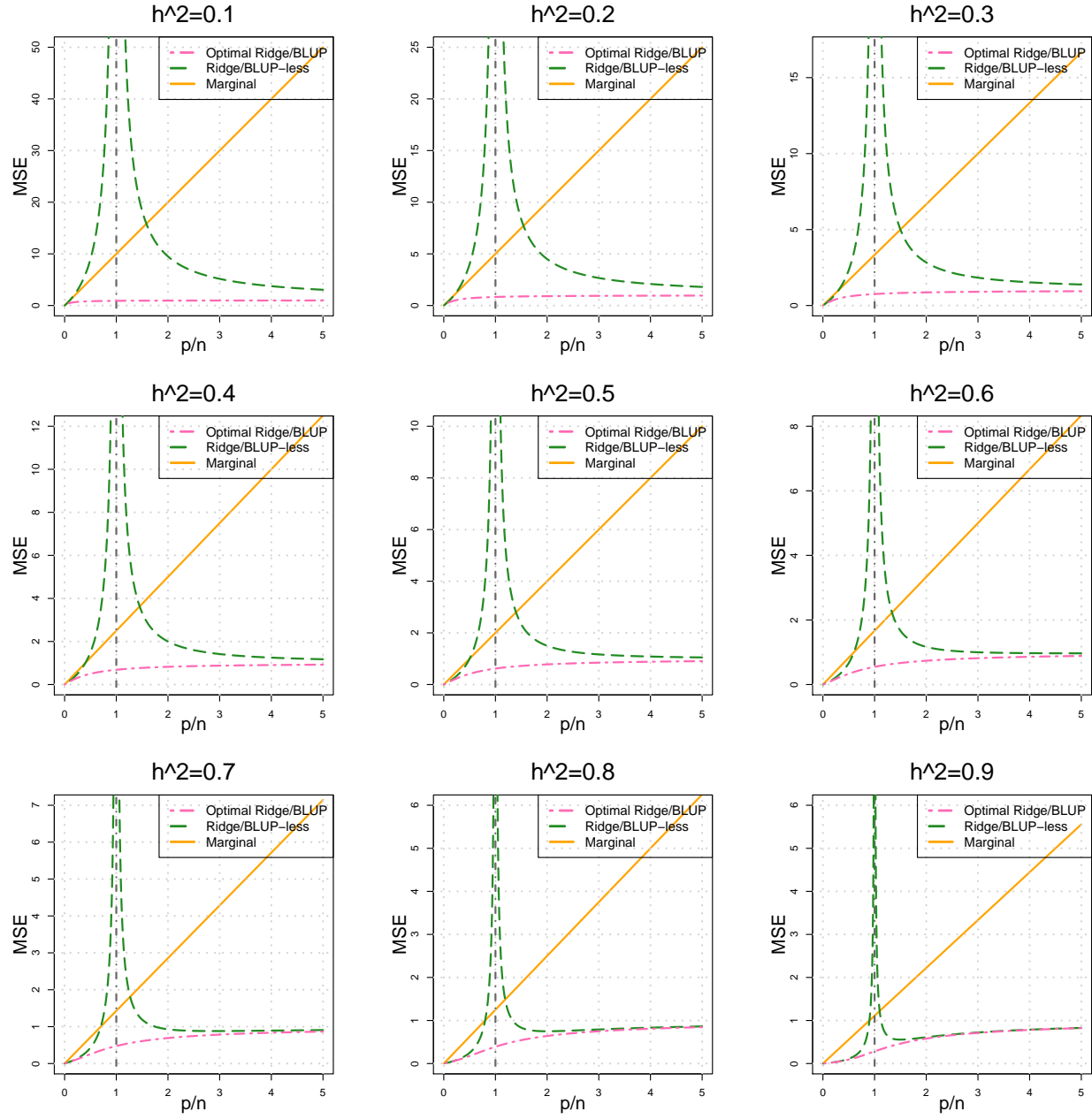
Supplementary Fig. 1: Out-of-sample R -squared $A_R^2(\lambda)$ of ridge-type estimators given different λ and heritability when $\Sigma = \mathbf{I}_p$. λ^* is the optimal λ value, 0^+ corresponds to the case $\lambda \rightarrow 0^+$, and $+\infty$ represents $\lambda \rightarrow +\infty$. We set $\varphi_{\beta\eta} = 1$, and vary $h_{\beta}^2 = h_{\eta}^2$ from 0.1 to 0.9.



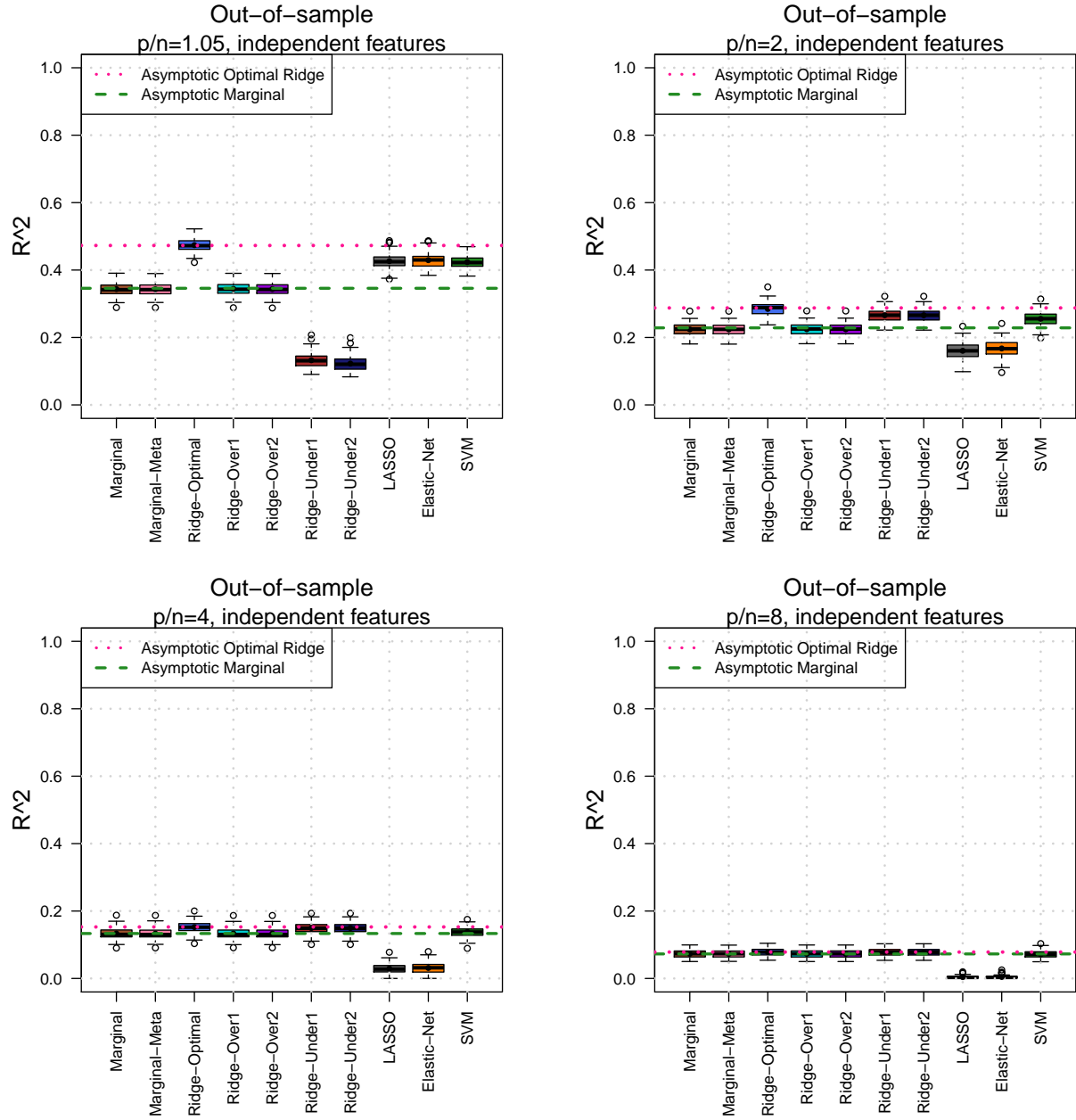
Supplementary Fig. 2: Out-of-sample R -squared of optimal ridge/BLUP estimators ($A_R^2(\lambda^*)=A_B^2(\lambda^*/\omega)$), ridge/BLUP-less estimators ($A_R^2(0^+)=A_B^2(0^+)$), and marginal estimator (A_S^2) when $\Sigma = I_p$. We set $\varphi_{\beta\eta} = 1$, and vary $h_\beta^2 = h_\eta^2$ from 0.1 to 0.9.



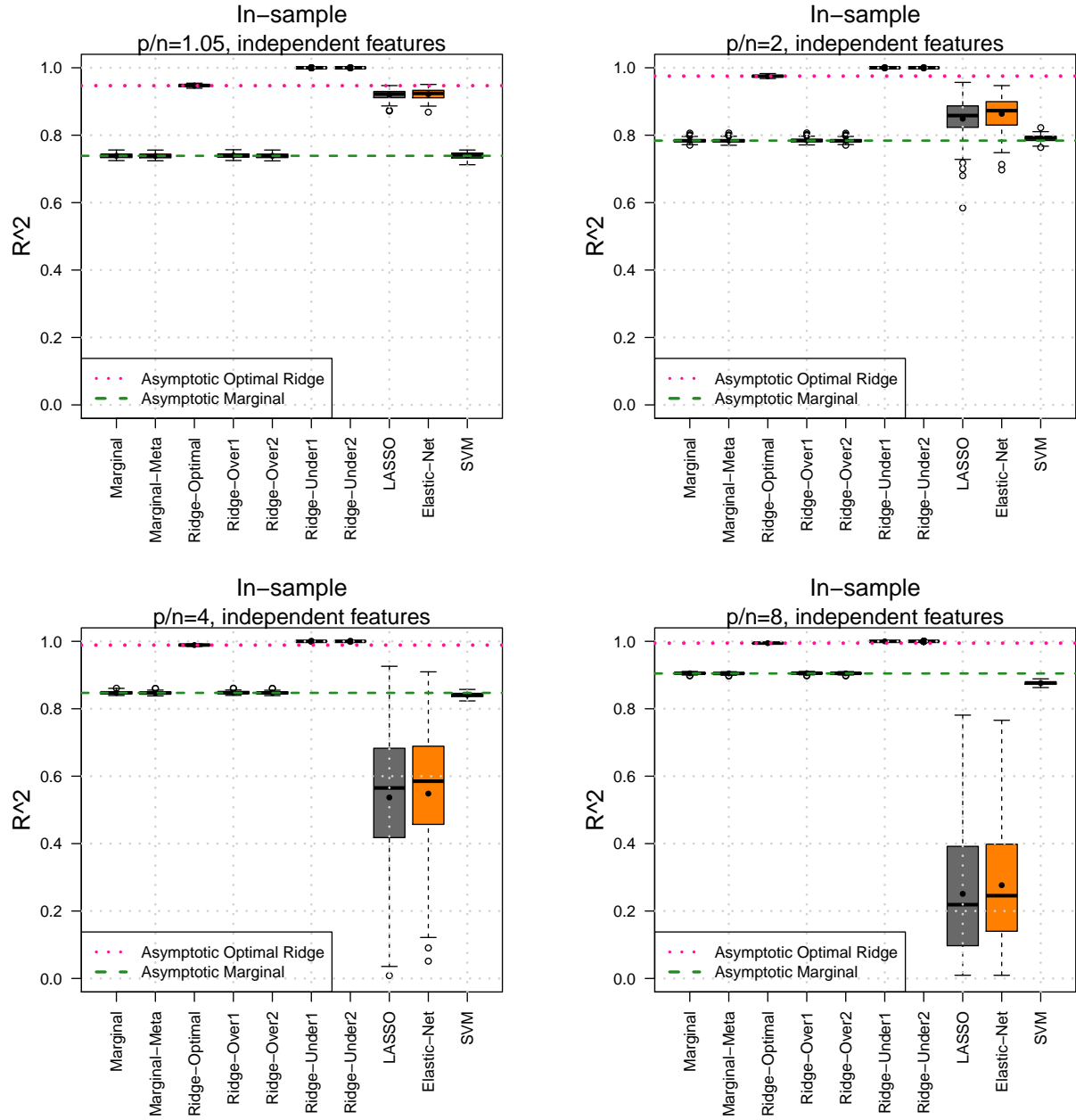
Supplementary Fig. 3: In-sample R -squared of ridge/BLUP-less estimators ($E_R^2(0^+) = E_B^2(0^+)$), optimal (out-of-sample) ridge/BLUP estimators ($E_R^2(\lambda^*) = E_B^2(\lambda^*/\omega)$), and marginal estimator (E_S^2) when $\Sigma = I_p$. We vary h_β^2 from 0.1 to 0.9.



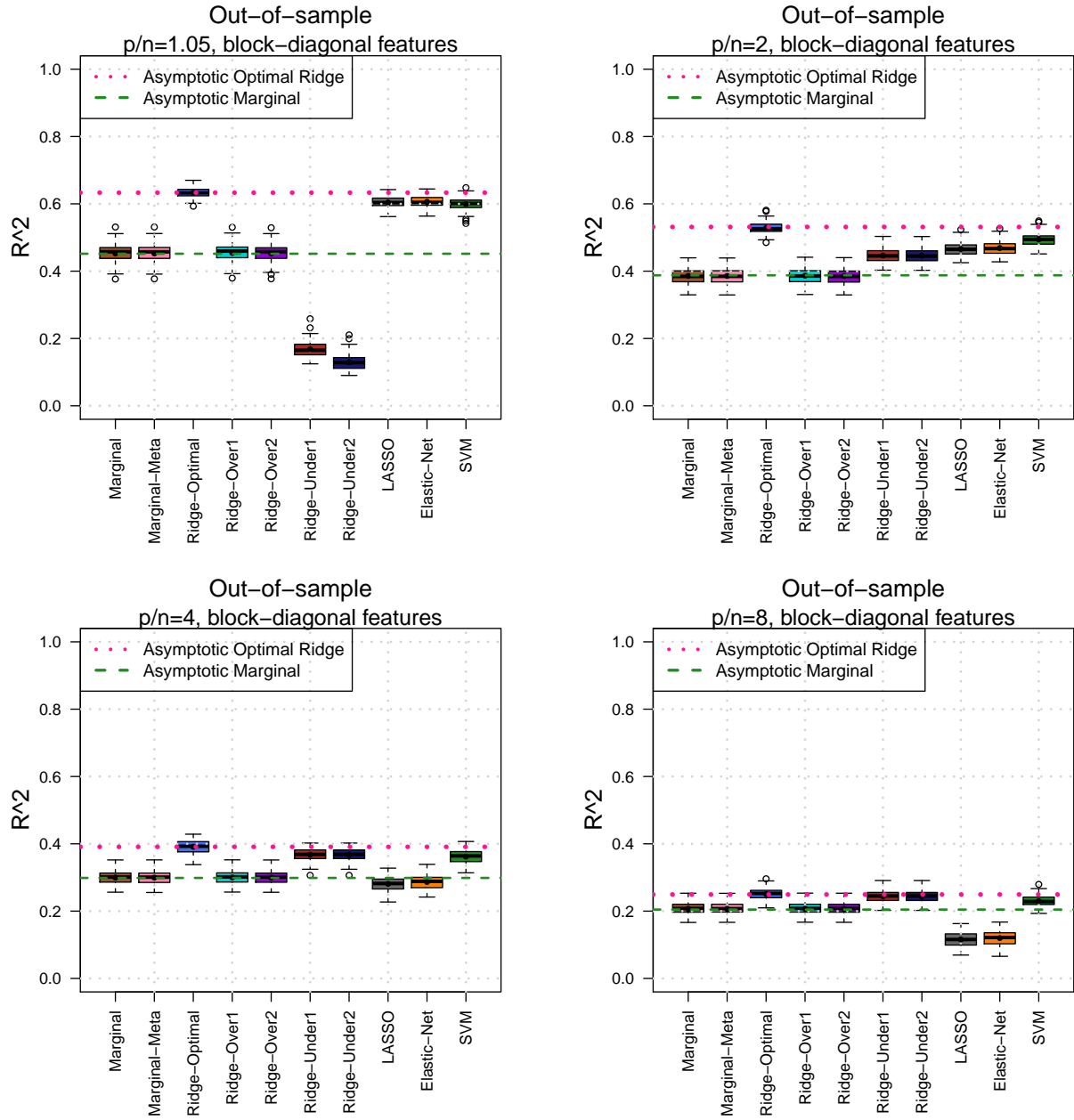
Supplementary Fig. 4: Mean squared prediction error (MSE) of marginal, ridge/BLUP, and ridge-less/BLUP-less estimators when $\Sigma = I_p$. We set $m_{\beta}\sigma_{\beta}^2/p = 1$, and vary h_{β}^2 from 0.1 to 0.9.



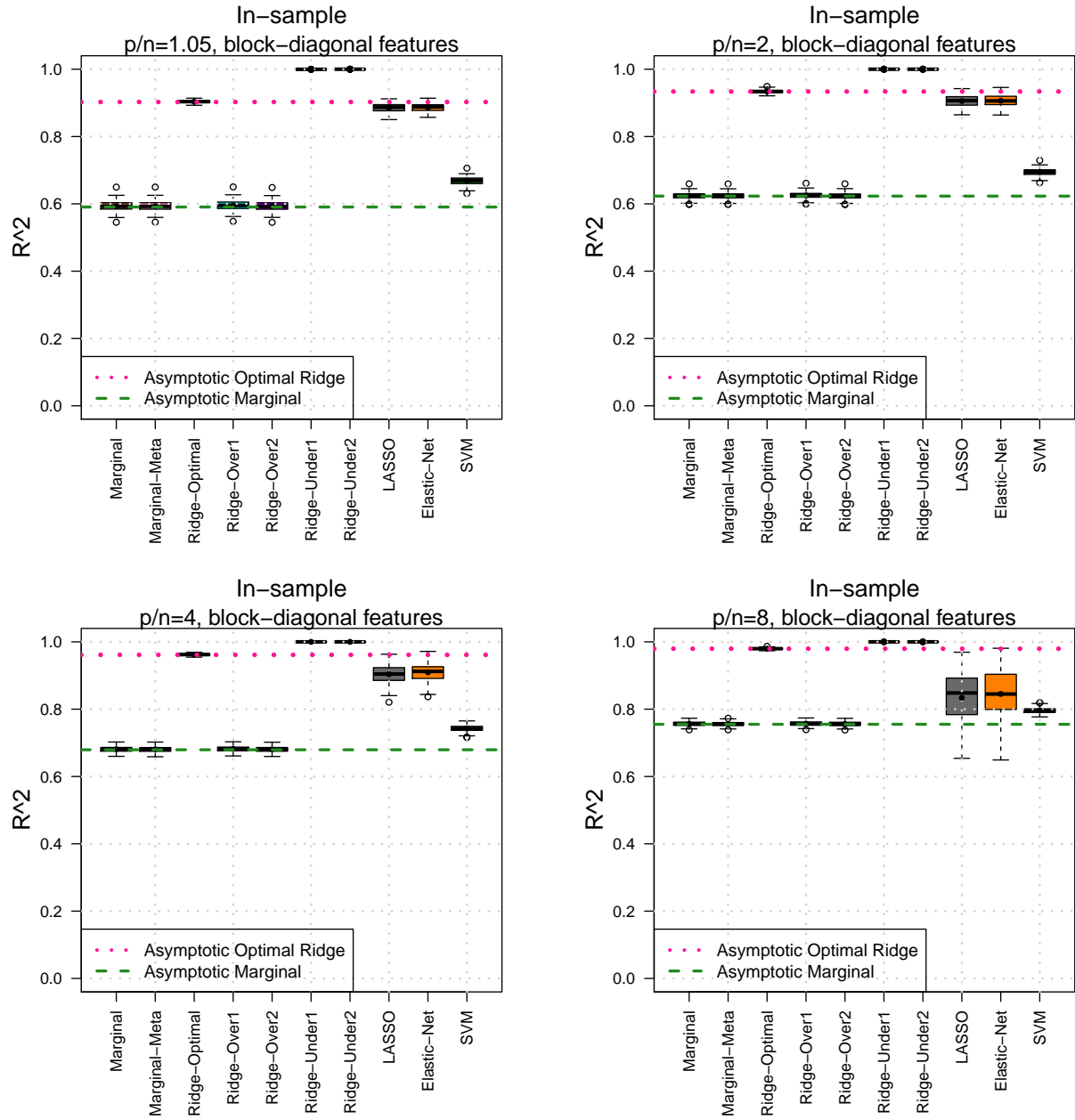
Supplementary Fig. 5: Out-of-sample R -squared of different estimators for independent features. See Figure 4 for figure notations. We set $n = 2000$, and vary $\omega =$ from 1.05 to 8. The dash lines represent the asymptotic limits of ridge (red) and marginal (green) estimators.



Supplementary Fig. 6: In-sample R -squared of different estimators for independent features. See Figure 4 for figure notations. We set $n = 2000$, and vary $\omega =$ from 1.05 to 8. The dash lines represent the asymptotic limits of ridge (red) and marginal (green) estimators.



Supplementary Fig. 7: Out-of-sample R -squared of different estimators for features with block-diagonal correlation structure. See Figure 4 for figure notations. We set $n = 2000$, and vary $\omega =$ from 1.05 to 8. The dash lines represent the asymptotic limits of ridge (red) and marginal (green) estimators.



Supplementary Fig. 8: In-sample R -squared of different estimators for features with block-diagonal correlation structure. See Figure 4 for figure notations. We set $n = 2000$, and vary ω from 1.05 to 8. The dash lines represent the asymptotic limits of ridge (red) and marginal (green) estimators.

Supplementary table

ROI ID	BLUP-IBAM	Marginal-IBAM	BLUP-LST	Marginal-LST
left.thalamus.proper	1.739E-02	3.501E-02	5.185E-02	3.895E-02
left.caudate	4.712E-02	1.377E-01	5.536E-02	4.042E-05
left.putamen	1.864E-01	2.224E-01	1.396E-02	3.509E-01
left.pallidum	1.839E-02	4.233E-02	9.342E-02	3.600E-02
left.hippocampus	8.727E-01	7.419E-02	4.957E-01	3.823E-02
left.amygdala	6.878E-01	9.384E-01	7.425E-01	7.848E-01
left.accumbens.area	6.475E-04	6.923E-02	1.647E-02	9.124E-03
right.thalamus.proper	4.950E-04	2.509E-04	1.205E-01	6.544E-03
right.caudate	1.549E-02	2.900E-01	1.513E-02	2.731E-02
right.putamen	2.607E-01	2.474E-01	3.173E-02	3.328E-01
right.pallidum	8.900E-02	9.409E-02	1.796E-01	6.048E-03
right.hippocampus	2.344E-01	3.116E-03	1.044E-01	1.666E-02
right.amygdala	2.369E-02	1.942E-01	1.181E-02	1.040E-01
right.accumbens.area	1.591E-02	2.564E-03	1.092E-02	4.209E-05

Supplementary Table 1: Partial R -squared ($\times 100\%$) of 14 subcortical ROI volumes to predict IBAM and LST cognitive test scores in the PING cohort. The partial R -squared is estimated from linear regression while adjusting for the effects of age and gender. BLUP: best linear unbiased prediction; Marginal: marginal estimator. IBAM: IBAM score; LST: list sort total score.